Removal and Recovery of Surfactants by Foam Fractionation

A thesis submitted in

partial fulfilment of the requirement for the degree of

DOCTOR OF PHILOSOPHY

by

Awadh Kishor Kumar

Department of Chemical Engineering

Indian Institute of Technology Guwahati

Guwahati – 781039, Assam, India

June 2022

Removal and Recovery of Surfactants by Foam Fractionation

A thesis submitted in

partial fulfilment of the requirement for the degree of

DOCTOR OF PHILOSOPHY

by

Awadh Kishor Kumar

Department of Chemical Engineering

Indian Institute of Technology Guwahati

Guwahati – 781039, Assam, India

June 2022

Dedicated to

My Family and Friends

Indian Institute of Technology Guwahati

Department of Chemical Engineering

STATEMENT

I hereby declare that the content embodied in the thesis titled **"Removal and Recovery of Surfactants by Foam Fractionation"** is the result of investigations carried out by me at the Department of Chemical Engineering, Indian Institute of Technology Guwahati, India, under the supervision of **Prof. Pallab Ghosh**.

In keeping with the standard practice of reporting scientific observations, due acknowledgments have been made on the findings of other investigators, wherever the work described is based.

Guwahati

June 2022

Awadh Kishor Kumar

Indian Institute of Technology Guwahati

Department of Chemical Engineering

CERTIFICATE

It is certified that the work described in the thesis titled **"Removal and Recovery of Surfactants by Foam Fractionation"** by Mr. Awadh Kishor Kumar for the award of the degree of Doctor of Philosophy is an authentic record of the results obtained from research work carried out under my supervision at the Department of Chemical Engineering, Indian Institute of Technology Guwahati, India, and this work has not been submitted elsewhere for a degree.

Dr. Pallab Ghosh
Professor
Department of Chemical Engineering
IIT Guwahati, Guwahati – 781039
Assam, India

ACKNOWLEDGMENTS

I would like to acknowledge all the people who contributed in some way to my Ph.D. thesis and helped me to complete it.

First and foremost, I offer my sincerest gratitude to my supervisor, Prof. Pallab Ghosh, for allowing me the opportunity to work in this fascinating area of research. I am very grateful to my supervisor for his continuous guidance, important advice, immense support, encouragement, and most importantly allowing me the freedom to work in my own way. I am very thankful to him for his enormous efforts on correcting all my mistakes, and making my work and research publications more valuable. It was really an honor to work under his supervision.

I would also like to thank my Doctoral Committee members, Prof. Mihir Kumar Purkait and Prof. Mahuya De of the Department of Chemical Engineering, and Dr. Tadikonda Venkata Bharat of the Department of Civil Engineering, for their valuable suggestions, which have improved the quality of this thesis.

I would also like to thank Prof. Subrata Kumar Majumder, Prof. Vimal Katiyar, Prof. Prakash Kotecha, and Prof. Tamal Banerzee for their research-oriented teaching during my coursework. I also thank Prof. Anugrah Singh (Head of the Department of Chemical Engineering) and Prof. Bishnupada Mandal (former Head of the Department of Chemical Engineering), for their administrative support. I shall always remain grateful to Prof. G. Pugazhenthi for his invaluable support throughout my entire journey during the Ph.D. Furthermore, I wish to thank all the technical staffs of my department, especially, Mr. Harsaraj Biswanath and Mr. Pankaj Kumar for their kind help.

I sincerely acknowledge the help and encouragement of my research-group members, i.e., Dr. Badri Vishal, Dr. Shailesh Ravi Varade, Dr. Abdisa Jabesa, Dr. Rima Biswas, Mr. Jinesh Machale, Mrs. Surabhi Patel, Mr. Shasahnk Shekhar Srinet, Ms. Ananya Basak, Ms. Ankita Jain, Ms. Neha Rawat, Mr. Nipu Kumar Das, Mr. Sandeep Kumar, and Mr. Anurag. I would also like to thank my friends who have helped me in various ways during my P.D.: i.e., Mr. Sunil Kumar Singh, Mr. Shivam Tiwari, Mr. Kaniska Murmu, Ms. Prerona Gogoi, Dr. Pritam Roy, Dr. Ankur Pandey, Mr. Anirudh Deb, Dr. Ranjeet Mishra, Dr. Nirmal Roy, Mr. Rupam Sinha, Dr. Kuldeep Roy, Mr. Bitang Tripura, Dr. Kuldeep Mahato, Dr. Pyarimohan Dehury, Dr. Upasana Mahanta, Dr. Debashis Kundu, Dr. Sourav Chattopadhaya, Dr. Rahul Kesarwani, Mr. Jitendra Rawat, Mr. Nabendu Paul, Mr. Nikhil Kumar, Mr. Dhiren Mishra, Mr. Naveen Kumar Verma, and Mr. Priyankar Talukdar who have made my stay pleasant at IIT Guwahati.

I will remain indebted forever to my parents who have provided me a great early-education. They have been a source of love and encouragement to me throughout, and without their emotional support, it would have been difficult to stay away from home all these years. Also, I would like to thank my brothers, sisters, uncles, aunties, cousins, brother-in-law, sister-in-law, and nephews for their love and support, which kept my morale high at difficult times (e.g., during the years of COVID-19 and lock-downs). Finally, I would like to thank my beloved wife Mrs. Neha Kumari for her love and support.

Awadh Kishor Kumar

ABSTRACT

Surfactants are used in many industries, and they are integrally related to many consumer products. However, at the same time, they contaminate water. The environmental fate of the surfactants is considerably important due to their effects on the health of human beings and animals. They are of interest because of their increasingly ubiquitous domestic and industrial use, and the difficulty in removing them by the traditional treatment methods. The removal of of different types of surfactant by foam fractionation has been practiced for water/wastewater treatment. This process and its applications in water/wastewater treatment have been discussed in the Chapter 1 of this thesis. Chapter 2 of this thesis focuses on the materials and experimental methods.

The Chapter 3 of this study focuses on the removal and recovery of a cationic surfactant [i.e., cetyltrimethylammonium bromide (CTAB)] by foam fractionation in batch mode. The surfactant concentration was five times its critical micellar concentration. About 60% of the surfactant was recovered from the top of the cylindrical column in the form of a semi-solid paste. Recovery of the surfactant in the presence of various inorganic salts (i.e., NaCl, $CaCl_2$, and Na_2SO_4) at different airflow rates was also investigated. Introduction of salt had a pronounced effect on the foaming characteristics. The foam volume and surfactant recovery were reduced by the addition of salt. The stability of the foam played a very important role in surfactant recovery, which was analyzed by the zeta potential measurements at the air–water interface.

The Chapter 4 of the study focuses on the removal and recovery of an anionic surfactant [i.e., sodium dodecyl sulfate (SDS)] from water by foam fractionation in the presence of oily effluents (i.e., benzene, toluene, and hexane). The presence of oily effluents in wastewater makes it more harmful so that it is essential to treat it before

discharging off. Surfactant-laden water containing oils may cause severe hazards to the animal and human health. In the presence study, the SDS concentration was above its critical micellar concentration. The effects of benzene, toluene, and hexane on the removal and recovery of SDS were studied at the airflow rates in the range of 0.4–1.6 dm^3 min^{-1}. About 72% recovery of SDS was achieved in the form of a semi-solid cake. Foam stability had a vital role in the SDS recovery, and it was affected by the presence of oil. The foam stability was analyzed by measuring the zeta potential at the air–water interface and through the entering, spreading, and bridging coefficients. The adsorption of the surfactant at the air–water interface was estimated from the surface tension measurements. The foam volume and SDS recovery decreased in the presence of oil.

Chapter 5 reports the effect of addition of methanol and ethanol on the removal and recovery of an anionic surfactant [i.e., sodium dodecylbenzene sulfonate (SDBS)]. This study was done at below and above the CMC of the SDBS. The concentrations of SDBS were 500, 1000, 2000, and 3000 mg dm^{-3}. The airflow rate was varied in the range 0.4 – 1.6 dm^3 min^{-1}. About 77% of the surfactant was recovered from the top of the column. The addition of alcohol lowered the foam volume and surfactant recovery. The zeta potential at the air–water interface was measured to determine the stability of the foam, which was highly significant in surfactant recovery. The zeta potential increased with the addition of alcohol. The Ross–Miles test also demonstrated that the production of foam and its stability increased with the increasing surfactant concentration and in the presence of alcohol. Surface tension measurements revealed the surfactant's adsorption at the air–water interface.

CONTENTS	Page no.

Acknowledgments	*i*
Abstract	*iii*
Contents	*v*
List of Figures	*ix*
List of Tables	*xii*
CHAPTER 1 INTRODUCTION	**1 – 50**
1.1. General overview	1
1.2. Surfactants	2
1.3. Classification of surfactants	5
1.3.1. Anionic surfactants	6
1.3.2. Cationic surfactants	6
1.3.3. Nonionic surfactants	7
1.3.4. Nonionic surfactants	7
1.4. Foams	8
1.4.1 Structure of foam	9
1.5. Foamability and foam stability	12
1.5.1. Marangoni effect	13
1.5.2. Film elasticity	14
1.5.3. Intermolecular and surface forces	15
1.5.4. Foam decay	19
1.5.5. Foam drainage	19
1.5.6. Coalescence of foam bubbles	20
1.6. Foam fractionation	21

1.6.1. Adsorption of surface active species at air–water interface 25

1.6.2. Modes of operation 27

1.6.3. Batch operation 29

1.6.4. Process performance indicators 30

1.7. Objectives of the work 31

1.8. Outline of the thesis 32

Nomenclature *35*

References *38*

CHAPTER 2 MATERIALS AND EXPERIMENTAL METHODS **51– 64**

2.1. Materials 51

2.2. Experimental setup 52

2.3. Measurement of surfactant concentration 53

2.3.1. Measurement of CTAB concentration 53

2.3.2. Measurement of SDS concentration 54

2.3.3. Measurement of SDBS concentration 56

2.4. Measurement of surface and interfacial tension 57

2.4.1. Wilhelmy plate method 59

2.4.2. du Noüy ring method 60

2.5. Measurement of zeta potential 62

2.6. Experimental conditions 63

References *64*

CHAPTER 3	**REMOVAL AND RECOVERY OF A CATIONIC SURFACTANT FROM ITS AQUEOUS SOLUTION BY FOAM FRACTIONATION**	**65 – 83**
3.1. Introduction		65
3.2. Results and discussion		66
3.2.1. Effect of surfactant and salt concentrations		66
3.2.2. Surfactant recovery		74
3.2.3. Foam volume		77
3.2.4. Water recovery		80
3.3. Conclusions		80
Nomenclature		*82*
References		*83*
CHAPTER 4	**REMOVAL AND RECOVERY OF AN ANIONIC SURFACTANT FROM ITS AQUEOUS SOLUTION BY FOAM FRACTIONATION**	**85 – 100**
4.1. Introduction		85
4.2. Results and discussion		86
4.2.1. Foam volume		86
4.2.2. Surfactant concentration profiles		92
4.2.3. Surface tension of the aqueous solutions		93
4.2.4. Zeta potential at the air–water interface		94
4.2.5. Surfactant recovery		96
4.2.6. Water recovery		97

4.3. Conclusions 97

Nomenclature 99

References 99

CHAPTER 5 REMOVAL AND RECOVERY OF AN ANIONIC SURFACTANT IN THE PRESENCE OF ALCOHOL BY FOAM FRACTIONATION **101 – 122**

5.1. Introduction 101

5.2. Results and discussion 102

5.2.1 Foam volume 102

5.2.2 Surfactant concentration profiles 108

5.2.3 Surface tension of the aqueous solutions 112

5.2.4. Zeta potential at the air–water interface 116

5.2.5. Surfactant recovery 119

5.2.6. Water recovery 121

5.3. Conclusions 121

Nomenclature *122*

References *123*

CHAPTER 6 SUMMARY AND SCOPE FOR FUTURE WORK **125 – 126**

6.1 Summary of the work 125

6.2 Future scope of research 126

Appendix A 127

Research Outcomes 129

LIST OF FIGURES

	Title	Page no.
Figure 1.1	Foaming in the Yamuna river (Delhi, India).	2
Figure 1.2	Schematic representation of a surfactant molecule.	3
Figure 1.3	Schematic representation of monolayer formation at the air–water interface and formation of micelles in the bulk phase when the surfactant concentration exceeds the CMC.	5
Figure 1.4	Structure of foam.	9
Figure 1.5	A generalized foam system.	11
Figure 1.6	Structure of a spherical foam bubble.	11
Figure 1.7	Schematic representation of Marangoni flow at the air–water interface caused by the surface surfactant gradient.	14
Figure 1.8	Coalescence of bubbles.	21
Figure 1.9	Simplest modes of operation: (a) batch and (b) continuous.	28
Figure 2.1	Foam fractionation setup.	53
Figure 2.2	Schematic diagram showing the two-phase titration for determining the concentration of CTAB (before and after): (a) aqueous phase and (b) organic phase.	55
Figure 2.3	Illustration of the titration for determining the concentration of SDS: (a) aqueous solution and (b) chloroform phase.	56
Figure 2.4	Absorption versus concentration calibration curve for UV–Vis spectrophotometry.	57
Figure 2.5	A photograph of the tensiometer used for the measurement of surface and interfacial tension.	58
Figure 2.6	Schematic illustration of the Wilhelmy plate method.	60
Figure 2.7	Schematic illustration of the du Noüy ring method.	61
Figure 2.8	A photograph of the zeta potentiometer.	63
Figure 3.1	The EDL when a cationic surfactant is adsorbed at a flat air-water interface in the presence of salt.	68

Figure 3.2	A comparison of the effects of 10 mol m^{-3} NaCl, $CaCl_2$, and Na_2SO_4 on the surfactant concentration profiles at different airflow rates: (a) 0.4, (b) 0.8, (c) 1.2, and (d) 1.6 dm^3 min^{-1}.	69
Figure 3.3	A comparison of the effects of 50 mol m^{-3} NaCl, $CaCl_2$, and Na_2SO_4 on the surfactant concentration profiles at different airflow rates: (a) 0.4, (b) 0.8, (c) 1.2, and (d) 1.6 dm^3 min^{-1}.	70
Figure 3.4	A comparison of the effects of 100 mol m^{-3} NaCl, $CaCl_2$, and Na_2SO_4 on the surfactant concentration profiles at different airflow rates: (a) 0.4, (b) 0.8, (c) 1.2, and (d) 1.6 dm^3 min^{-1}.	71
Figure 3.5	Variation of surfactant recovery with airflow rate at different NaCl concentrations.	75
Figure 3.6	Variation of surfactant recovery with airflow rate at different $CaCl_2$ concentrations.	75
Figure 3.7	Variation of surfactant recovery with airflow rate at different Na_2SO_4 concentrations.	76
Figure 3.8	The effect of NaCl on foam volume at different airflow rates: (a) 0.4, (b) 0.8, (c) 1.2, and (d) 1.6 dm^3 min^{-1}.	77
Figure 3.9	The effect of $CaCl_2$ on foam volume at different airflow rates: (a) 0.4, (b) 0.8, (c) 1.2, and (d) 1.6 dm^3 min^{-1}.	78
Figure 3.10	The effect of Na_2SO_4 on foam volume at different airflow rates: (a) 0.4, (b) 0.8, (c) 1.2, and (d) 1.6 dm^3 min^{-1}.	79
Figure 4.1	The EDL when an anionic surfactant is adsorbed at a flat air–water interface.	87
Figure 4.2	Schematic presentation of the spreading-oil entrainment mechanism of foam film rupture.	89
Figure 4.3	The effects of benzene, toluene, and hexane on foam volume at various airflow rates: (a) 0.4, (b) 0.8, (c) 1.2, and (d) 1.6 dm^3 min^{-1}.	90

Figure 4.4	The effects of benzene, toluene, and hexane on the SDS concentration at various airflow rates: (a) 0.4, (b) 0.8, (c) 1.2, and (d) 1.6 dm^3 min^{-1}.	91
Figure 4.5	The effect of different airflow rates on the recovery of surfactant in the presence of benzene, hexane, and toluene.	95
Figure 5.1	Adsorption of surfactant/alcohol molecules at air-water interface.	104
Figure 5.2	Variation of foam volume with time at different airflow rates at 500 mg dm^{-3} SDBS: (a) 0.4, (b) 0.8, (c) 1.2, and (d) 1.6 dm^3 min^{-1}.	104
Figure 5.3	Variation of foam volume with time at different airflow rates at 1000 mg dm^{-3} SDBS: (a) 0.4, (b) 0.8, (c) 1.2, and (d) 1.6 dm^3 min^{-1}.	105
Figure 5.4	Variation of foam volume with time at different airflow rates at 2000 mg dm^{-3} SDBS: (a) 0.4, (b) 0.8, (c) 1.2, and (d) 1.6 dm^3 min^{-1}.	106
Figure 5.5	Variation of foam volume with time at different airflow rates at 3000 mg dm^{-3} SDBS: (a) 0.4, (b) 0.8, (c) 1.2, and (d) 1.6 dm^3 min^{-1}.	107
Figure 5.6	Variation of foam height with time at different surfactant concentrations: (a) 500, (b) 1000, (c) 2000, and (d) 3000 mg dm^{-3}.	108
Figure 5.7	Effect of airflow rate on the concentration profiles at 500 mg dm^{-3} of SDBS with time: (a) 0.4, (b) 0.8, (c) 1.2, and (d) 1.6 dm^3 min^{-1}.	109
Figure 5.8	Effect of airflow rate on the concentration profiles at 1000 mg dm^{-3} of SDBS with time: (a) 0.4, (b) 0.8, (c) 1.2, and (d) 1.6 dm^3 min^{-1}.	110
Figure 5.9	Effect of airflow rate on the concentration profiles at 2000 mg dm^{-3} of SDBS with time: (a) 0.4, (b) 0.8, (c) 1.2, and (d) 1.6 dm^3 min^{-1}.	111

Figure 5.10 Effect of airflow rate on the concentration profiles at 3000 mg dm^{-3} of SDBS with time: (a) 0.4, (b) 0.8, (c) 1.2, and (d) 1.6 $dm^3 min^{-1}$. 111

Figure 5.11 Surfactant recovery at different airflow rates: (a) 500, (b) 1000, (c) 2000, and (d) 3000 mg dm^{-3} SDBS concentrations. 120

LIST OF TABLES

	Title	Page no.
Table 1.1	Examples of commonly used surfactants of various types	5
Table 1.2	Some examples of foams in everyday experience	8
Table 2.1	Chemicals used in this work	51
Table 3.1	Effect of salt on surface tension of the feed solutions	71
Table 3.2	Effect of salt on the zeta potential at the air–water interface	73
Table 4.1	Entering, spreading, and bridging coefficients in the presence of oil	89
Table 4.2	Surface tension of the oil-based surfactant solutions at different airflow rates (after the experiments)	92
Table 4.3	Zeta potential of the oil-based surfactant solutions at different airflow rates (after the experiments)	94
Table 5.1	Surface tensions of the feed solutions at different concentrations of SDBS	113
Table 5.2	Surface tensions of the alcohol-based surfactant solutions at 500 mg dm^{-3} after the experiment at different airflow rates	113
Table 5.3	Surface tensions of the alcohol-based surfactant solutions at 1000 mg dm^{-3} after the experiment at different airflow rates	114
Table 5.4	Surface tensions of the alcohol-based surfactant solutions at 2000 mg dm^{-3} after the experiment at different airflow rates	114
Table 5.5	Surface tensions of the alcohol-based surfactant solutions at 3000 mg dm^{-3} after the experiment at different airflow rates	115
Table 5.6	Zeta potential of the feed solutions at different concentrations of SDBS	116

Table 5.7	Zeta potentials at the air–water interfaces after the experiments at different airflow rates at 500 mg dm^{-3} surfactant concentration	116
Table 5.8	Zeta potentials at the air–water interfaces after the experiments at different airflow rates at 1000 mg dm^{-3} surfactant concentration	117
Table 5.9	Zeta potentials at the air–water interfaces after the experiments at different airflow rates at 2000 mg dm^{-3} surfactant concentration	118
Table 5.10	Zeta potentials at the air–water interfaces after the experiments at different airflow rates at 3000 mg dm^{-3} surfactant concentration	119

Chapter 1

Introduction

CHAPTER 1

INTRODUCTION

1.1. General overview

Water pollution has become a global concern due to its impact on the human health as well as aquatic life. There are numerous sources of water pollution where surfactants are considered as major pollutants [1, 2]. A huge amount of surfactants (e.g., soaps and detergents) is released from the laundries, washing and cleaning operations, and various industries (e.g., sugar, petroleum, personal care products, food, fabric, and pulp and paper) (see Figure 1.1) [3]. Surfactant-based products can have a negative effect on the surface water such as a decrease in oxygen transfer, damage in water quality due to foaming, and a reduction in the self-cleaning capacity of the river. Human health can be adversely affected by drinking the water contaminated with surfactants. A variety of diseases such as skin irritation, liver damage, stomach cramps, sore throat, and nausea can occur. This can lead to death in the severe cases. Surfactants can have toxic and harmful effects on all types of amphibian life at the high concentrations. They can damage the outer mucus layers, which protect the fishes from bacteria and parasites [4]. Surfactants can cause severe damage to their gills [5]. If the surface tension of the water becomes low, fishes may consume toxic organic chemicals like phenol and pesticides. Since most surfactants reduce the surface tension, fishes easily consume these chemicals. When such fish is consumed as food, humans can get diseases like liver and kidney damage.

Surfactants and detergents used for the industrial purposes and household products are responsible for diminishing the breeding capability of the amphibian organisms. The phosphate-rich surfactants lead to an algal bloom in the freshwater and decrease oxygen in the waterways. The decomposition of the algae consumes the oxygen, which could have

been otherwise used by the aquatic life [6]. Wastewater containing phosphates and ammonia creates a nuisance for human life by generating a large amount of foam in the lake and river. Such excessive foaming creates an unbearable stench causing suffocation to the residents and passers-by. To meet the stringent environmental regulations, the surfactant concentration in the effluent streams must be reduced.

Figure 1.1 Foaming in the Yamuna river (Delhi, India).

For the removal of non-biodegradable surfactants, standard oxidation methods are not effective. One of the promising methods to remove such surfactants from wastewater is foam fractionation. In this method, the surfactant solution is bubbled with air in a column to adsorb the surfactant molecules at the gas–liquid interface, which are then carried along the column to its top in the form of foam [4, 7]. A significant portion of the surfactant can be recovered by this method.

1.2. Surfactants

The term “surfactant” refers to a substance that acts as a surface active agent. In other words, a surfactant is defined by its ability to adsorb at the surfaces and interfaces [8]. Surfactants have numerous applications in the industrial processes. They are widely used in the household products, food processing [9], foaming [10], oil recovery [11], cosmetics [12, 13], paints [14,

15], biomedical applications [16, 17], and polymerization [18]. Surfactants are also known as amphiphilic or amphipathic molecules with a polar head group (which is hydrophilic) and a long hydrocarbon tail (which is hydrophobic). When the surfactant is dissolved in water, its hydrophilic head group always remains in the aqueous phase, while the hydrophobic tail group stays in the air (or in the oil phase). The name "amphiphilic" derives from the Greek word "amphi", which means "of both kinds". The hydrophilic head groups can be polar end-groups like the amino, carboxylate, sulfate, sulfonate, quaternary ammonium, hydroxyl, and polyoxyethylene, while the hydrophobic tails are usually long hydrocarbon chains. Figure 1.2 shows the schematic representation of a surfactant molecule.

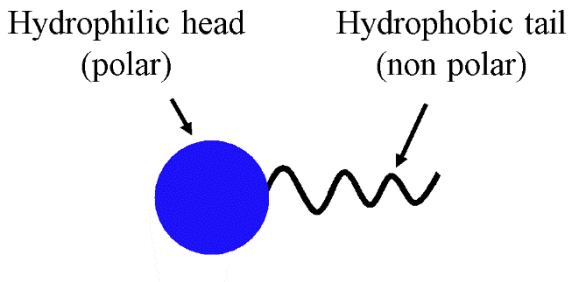

Figure 1.2 Schematic representation of a surfactant molecule.

Surfactants have the ability to adsorb on the surfaces and interfaces, changing their free energy. The decrease of the phase boundary's free energy is the driving factor for surfactant adsorption. The amount of work required to expand the interface is the interfacial free energy per unit area. This interfacial free energy is measured in J m^{-2}. It is equivalent to interfacial tension, which is measured in N m^{-1}. The surface tension (at the air–liquid interface) or interfacial tension (at the oil–water interface) is reduced by the adsorption of surfactant [19]. The surface tension reduces with increasing surfactant adsorption. Surfactant adsorption at the

interface is determined by the structure of the surfactant and the nature of the two phases that meet at the interface.

As mentioned earlier, when the surfactant is dissolved in water, the hydrophilic head group is oriented toward the aqueous phase, while the hydrophobic tail group is oriented towards the air (or oil) phase. This process decreases the surface free energy by forming a layer of the surfactant molecules at the air–water interface. When the air–water interface is entirely covered with the surfactant molecules, a monolayer is formed, and those molecules present in the bulk aqueous phase form self-assembled structures known as *micelles*. The surfactant concentration at which this phenomenon occurs is called critical micelle concentration (CMC). The hydrophobic tail groups in the micelle reduce their interaction with water, forming a hydrophobic core. On the other side, the hydrophilic head groups optimize their interaction with water and develop a surface layer. Between the micelles and the monolayer, there is a dynamic equilibrium of surfactant molecules [20, 21]. The number of micelles grows as the surfactant concentration rises. The morphology of the micelles can change as the surfactant concentration rises. It is common to see a transition from spherical to cylindrical micelles. Surfactants can create micelles having complex microstructures that look like worms. As these changes occur, the physical properties of the micellar solution alter significantly [22]. When the surfactant molecules dissolve in oil and form aggregates there, reverse micelles can form [23].

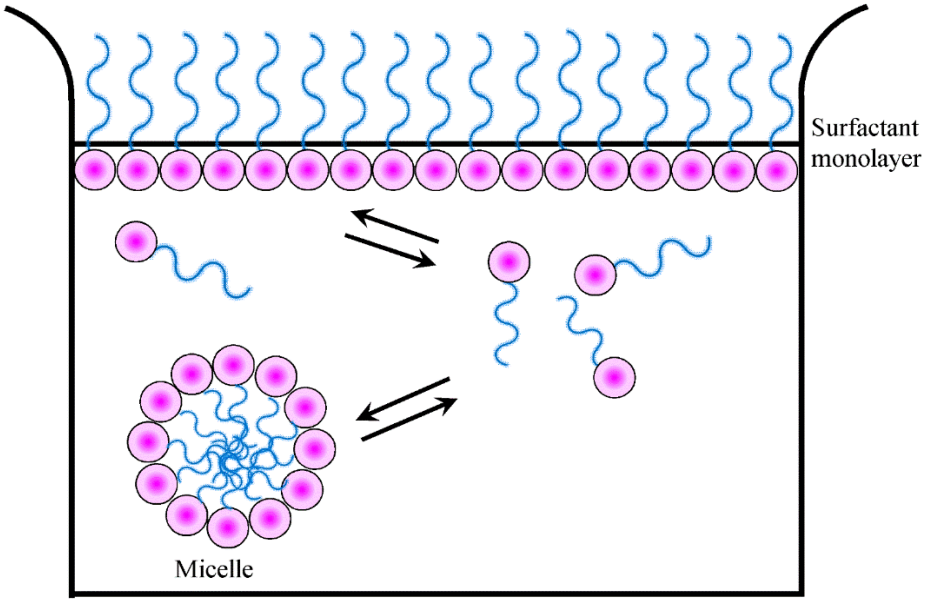

Figure 1.3 Schematic representation of monolayer formation at the air–water interface and formation of micelles in the bulk phase when the surfactant concentration exceeds the CMC.

1.3. Classification of surfactants

Based on the charge on their head group, surfactants can be classified as cationic (positively charged), anionic (negatively charged), nonionic (no charge), and zwitterionic (both positive and negative charges). Examples of different types of commonly-used surfactants are given in Table 1.1.

Table 1.1 Examples of commonly-used surfactants of various types

Surfactant	*Type*	*Mol. wt. (g mol^{-1})*	*Formula*
Sodium dodecyl sulfate (SDS)	Anionic	288.4	$CH_3(CH_2)_{11}OSO_3Na$
Cetyltrimethylammonium bromide (CTAB)	Cationic	364.5	$CH_3(CH_2)_{15}N(Br)(CH_3)_3$

Triton X-100	Nonionic	647.0	$C_{14}H_{22}O(C_2H_4O)_n$ (n = 9 - 10)
Didodecyldimethylammonium bromide	Zwitterionic	462.6	$[CH_3(CH_2)_{11}]_2N(CH_3)_2(Br)$

1.3.1. Anionic surfactants

Surfactants with anionic functional groups at their heads, such as sulfonate, phosphate, sulfate, and carboxylate, are known as anionic surfactants [24]. The most commonly used surfactants are of this type, which account for nearly 50% of all surfactant production worldwide [25]. Ammonium lauryl sulfate, sodium lauryl sulfate, sodium laureth sulfate (sometimes known as sodium lauryl ether sulfate, SLES), and sodium myreth sulfate are all anionic surfactants extensively used in the various industries. The alkyl carboxylates (i.e., soaps), e.g., sodium stearate, are the most common surfactants used for personal hygiene care. Stearates account for more than half of all surfactant used worldwide.

1.3.2. Cationic surfactants

When cationic surfactants are dissolved in the aqueous phase, they have positive charges on their head groups. The cationic surfactants like benzalkonium chloride (BAC), cetylpyridinium chloride (CPC), and benzethonium chloride (BZT) are used as antimicrobials and antifungals in domestic, institutional, and industrial cleansers. These surfactants can destroy bacterial and viral cell membranes. Alkyltrimethylammonium salts, such as cetyltrimethylammonium bromide (CTAB) and cetyltrimethylammonium chloride possess permanently-charged quaternary ammonium cations.

1.3.3. Nonionic surfactants

Nonionic surfactants (such as alcohols, phenols, ethers, esters, or amides) do not ionize in water because their hydrophilic portion is non-dissociable. These surfactants account for over 40% of the total industrial surfactant output worldwide, and they are often good dispersing agents for carbon. Fatty acid ethoxylates, alcohol ethoxylates, alkyl phenol ethoxylates, POE mercaptans, sorbitan ester ethoxylates, fatty amine ethoxylates, and tertiary acetylenic glycols are a few examples of commonly-used nonionic surfactants.

1.3.4. Zwitterionic surfactants

Both the cationic and anionic centers are linked to the same molecule in this type of surfactant. The cationic component is preferably based on the ammonium group, while the anionic component can be varied and include sulfonates, carboxlic acids, and sulphuric acid esters. The zwitterionic surfactant is generally pH sensitive, and it behaves as anionic or cationic depending on the pH. A few examples of the zwitterionic surfactant are β-N-alkylaminopropionic acids, N-alkyl-β-iminodipropionic acids, imidazoline carboxylates, N-alkylbetaines, amidoamines, amine oxides, sulfobetaines, and sultaines.

1.4. Foams

Foam is a dispersion of gas bubbles separated by liquid films [26]. Foams are two-phase systems consisting of a dispersed gaseous phase and a continuous liquid phase, forming a closed-cell structure [27]. The dispersed (gas) and continuous (liquid) phases in foams are immiscible. The gas fraction in a foam may be 80% or higher [27-29]. In order to generate foam, energy equal to γA (where γ is the surface tension and A the area created) is needed to create the bubble surfaces. Foams are widely employed in petroleum oil recovery,

manufacturing processes, and also in our everyday life due to their unique properties such as large specific area, low density, and high thermal insulation. Table 1.2 shows some examples of foams in day-to-day life.

Table 1.2 Some examples of foams in everyday experience [11]

Group	*Applications*
Foods	Champagne, soda head, beer head, whipped cream, and meringue
Detergency	Manual and machine dishwashing, commercial bottle-cleaning, and machine washing of clothes
Personal care products	Shaving cream, hair shampoo, and bubble bath
Process industries	Foam blankets on electroplating baths, sewage treatment effluent foams, mineral or oil flotation froths, foam fractionation, and pulping black liquor foams
Other	Fire extinguishing liquor foam, explosion suppressing foam blankets, fumigants, insecticides, mattresses, and herbicide blankets

Some well-known foams are bubble baths, dishwater detergents, and foam heads on the beers. Foams are very important in many industrial, environmental, and biological processes. They are of great practical importance for the synthesis of new materials such as superhydrophobic organosilica sol-gel foams [30-32]. They are used in many important technologies, either intermediate or end products. Foam is one of the dominant factors that determine the commercial value of various cosmetic products such as soap, shampoo, shaving foam, cleansing foam, and toothpaste. [33-35]. The acceptability of many consumer products

is closely linked to the quality and texture of the foam they produce (e.g., shaving foams and creams, shampoos, etc.) [36, 37]. As a result, the study of foam stability has kindled the interest of researchers and product manufacturers.

1.4.1. Structure of foam

A wide range of research on the surface phenomena has been carried out on foams and foam films. Contact between the gas bubbles in the foam occurs through the liquid films, which contain surfactant molecules. Foam films are the essential structural elements of the foam, and they determine, to a great extent, the stability and properties of the foam. The liquid phase may change to a gel or solid after making the dispersion, which leads to a solid foam. Solid foams typically evolve from the liquid state and share the same basic cell structure as the liquid foams.

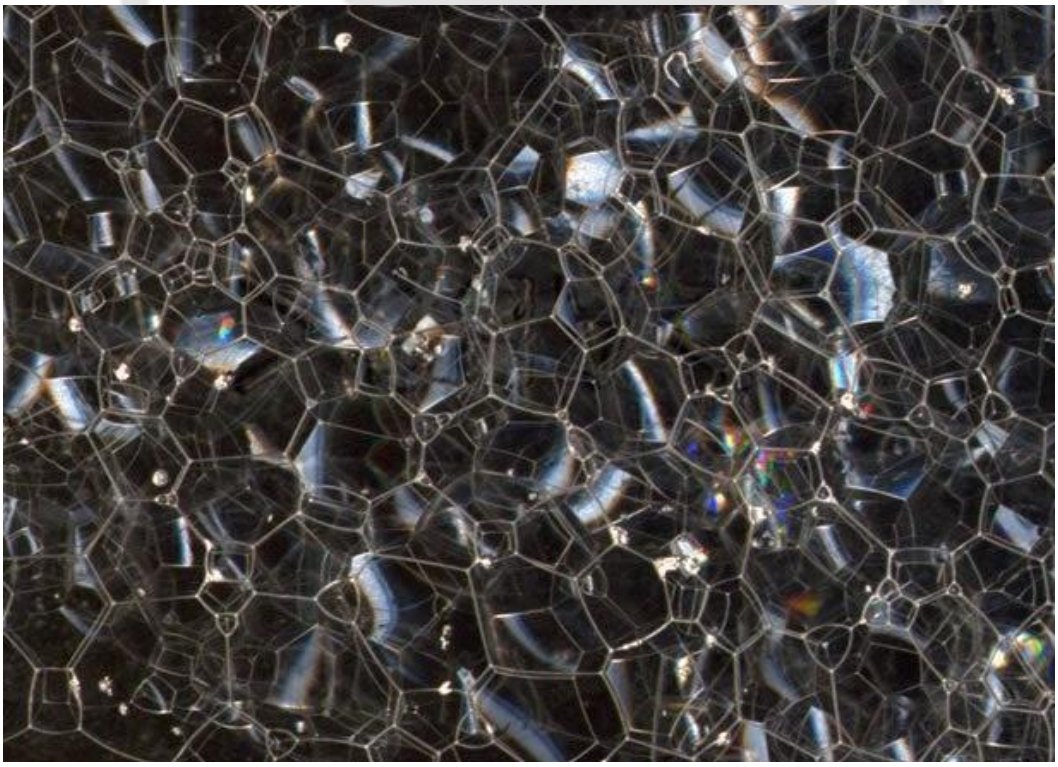

Figure 1.4 Structure of foam [32].

The total area of the gas–liquid interface dictates the energy of the foam. Foams are generally characterized by their quality (Φ), which is defined as

$$\Phi = \left(\frac{V_g}{V_g + V_l} \right) \times 100 \tag{1.1}$$

The structure of foam depends on the amount of liquid and gas present in it. Based on the circumstances, a foam may contain a high or a low amount of liquid [27]. Foams with a minimal amount of liquid (e.g., 2%) are almost completely dry and polyhedral. These are termed as *dry foam* or *polyederschaum*. If the liquid fraction is greater than 36%, then the quality of foam would be very low, and the bubbles would be spherical. Such type of foam is known as *wet foam* or *kugelschaum*. Wet foams are transient and exist for a few tens of seconds. In contrast, dry foams can be stable for hours to days after formation [38]. Polyhedral or dry foams have a complex structure. The formation of polyhedral bubbles and Plateau borders takes place at the edges. The junction of these films is known as the Plateau border (see Figure 1.5). Two-dimensional thin flat liquid films are known as *lamellae* or *laminae*. Three lamellae meet at the Plateau border, which is shown in Figure 1.5. The liquid begins to drain following the foam generation, leaving behind a collection of thin liquid films joined together through a network of these Plateau borders. The Plateau borders are indistinct from the nodes in the wet foams. The angle between them is known as *Steiner angle*.

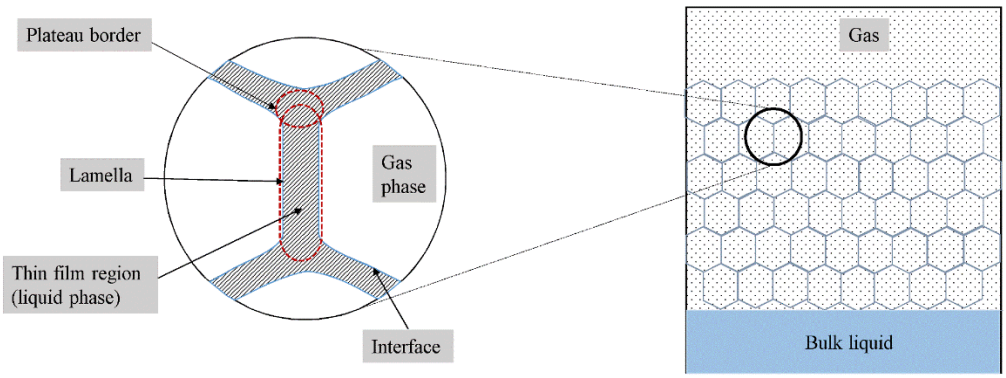

Figure 1.5 A generalized foam system [11].

When a surfactant is added to water, it spontaneously adsorbs at the air–water interface and decreases the interfacial energy (otherwise, there would be no spontaneous adsorption). At the air–water interface, the polar part of the adsorbed surfactant molecules remains in contact with water and the hydrophobic part is oriented in the air. This leads to the formation of a monolayer. The foam films have surfactant monolayers on their air–water interfaces. The foam films formed from the detergent solutions are initially thick (i.e., a few μm). The film becomes thin as the fluid drains away due to gravity, capillary forces, or surface evaporation, to about 100 nm or less.

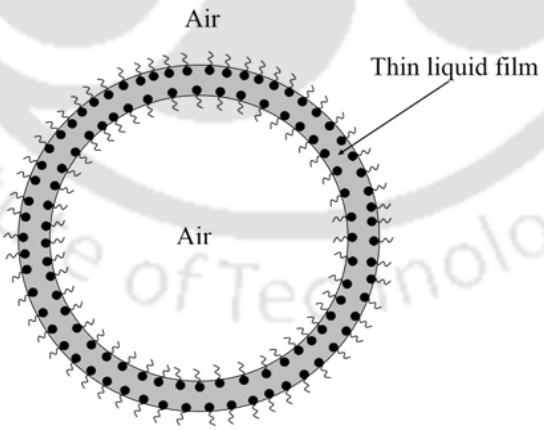

Figure 1.6 Structure of a spherical foam bubble.

Foam formation involves dynamic adsorption of surfactant molecules at the air–water interface. The structure and stability of foams are determined by the concentration of surfactant in the bulk solution and the ability of the surfactant molecules to stabilize the thin foam films.

After forming a foam, its stability depends on factors such as the gravity drainage, capillary suction, surface elasticity, surface and bulk viscosity, attraction due to van der Waals force, and repulsion due to electrostatic double layer and steric forces [39].

Foams are metastable non-equilibrium systems. The smaller bubbles have a higher internal pressure than the larger ones. The Young–Laplace equation gives the excess pressure inside the spherical bubbles.

$$\Delta P = 2\gamma / r \tag{1.2}$$

Due to the excess pressure inside the smaller bubbles, the air inside them diffuses into the larger bubbles. Therefore, the larger bubbles coarsen and increase in size with time, which is known as *Ostwald ripening*. The coarsening of foam causes the tiny bubbles to disappear eventually. As the bubble area increases, bubbles of five or fewer sides shrink, and those of seven or more sides grow. This evolution of foam causes the thin films to get stretched and dilated. In such thin foam films, surface waves are generated due to mechanical and thermal disturbances, leading to the rupture of the film.

1.5. Foamability and foam stability

Foams are usually characterized by *foamability* and *foam stability*. The foamability or foam generation capacity of a surfactant solution determines its ability to form foam. As mentioned in Section 1.2.1, foams are thermodynamically unstable or metastable, and they collapse or break down eventually [10, 40]. As a result, the study of foam stability has kindled the interest of researchers and product manufacturers. As mentioned in Section 1.2.1, surfactant is the main stabilizing ingredient for the foams. The commercial foams are often stabilized employing surfactants with the help of additives such as inorganic salt, protein etc. [41, 42]. The foam generation mechanism substantially impacts foamability and stability, and these two parameters frequently define the surfactant's effectiveness. Foam formation is influenced by

surfactant concentration, type of the medium (which is water in most of the cases), and the gas. The foam can be brittle, short-lived, and dissipate quickly. The capacity of the surfactant solution to generate a robust, flexible, and cohesive film that can minimize gas permeability and prevent bubble coalescence, is critical to foam stability. Film elasticity, the Marangoni effect, gas diffusion through the lamellae, interfacial rheology, and intermolecular and surface forces play an essential role in foam stabilization.

The mechanism of foaming and its stability in the aqueous surfactant solutions have been reported by a number of researchers [37, 43-46]. Behera et al. [47] studied foaming in micellar solutions in the presence of a surfactant, salt, and oil. They found that the foam stability decreased in the presence of oil. Yekeen et al. [48] found that the inhibition of bubble coalescence and foam stability decreased in the presence of salt. Simjoo et al. [43] found that the foam stability was influenced by the chain length of an alkane dissolved in the medium. The small-chain alkanes were more effective in destabilizing the foam. Osei-Bonsu et al. [49] found that the stability of foam decreased in the presence of oil. Their findings suggest that the foam stability in the presence of oil largely depends on the properties of the latter. Vikingstad et al. [50] found that the larger alkanes stabilized the foam, while the alkanes with lower molecular weight destabilized the foam.

1.5.1. Marangoni effect

Transport of surfactant molecules takes place as the foam film drains from its center towards the Plateau border under dynamic conditions. The surfactant molecules are transported towards the periphery of the film. The Marangoni effect is caused by a surfactant concentration gradient across the foam film. As the surfactant molecules diffuse back from the film periphery towards its center, a flow originates from an area of high surfactant concentration to a region of low

surfactant concentration [51, 52]. Because it works on both expanding and contracting foam films, the Marangoni effect plays a vital role in stabilizing the thick foam films. The Marangoni effect is weak at the low surfactant concentrations. This is due to a low surface tension gradient, a slow diffusion of the surfactant molecules at the air–water interface, and less diffusion of the surfactant molecules from the core of the film to the Plateau borders. As a result, at the low surfactant concentrations, the Marangoni effect has little effect on film drainage. However, at the high surfactant concentrations, the density of surfactant molecules at the interface is high, resulting in molecular migration from the surfactant-rich area of the film to the surfactant-lean region. This creates a significant surface tension differential at the air–water interface, attracting surfactant molecules and liquid into the film. As a result, the foam film is stabilized by a strong Marangoni effect. Therefore, the risk of film rupture is reduced.

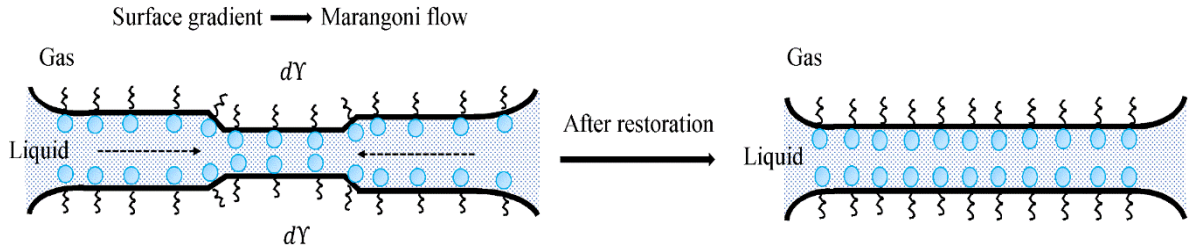

Figure 1.7 Schematic representation of Marangoni flow at the air–water interface caused by the surface surfactant gradient.

1.5.2. Film elasticity

Elasticity is defined as the ratio of stress to strain. It is a measure of a material's proclivity to return to its original state after being deformed. It refers to the "self-healing" ability of the foam film to recover from any external disruption. The elasticity of foams is determined by the relationship between surface tension and film surface area. The Gibbs elasticity $\left(E_G\right)$ is defined as

$$E_G = 2A\left(\frac{d\gamma}{dA}\right) \tag{1.3}$$

where $d\gamma$ is the change in the surface tension and dA is the change in the film surface area. The Gibbs elasticity describes the increase in the surface tension of the film induced by a drop in surfactant concentration inside the interlamellar solution due to the film's limited extension relative to its size [53]. The surfactant redistribution between the bulk of the film and its two surfaces, which occurs after stretching, affects the elasticity of the foam film. The Gibbs elasticity is frequently used to explain the stability of static foams, but the elasticity owing to the Marangoni effect is more appropriate for the dynamic foams [54]. A dynamic surface tensiometer capable of monitoring changes in surface area can be used to determine the Marangoni elasticity.

1.5.3. Intermolecular and surface forces

The stability of thin foam films is influenced by intermolecular and surface forces. As a result, understanding the relationship between these forces and the stability of the foam is crucial. Interfacial forces act between the two air–water interfaces when the foam film gets thin. The forces present in the thin foam films have been interpreted by using the DLVO and non-DLVO theories. Derjaguin introduced the concept of disjoining pressure to explain the forces between the two surfaces of a thin foam film [55, 56]. The difference between the pressure in the thin liquid film normal to the plane-parallel film surfaces and the intrinsic pressure in the bulk phase of thickness h is the disjoining pressure (Π). The disjoining pressure in the thin liquid film of thickness h is equal to the difference between the pressure in the film normal to the plane-parallel film surfaces (P_N) and the intrinsic pressure in the bulk phase (P_B) [57], i.e.,

$$\Pi(h) = P_N - P_B \tag{1.4}$$

For a thin liquid film, the thermodynamic definition of disjoining pressure is given in terms of the change in the Gibbs free energy (G) with the film thickness (h), i.e.,

$$\Pi(h) = -\left(\frac{dG}{dh}\right)_{T,P,A,N_i} \tag{1.5}$$

where T, P, A, and N_i represent temperature, overall pressure, cross-sectional area of the film, and the number of moles of the substances, respectively.

The disjoining pressures due to the electrostatic double layer (EDL) and van der Waals (vdW) forces form the basis of the DLVO theory [58-62]. The electrostatic interaction develops when the surfaces become electrically charged as a result of adsorption of ionic surfactant. The disjoining pressure $\left(\Pi_{\mathrm{EDL}}\right)$ is caused by the overlap of the diffuse double layers on the two film surfaces at a small separation. The confinement of the counterions of the double layers in a narrow region is primarily responsible for this repulsive force. The foam films are stabilized as a result of this repulsion. According to the Debye–Hückel theory, the thickness of the diffuse ionic atmosphere $\left(\kappa^{-1}\right)$ is given by [63]

$$\kappa^{-1} = \left(\frac{\varepsilon\varepsilon_0 k_B T}{e^2 N_A \sum z_i^2 c_i}\right)^{1/2} \tag{1.6}$$

where κ^{-1} is termed as *Debye length*, ε is the dielectric constant of the medium, ε_0 is the permittivity of free space, k_B is the Boltzmann constant, T is the temperature, e is the elementary charge, N_A is the Avogadro's number, and z is the valence of the electrolyte. This repulsion is screened by the presence of salt (e.g., NaCl). According to Equation (1.6), the Debye length reduces as the electrolyte concentration rises, indicating that the interaction happens over a smaller range due to the ionic screening. The *ionic strength* (I) of the medium

is defined as

$$I = \frac{1}{2}\sum z_i^2 c_i \tag{1.7}$$

When the ionic strength of the aqueous solution is increased, the Debye length decreases. In a thin flat foam film, the disjoining pressure due to EDL is given by [64]

$$\Pi_{\mathrm{EDL}} = 64RTc\tanh^2\left(\frac{ze\psi_0}{4k_BT}\right)\exp\left(-\kappa h\right) \tag{1.8}$$

where ψ_0 is to the potential at the surface. Π_{EDL} is positive because the equally charged film surfaces repel each other (i.e., disjoins the two surfaces).

The van der Waals interaction is the other vital force in the thin foam film. The electromagnetic fields between two dipoles cause the attractive van der Waals disjoining pressure $\left(\Pi_{\mathrm{vdW}}\right)$. It is relatively unaffected by the changes in the electrolyte concentration and pH. Its magnitude can be greater than the EDL repulsion at a very low film thickness. Like the Π_{EDL}, Π_{vdW} also depends on the separation between the surfaces. The disjoining pressure for two flat surfaces is given by [65, 66]

$$\Pi_{\mathrm{vdW}} = -\frac{A_H}{6\pi h^3} \tag{1.9}$$

where A_H represents the Hamaker constant and h is the film thickness. For the air–water–air system (i.e., aqueous foam films), the value of A_H is about 3.7×10^{-20} J [67]. The foam films are destabilized due to the attractive van der Waals attraction. They ultimately rupture due to this force. The EDL repulsive force generated by the surfactant molecules must overcome the attractive van der Waals force in order to stabilize the foam film.

The DLVO theory hypothesizes that the net disjoining pressure in the foam film can be approximated by a superposition of the electrostatic double layer and the van der Waals forces as

$$\Pi(h) = \Pi_{EDL} + \Pi_{vdW} \tag{1.10}$$

According to this theory, the repulsive EDL force creates an energy barrier that prevents the thin film from rupturing. The van der Waals attractive force would cause the film to rupture if this energy barrier is overcome. The film would be stable and prevent the foam from collapsing if the EDL repulsion is dominant. At a very small separation between the surfaces, the van der Waals force is dominant, whereas the EDL force is dominant at wider separations. The DLVO theory assumes that the solvent may be viewed as a continuous medium characterized by a dielectric constant, the ions can be treated as point charges, and the EDL and van der Waals forces are independent and additive.

A thick non-equilibrium coating of liquid film forms during the early phases of foam production. Various forces work in this film, such as capillary pressure, gravity, and surface forces, causing it to thin over time [68-70]. Over time, during which the film thins, a foam film of uniform thickness is generated, which is determined by the thermodynamic equilibrium of the foam system. If the thinning process is continued, a very thin film may form, which appears black in the reflected light. These films are called “black films.” The black films are divided into two categories, i.e., common black film (CBF) and the Newton black film (NBF). The stability of the CBF is controlled by the repulsive EDL force, which is consistent with the standard DLVO theory. The thickness of the CBF is usually between 20 and 30 nm. The EDL repulsion is diminished at the high electrolyte concentrations, and a very thin NBF is formed, which has a thickness of less than 10 nm. The salt concentration determines the thickness of the film. It also depends on the interaction of short-range (i.e., van der Waals) forces between the adsorbed surfactant layers. The efficiency of the overall foam system is determined by the formation and stability of these thin foam films.

Non-DLVO forces (such as steric, hydration, and hydrophobic forces) may also act in the foam films in addition to the DLVO forces [71, 72]. The DLVO theory occasionally fails

to characterize interactions at short distances (such as a few nanometers) when the non-DLVO forces are present. These forces can be attractive and repulsive, and can be more potent than the DLVO forces. In some cases, the disjoining pressure due to the short range force (i.e., Π_{sr}) is included as the third term in Equation (1.10) [39].

1.5.4. Foam decay

Many phenomena, operating at the microscopic level within the foam film, control foam generation and evolution. All these factors work together to determine the stability of the foam. They have their own length and time scales based on the liquid fraction and bubble size. Foam begins to decompose almost immediately after its formation. Foam degradation can be slow or rapid, depending on various factors such as structural changes in the bubbles (i.e., from spherical to polyhedral). Foam degradation is caused by a complex interaction of events resulting in the thinning of the foam film due to drainage, coalescence, and coarsening. Evaporation, temperature gradients, and humidity are the other elements that contribute to deterioration of the foam.

1.5.5. Foam drainage

The collapse of the foam is mostly due to the liquid drainage from the foam film, capillary suction, and ultimately, the instability in the thin foam film [73, 74]. Drainage plays an essential part in the stability of the overall foam system. There is a constant interplay between drainage and foam film collapse [75]. Gravity and capillary forces cause an irreversible flow of aqueous solution across the foam network through the lamellae and Plateau borders, resulting in foam drainage. The drainage is influenced by the Marangoni effect and hydrostatic forces. The Marangoni effect is crucial in a premicellar aqueous surfactant solution. On the other hand, the

interaction between the adsorbed surfactant layer and the micelles governs the stability of the foam at surfactant concentrations above the CMC. The foam films generated from the micellar surfactant solutions show stratification or step-wise thinning. It entails destroying the micellar structures within the film layer by layer. Stratification is affected by many parameters, including film area, temperature, the concentration of added electrolyte, surfactant concentration, and the concentration of the micelles present in the solution and the interaction between them [76]. Drainage may also cause the surfactant molecules in the foam film to be distributed in a non-uniform manner [77]. Drainage causes the spherical foam to mature into a polyhedral foam. Shock, vibration, and temperature gradient are more likely to cause the films in the polyhedral foam to rupture. Drainage starts shortly after the foam production in the low-stability foams, causing a substantial surface tension differential at the surfaces of the foam films. Because this gradient slows the drainage, the rate of foam degradation is significantly reduced.

Several researchers have studied liquid drainage in foams [53, 78-83]. Weaire and Phelan [84] have demonstrated the estimation of the liquid fraction of the foam by analyzing its conductivity. They developed models to describe the swelling of the Plateau borders. Their findings reveal that channel-dominated drainage was the primary mechanism of drainage, particularly at the dry foam limit. This was a step forward from Lemlich's work [85], which demonstrated that the volume fraction of the foam phase was 3-times the relative conductivity of the foam, which had a low liquid content (3%).

1.5.6. Coalescence of foam bubbles

The bubble coalescence time is often considered as an indication of the stability of foam. Coalescence occurs when the thin liquid film that separates the adjacent foam cells (or bubbles)

ruptures, causing them to merge (see Figure 1.7). It causes a decrease in the number of bubbles in the foam and the mean bubble volume increases. Coalescence begins with the stretching and dilatation of the film, followed by its rupture. The *critical liquid fraction* is an essential factor in coalescence. The initial liquid fraction in the freshly generated foam is nearly constant throughout the system. The reduction in liquid fraction after drainage is substantially slower for the smaller foam bubbles. This could be due to the slower velocity of the liquid at the Plateau border or nodes in the foam. This explains the fact that foams with small bubbles are more stable. On the other hand, the large bubbles show the opposite phenomena, with a fast drop in the liquid percentage corresponding to the commencement of the rupture point. Avalanches occur from the coalescence of large bubbles, whereas the height of foam containing small bubbles remains essentially constant. Coalescence is intensified below a critical liquid fraction, which varies depending on the nature of the surfactant and its concentration. The non-uniformity in the size and shape of the films that comprise the faces of the polyhedral bubbles may cause a faster rate of bubble coalescence. As a result, the film-drainage rate and the film thickness within any volume element of the foam become non-uniform. Several researchers have studied the coalescence of foam bubbles [73, 86-96].

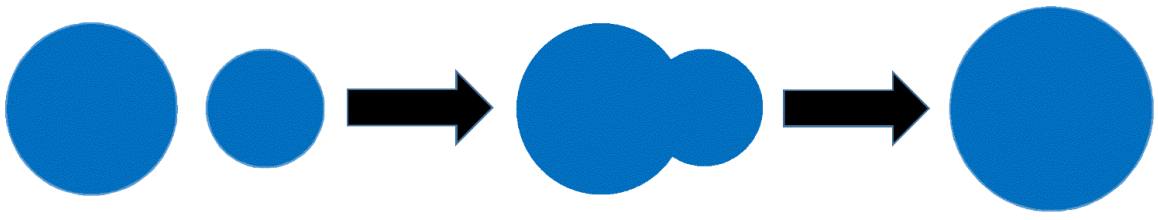

Figure 1.8 Coalescence of bubbles.

1.6. Foam fractionation

Foam fractionation is a physiochemical procedure that involves extraction of surface active molecules from a growing foam and separating them from the solution. It is one of the

promising strategies for separating surfactants from wastewater [4, 7, 97-101]. It is a well-explored topic applied to various industries, including biological protein and metabolite purification, mineral processing, and agriculture [102-105]. Some of the non-surface active materials can also be removed by interaction with the surfactant and carried along into the foam. The surfactant in this circumstance is termed as *collector*. Foam fractionation is also used for the separation of one or more species from a complex mixture based on their surface activity. The following are the main steps involved in foam fractionation: (i) the surface active substance present in the bulk solution preferentially adsorbs on the air–water interface (i.e., the surface of the foam bubbles) based on its surface activity, (ii) the bubbles rise through the solution and form a foam phase in which a very small amount of liquid is trapped in the foam lamellae, and (iii) gravity causes this liquid to drain downwards towards the bulk liquid phase, thereby drying the foam phase. Consequently, factors such as the physiochemical properties of the surface active substance (i.e., surfactant), foam properties, and the operating variables (e.g., airflow rate, surfactant concentration, and temperature) govern the efficiency of foam fractionation.

In the foam fractionation process, the air bubbles carry the surfactant molecules along the column to its top. Consequently, the foam phase gets richer in the surfactant and the bulk liquid phase is depleted. This develops a concentration gradient in the foam column [106]. The maximum transfer in the column occurs when the concentration of the surfactant solution flowing upward is at its lowest at the bottom and highest possible at the top of the column. A well-known equipment employing the foam fractionation is “protein skimmer”, which removes the organic waste from the aquariums, and proteins from the wastewater stream in the food industries [2]. Foam is a good medium for adsorptive separation because of its high specific surface area on which the surfactant molecules adsorb. Also, the amount of interstitial fluid is low, especially if the foam is dry. As opposed to the interstitial liquid, the surface influences

the separation process inasmuch as the surfactant molecules tend to move from the interstitial liquid to the surface.

The film enveloping the rising air bubbles becomes stable when the surface tension is low enough. Drainage of the liquid in the lamellae, coarsening, gas transfer from the smaller bubbles to the bigger ones, and coalescence of the bubbles are the main phenomena that influence foam creation and stability. The instability of the liquid films induces the bubbles within the foam to coalesce [107]. Due to the film rupture, coalescence releases more water and the adsorbed material, which drain downward through the foam matrix due to gravity. Due to the gravity and bubble coalescence, the amount of interstitial liquid entrained in the foam may decrease as the foam rises, depending on the stability of the foam.

Interest in foam fractionation has grown in the recent years, leading to a better knowledge of the process and novel uses for what may appear to be a well-established technique [108]. Foam fractionation, in particular, has been utilized to augment existing wastewater treatment plants because of its capacity to remove refractory chemicals that are difficult to treat by modern municipal treatment systems [109]. Low capital cost, low energy requirement, environment friendliness, and low operational expenses are some of the inherent advantages of foam fractionation as a water treatment technique [110, 111]. Burghoff [97] has offered a more recent and comprehensive study, focusing mostly on biotechnological applications such as phytonutrient, metabolites, and protein enrichment. Jenkins [112] studied the applicability of foam fractionation as a method for integration with the industrial wastewater treatment plants, so that the surface active chemicals do not cause any issue in the microbial degradation process. A few scientists have studied the applications of foam fractionation focusing on the removal of pollutants from a waste stream as well as concentrating them in the foam phase [107, 113, 114]. Somasundaran [114] presented a detailed list of compounds that can be removed via foam fractionation, foam flotation,

precipitate flotation, or froth flotation. Boonyasuwat et al. [99] have found that a number of variables such as decreasing airflow rate, increasing foam height, and increasing the number of stages in a multi-stage foam fractionator could completely remove the surfactant from water. Tharapiwattananon et al. [115] investigated the effects of airflow rate, foam height, liquid height, surfactant concentration in the liquid feed, and sparger porosity on the recovery of surfactant. They found that the increasing airflow resulted in a decrease in the enrichment ratio and an increase in the rate of surfactant recovery. Kumpabooth et al. [116] studied the effects of temperature and added salt on foam flow rate, enrichment ratio, foam wetness, and the rate of surfactant recovery. They found that an increase in temperature generally had a positive impact on foam fractionation as a more concentrated foam liquid was recovered as the overhead.

Rubin and Jorne [117] found that the foam fractionation technique may be applied to separate two surfactants by using their relative distribution coefficient. They found that the calculations based on the Langmuir isotherm may be used for a conservative estimation of the relative distribution coefficient at very low surfactant concentrations. Šonc and Grilc [98] developed a mathematical model to describe the changes in the concentration of the surfactant, and tested optimal conditions of many processes and material parameters on an actual industrial sample. The optimal parameters for the surfactant solutions were applied to model the purification of actual wastewater samples containing surfactants from various industrial cleaning operations. Qu et al. [118] investigated the recovery of surfactants and metal ions in the permeate of micellar-enhanced ultrafiltration (MEUF) process. They found that the changes in the airflow rate had a substantial effect on the enrichment ratio and removal of SDS and Cd^{2+}. Srinet et al. [106] observed that the foam volume increased with increasing the airflow rate. They observed that the feeds with a lower initial surfactant concentration showed a higher separation efficiency and surfactant recovery. They studied the effect of salt and observed that

the surfactant recovery and separation efficiency reduced in the presence of salt. Tadakamalla and Marathe [119] optimized important parameters such as the airflow rate, foam height, influent concentration, variation of the pH of the feed solution, and duration of operation for a cationic surfactant, cetyl pyridinium chloride. They found that the effectiveness of the foam fractionation process in recovering a single surfactant was better than that of a mixture of cationic and nonionic surfactants.

1.6.1. Adsorption of surface active species at air–water interface

Foam fractionation is effective when the compound to be removed from water adsorbs at the gas–liquid interface. The adsorption of such a molecule to the surface results in a reduction in surface tension. The interfacial Gibbs free energy of the system decreases, and it is this potential for energy reduction that causes adsorption. Eventually, a surface concentration is attained at which any further adsorption will not reduce the Gibbs free energy further, and the system will reach its equilibrium. The equilibrium relationship between the bulk concentration of the surfactant and its surface excess concentration at a particular temperature is known as the *adsorption isotherm*. Although the surface concentration is difficult to measure, it can be conveniently estimated indirectly by measuring the equilibrium surface tension (γ) at different concentrations of the surfactant (c), by using the Gibbs adsorption isotherm, which states that

$$\Gamma_G = -\frac{1}{\nu RT}\left(\frac{d\gamma}{d\ln c}\right) \tag{1.11}$$

In Equation (1.11) it has been assumed that the activity coefficient is unity, which us true at the low surfactant concentrations. According to the Langmuir adsorption isotherm, the surface excess concentration (Γ_L) is related to the concentration of the surfactant in the bulk solution as

$$\Gamma_L = \Gamma_\infty \left(\frac{K_L c}{1 + K_L c} \right) \tag{1.12}$$

where Γ_∞ is the adsorption capacity. Its value depends on the minimum surface area occupied by an adsorbed surfactant molecule. The equilibrium constant, K_L, is the ratio of the constants for adsorption and desorption. The Langmuir model assumes that both the solution and the interface are ideal. However, for the ionic surfactants, there is a significant electrostatic interaction between the molecules adsorbed at the air–water interface. Therefore, the Langmuir model is expected to be valid at concentrations below the CMC. For dilute surfactant solutions, the surface excess concentration may be approximated by the adsorbed surface concentration, i.e., $\Gamma_G \approx \Gamma_L$. Therefore, from equations (1.11) and (1.12), we can write

$$d\gamma = -\nu RT\Gamma_\infty \left(\frac{K_L c}{1 + K_L c} \right) d\ln c \tag{1.13}$$

If the surface tension of pure water is represented by γ_0, integration of Equation (1.13) gives,

$$\gamma = \gamma_0 - 2RT\Gamma_\infty \ln\left(1 + K_L c\right) \tag{1.14}$$

Equation (1.14) is known as the *Langmuir–Szyszkowski equation* [90], which is the simplest surface EOS that correlates surface tension with the concentration of the surfactant in the bulk solution. This equation has two unknown parameters, viz., Γ_∞ and K_L, which can be obtained by fitting the EOS to the experimental surface tension profile.

Adsorption of surfactants is a very important phenomenon in foam fractionation [120-124]. Kamalanathan and Martin [125] have investigated the adsorption and transport of Triton X 100/BSA mixtures in a foam fractionation column. They found that Triton X-100 dominated the surface adsorption by diffusing to the surface and adsorbing there in a faster and more prominent manner than BSA. Eastoe et al. [126] used neutron reflection and surface tension

methods to access the equilibrium adsorption isotherm of various ionic surfactants at the air–water interface. Chang and Franses [127] have reviewed equilibrium and dynamic aspects of surface tension and adsorption, primarily of single micellar or premicellar surfactants at the air–water interface. They have discussed the dynamic adsorption models with the diffusion-controlled and mixed-kinetic mechanisms. The adsorption of most of the surfactants was slower than that predicted by the diffusion-controlled models [128].

Several studies have been made on the effect of various electrolytes, oils, and alcohols on the adsorption of surfactants at the fluid–fluid interfaces. Additives present in the aqueous phase may improve the viscosity of the foam and affect the charge of the air–water interface [129, 130]. Kumar and Ghosh [92] have studied the adsorption of cationic and anionic surfactants at the air–water interface in the presence of a monovalent inorganic salt (NaCl). It was found that the adsorption was strongly amplified by the presence of salt at the low surfactant concentration. They observed significant effects of salt on surface tension and coalescence of air bubbles. Ruckenstein and Bhakta [131] presented an improved model for foams involving ionic surfactants, which accounted for the effect of surfactant and salt concentrations. They also analyzed the effect of these parameters on the drainage and collapse of foams involving the ionic surfactants. Dutkiewicz and Jakubowska [132] analyzed the effect of electrolytes on the physicochemical behavior of the SDS micelles. They observed that the value of the CMC of SDS decreased in the presence of electrolytes.

1.6.2. Modes of operation

Foam fractionation is a versatile process that can be performed in batch, semi-batch, and continuous modes [107]. There are some other advanced modes of operation incorporating enrichment and stripping. The operating modes usually follow single or multi-stage processes. There are various pros and cons associated with these methods. For instance, a multi-stage

foam fractionator has been preferred over a single-stage due to the high removal efficiency of the former [99]. Figure 1.8 shows the simplest modes of the batch and continuous operations.

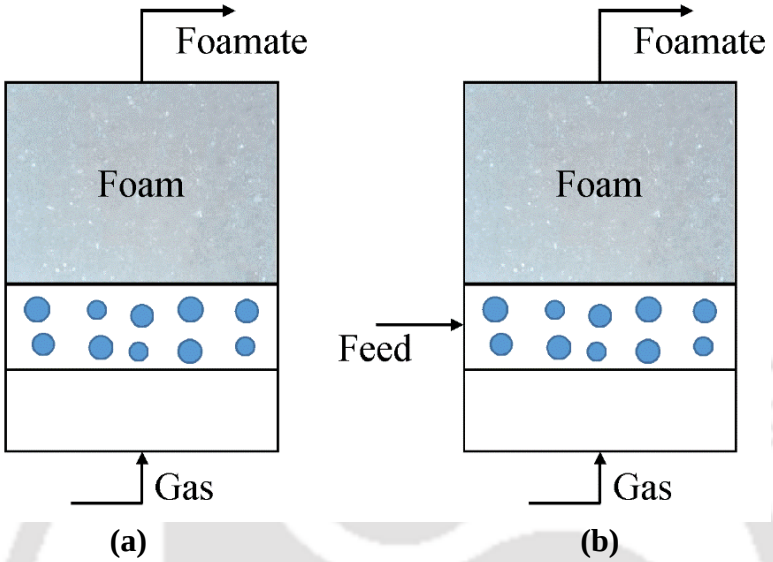

Figure 1.9 Simplest modes of operation: (a) batch and (b) continuous.

In the batch process, the foam fractionation column contains the aqueous surfactant solution and air is sparged into it from the bottom. This process is continued until the amount of foam generated is very low (i.e., the aqueous solution inside the column is significantly depleted of the surfactant and it no longer has a sufficient foaming capacity).

The liquid in the column is constantly refilled by a fresh feed in the continuous operation, resulting in a steady state foam generation, foam harvesting, and liquid concentration. The position of the polluted water, which flows into the column, determines the different modes of operation. The stripping mode of operation occurs when the feed stream is placed above the foam–water interface in the column. On the other hand, the enrichment mode occurs when the feeding point is below the foam–water contact. A constant liquid–foam interface, which allows the system to operate under steady state, is one of the essential requirements for consistent functioning as a continuous process.

1.6.3. Batch operation

The most straightforward method of performing foam fractionation is to charge the surfactant solution into a column and then sparge gas bubbles into it from the bottom so that a foam is formed above the liquid layer. The liquid drains from the foam to make it dry. The foam is drier at the top of the column. The usual assumption made is that the interstitial liquid within the foam has the same concentration of the adsorbing species as that within the liquid layer. This is approximately valid because the action of molecular diffusion will tend to equilibrate the liquid concentration throughout the system. Further, it is assumed that for every cycle of operation, the recovery is low, so the depletion of the liquid layer is insignificant, and the concentration stays approximately constant throughout the process, i.e., C_0. By assuming equilibrium between the concentration of the interstitial liquid and the surface excess concentration via an adsorption isotherm, we can write that

$$\Gamma = f(C_0) \tag{1.15}$$

and this surface excess is constant through the foam. The reason for this assumption is that any concentration gradient in the interstitial liquid within the foam phase tends to be eradicated by molecular diffusion. Thus, the amount of adsorbed species with the foam layer per unit cross-sectional area of the column is $\int_0^H S\Gamma dx$. The volume of liquid within the foam per unit cross-sectional area of the column can be expressed as $Q_P = \int_0^H \varepsilon(x)dx$, where $\varepsilon(x)$ is the distance from the liquid–foam interface. So, the amount of target species dissolved in the interstitial liquid per unit cross-sectional area of the column is $C_0 \int_0^H \varepsilon(x)dx$. Thus, the concentration of the

foamate product is obtained by summing the amount of target species in both the interstitial liquid and that adsorbed at the gas–liquid interfaces, and dividing by the product volume, Q_P [4], i.e.,

$$C_P = C_0 + \frac{\Gamma \int_0^H \frac{3[1-\varepsilon(x)]dx}{r_{32}(x)}}{Q_P} \tag{1.16}$$

The expressions for enrichment and recovery are complicated by the fact that the bubble size and liquid fraction are allowed to vary as a function of the height up the column, *x*. A higher enrichment is obtained if the period for free drainage is increased.

Equation (1.16) shows that the enrichment is strongly affected by the liquid hold-up, which will decrease up a riser as the liquid drains down due to gravity. Therefore, it is seen that the enrichment in foam fractionation is affected by the drying of foam in a riser due to the drainage as well as by surfactant adsorption on the bubble surfaces.

1.6.4. Process performance indicators

The terms *enrichment* (*E*) and *recovery* (*X*) of the target component in the top stream are frequently used to describe the performance of a foam fractionation system [4, 99, 133]. The enrichment of a species is defined as the ratio of the concentration of the target species in the foamate product (C_P) and in the feed (C_0), i.e.,

$$E = \frac{C_P}{C_0} \tag{1.17}$$

In a semi-batch process (i.e., batch with respect to the liquid phase), the concentration of the foamate product decreases over time as the liquid pool becomes depleted in the target species. The enrichment is defined as the average value taken over the whole process (i.e., the quotient

of the final concentration of the foamate collected and the feed concentration). In a system with more than one adsorbing species, the enrichment must be defined with respect to a particular species. In the foregoing discussion, it is assumed that there is only one adsorbing species.

The recovery is defined as the ratio of the amount of target species citing to the foamate product to the amount present in the feed. It can be expressed as follows:

$$X = \frac{C_P Q_P}{C_0 Q_0} \tag{1.18}$$

where, Q_0 is the volume of the liquid delivered as feed and Q_P is the volume of the recovered foamate product. Again, if there are multiple adsorbing species, the recovery with respect to a particular species must be defined. In general, there exists a trade-off between high recovery and high enrichment. A product stream that is highly concentrated in the target species is often obtained at the expense of low recovery, and vice versa.

Separation efficiency (ϕ) of the batch process helps us in ascertaining how much surfactant can be recovered in the targeted interval of time. It is determined by using the following equation:

$$\phi = \frac{C_0 - C_e}{C_0} \tag{1.19}$$

1.7. Objectives of the work

The main objective of this work was to study the removal and recovery of surfactants by foam fractionation in the presence of inorganic salts, oily effluents, and alcohols in the batch mode. The objectives of this research are as follows:

1. Removal and recovery of a cationic surfactant from its aqueous solution

2. Removal and recovery of an anionic surfactant from aqueous solution in the presence of benzene, toluene, and hexane
3. Removal and recovery of an anionic surfactant from its aqueous solution in the presence of alcohols
4. Investigate the effects of process variables such as airflow rate, surfactant feed concentration, salt concentration, oil, alcohols, operation time, and water recovery on the separation of the surfactant

Outline of the thesis

Each chapter of this thesis deals with a specific topic, which is important in foam fractionation. The literature relevant to the topic is reviewed separately in the corresponding chapter. The structure of this thesis is described below.

Chapter 1 **(Introduction):** This chapter presents the general overview of the foam fractionation process, emphasizing the importance of the stability of foam. The fundamentals of the colloidal and interfacial phenomena involved in the process are discussed in detail. The research problem is identified, and the objectives of this thesis are given.

Chapter 2 **(Materials and experimental methods)**: This chapter lists the materials used in the experimental studies and their sources. A detailed information on sample preparation, equipment used, and the experimental procedure for foam fractionation in the batch mode is provided.

The detailed procedure of the measurement of surfactant concentration by two-phase titration has been given. The equipment used in this work includes a tensiometer, zeta potentiometer, HPLC, and UV-Vis spectrophotometer.

Chapter 3 **(Removal and recovery of a cationic surfactant from its aqueous solution by foam fractionation)**: This chapter focuses on the removal and recovery of a cationic surfactant [i.e., cetyltrimethylammonium bromide (CTAB)] from the aqueous medium by using foam fractionation. The surfactant concentration was five times its CMC. The effects of different salts (i.e., NaCl, $CaCl_2$, and Na_2SO_4) and airflow rate on the recovery of surfactant have been reported. The surface tension of the surfactant solution was measured by a tensiometer, and the electric charge at the air–water interface was determined by the zeta potential measurements. The stability of foam was correlated with these two parameters.

The results indicate that nearly 60% of the surfactant was recovered from the top of the column in the form of a semi-solid paste. The addition of salt reduced the foam volume and surfactant recovery. Since the surfactant concentration was far above its CMC, the addition of salt did not have much effect on the surface tension. The stability of the foam played a significant role in surfactant recovery. The zeta potential decreased with increasing salt concentration. The zeta potential was highest in the presence of NaCl, and lowest for Na_2SO_4. The recovery of water was excellent.

Chapter 4 **(Removal and recovery of an anionic surfactant from aqueous solution in the presence of benzene, toluene, and hexane by foam fractionation)**: This chapter focuses on the removal and recovery of an anionic surfactant (i.e., SDS) from water by foam fractionation in the batch mode in the presence of oily effluents such as benzene, toluene, and hexane.

The SDS concentration was above its CMC. The SDS concentration in the samples collected from the column was measured by two-phase titration. The airflow rate was varied in the range of 0.4–1.6 $dm^3\ min^{-1}$. The adsorption of the surfactant at the air–water interface was measured by surface tension. About 72% of the SDS was recovered in the form of a semi-solid cake. Nearly 97.5% of water was recovered in this process. The removal and recovery of SDS

increased with increasing airflow rate. Foam stability had a serious impact on the recovery of SDS. The oils had an antifoaming effect, which reduced the foam volume. The foam stability was higher in the absence of the oils. The foam stability was analyzed by the measurement of zeta potential, and the entering, spreading, and bridging coefficients.

Chapter 5 **(Removal and recovery of an anionic surfactant from its aqueous solution in the presence of alcohols by foam fractionation)**: This chapter mainly focuses on the removal and recovery of an anionic surfactant [i.e., sodium dodecylbenzene sulfonate (SDBS)] in the presence of two short-chain alcohols, i.e., methanol and ethanol.

The experiment was performed below and above the CMC of the SDBS. The concentration of SDBS was 500, 1000, 2000, and 3000 mg dm^{-3}. The airflow rate was varied in the range 0.4 – 1.6 dm^3 min^{-1}. About 77% of the surfactant was recovered from the top of the column in the form of a semi-solid cake. The addition of alcohol lowered the foam volume and surfactant recovery. The enrichment ratio decreased with increasing airflow rate. The zeta potential at the air–water interface was measured to determine the stability of the foam, which was highly significant in surfactant recovery. The surface tension measurements revealed that the addition of alcohol lowered the surface tension of the surfactant solutions. About 95% water was recovered in the process.

Chapter 6 **(Summary and scope for future work):** This chapter summarizes the work and provides new directions for future research.

Nomenclature

Symbols

A	surface area of foam lamella, m^2
A_H	Hamaker constant, J
C	bulk concentration of salt, mol m^{-3}
C_e	concentration of the surfactant in the effluent stream, mg dm^{-3}
C_P	concentration of the surfactant in the foamate product, mg dm^{-3}
C_0	concentration of the surfactant in the original feed solution, mg dm^{-3}
e	electronic charge, C
E	enrichment
E_G	Gibbs film elasticity, N m^{-1}
G	Gibbs free energy, J
h	thickness of foam film, m
H	height of the foam layer, m
I	ionic strength, mol kg^{-1}
k_B	Boltzmann's constant, J K^{-1}
K_L	equilibrium constant in the Langmuir isotherm, m^3 mol^{-1}
N_A	Avogadro's number, mol^{-1}
N_i	number of moles of the substances, mol
ΔP	excess pressure inside the spherical bubbles, Pa
P_N	pressure in the film normal to the plane-parallel film surfaces, Pa

P_B	intrinsic pressure in the bulk phase, Pa
Q_0	volumetric flow rate of the bulk solution, $dm^3\ min^{-1}$
Q_P	volumetric flow rate of the foamate, $dm^3\ min^{-1}$
r	radius of the bubble, m
R	gas constant, $J\ mol^{-1}\ K^{-1}$
r_{32}	Sauter mean bubble radius, m
T	temperature, K
V_g	gas volume, dm^3
V_l	liquid volume, dm^3
X	recovery
z	valence of ion

Greek letters

γ	surface tension, $N\ m^{-1}$
Φ	foam quality, %
γ_0	surface tension of pure water, $N\ m^{-1}$
Γ	surface excess concentration of surfactant, $mol\ m^{-2}$
Γ_G	surface excess concentration calculated by Gibbs adsorption isotherm, $mol\ m^{-2}$
Γ_L	surface excess concentration calculated by Langmuir adsorption isotherm, $mol\ m^{-2}$
Γ_∞	adsorption capacity, $mol\ m^{-2}$
ε	dielectric constant of the medium

ε_0	permittivity of free space, $C^2\ J^{-1}\ m^{-1}$
κ	Debye–Hückel parameter, m^{-1}
λ	interfacial dilatational viscosity, Pa s m
ν	constant (ν = 1 for a non-ionic surfactant and ν = 2 for a 1:1 ionic surfactant)
$\Pi(h)$	disjoining pressure in the thin liquid film, Pa
Π_{vdW}	disjoining pressure due to the van der Waals force, Pa
Π_{EDL}	disjoining pressure due to electrostatic double layer force, Pa
Π_{SR}	disjoining pressure due to the short-range repulsive forces (e.g., the hydration force), Pa
ϕ	separation efficiency, %
ψ_0	potential at the surface (or interface), V

Abbreviations

BAC	benzalkonium chloride
BZT	benzethonium chloride
CBF	common black film
CMC	critical micelle concentration
CPC	cetylpyridinium chloride
CTAB	cetyltrimethylammonium bromide
DLVO	Derjaguin–Landau–Verwey–Overbeek
EDL	electrostatic double layer
HPLC	high-performance liquid chromatography
NBF	Newton black film

SDBS	sodium dodecylbenzenesulfonate
SDS	sodium dodecyl sulfate
SLES	sodium lauryl ether sulfate
TX-100	Triton X-100

References

[1] A.M. Becker, S. Gerstmann, H. Frank, Perfluorooctane surfactants in waste waters, the major source of river pollution, Chemosphere 72 (2008) 115–121.

[2] E. Önder, A.S. Koparal, Ü.B. Öğütveren, An alternative method for the removal of surfactants from water: electrochemical coagulation, Sep. Purif. Technol. 52 (2007) 527–532.

[3] P. Wungrattanasopon, J.F. Scamehorn, S. Chavedej, C. Saiwan, J.H. Harwell, Use of foam flotation to remove tert-butylphenol from water, Sep. Sci. Technol. 31 (1996) 1523–1540.

[4] P. Stevenson, X. Li, Foam fractionation: principles and process design, CRC Press, Boca Raton, 2014.

[5] P.D. Abel, Toxicity of synthetic detergents to fish and aquatic invertebrates, J. Fish Biol. 6 (1974) 279–298.

[6] D. Bajpai, V.K. Tyagi, Laundry detergents: an overview, J. Oleo Sci. 56 (2007) 327–340.

[7] S. Chen, M.B. Timmons, J.J. Bisogni, D.J. Aneshansley, Modeling surfactant removal in foam fractionation: II – experimental investigations, Aquac. Eng. 13 (1994) 183–200.

[8] B. Krister Holmberg, B. Kronberg, B. Lindman, Surfactants and polymers in aqueous solution, John Wiley & Sons, New York, 2002.

[9] I. Kralova, J. Sjöblom, Surfactants used in food industry: a review, J. Dispersion Sci. Technol. 30 (2009) 1363–1383.

[10] R. Pugh, Foaming, foam films, antifoaming and defoaming, Adv. Colloid Interface Sci. 64 (1996) 67–142.

[11] L.L. Schramm, Foams: fundamentals and applications in the petroleum industry, American Chemical Society, Washington DC, 1994.

[12] S. Chen, S. Hanning, J. Falconer, M. Locke, J. Wen, Recent advances in non-ionic surfactant vesicles (niosomes): fabrication, characterization, pharmaceutical and cosmetic applications, Eur. J. Pharm. Biopharm. 144 (2019) 18–39.

[13] M. Rieger, Surfactants in cosmetics, Marcel Dekker, New York, 2017.

[14] D. Myers, Surfactant science and technology, John Wiley & Sons, New Jersey, 2020.

[15] P. Sar, A. Ghosh, A. Scarso, B. Saha, Surfactant for better tomorrow: applied aspect of surfactant aggregates from laboratory to industry, Res. Chem. Intermed. 45 (2019) 6021–6041.

[16] M.J. Lawrence, Surfactant systems: their use in drug delivery, Chem. Soc. Rev. 23 (1994) 417–424.

[17] A. Panda, A. Kumar, S. Mishra, S. Mohapatra, Soapnut: a replacement of synthetic surfactant for cosmetic and biomedical applications, Sustain. Chem. Pharm. 17 (2020) 100297.

[18] D.R. Karsa, Industrial applications of surfactants IV, Elsevier, Manchester, 1999.

[19] S. Ghosh, A. Ray, N. Pramanik, Self-assembly of surfactants: an overview on general aspects of amphiphiles, Biophys. Chem. 265 (2020) 106429.

[20] X.Y. Hua, M.J. Rosen, Dynamic surface tension of aqueous surfactant solutions: I. basic paremeters, J. Colloid Interface Sci. 124 (1988) 652–659.

[21] R.M. Manglik, V.M. Wasekar, J. Zhang, Dynamic and equilibrium surface tension of aqueous surfactant and polymeric solutions, Exp. Therm. Fluid Sci. 25 (2001) 55–64.

[22] A. Shiloach, D. Blankschtein, Predicting micellar solution properties of binary surfactant mixtures, Langmuir 14 (1998) 1618–1636.

[23] M. Pileni, Reverse micelles as microreactors, J. Phys. Chem. 97 (1993) 6961–6973.

[24] B. Kronberg, K. Holmberg, B. Lindman, Surface chemistry of surfactants and polymers, John Wiley & Sons, West Sussex, 2014.

[25] L.L. Schramm, E.N. Stasiuk, D.G. Marangoni, Surfactants and their applications, Annu. Rep. Prog. Chem., Sect. C: Phys. Chem. 99 (2003) 3–48.

[26] A.J. Wilson, Foams: physics, chemistry and structure, Springer, New York, 2013.

[27] D.L. Weaire, S. Hutzler, The physics of foams, Oxford University Press, New York, 2001.

[28] P. Stevenson, Foam engineering: fundamentals and applications, John Wiley & Sons, West Sussex, 2012.

[29] I. Cantat, S. Cohen-Addad, F. Elias, F. Graner, R. Höhler, O. Pitois, F. Rouyer, A. Saint-Jalmes, Foams: structure and dynamics, Oxford University Press, New York, 2013.

[30] N. Shirtcliffe, G. McHale, M. Newton, C. Perry, Intrinsically superhydrophobic organosilica sol-gel foams, Langmuir 19 (2003) 5626–5631.

[31] R. Aveyard, B. Binks, P. Fletcher, T. Peck, C. Rutherford, Aspects of aqueous foam stability in the presence of hydrocarbon oils and solid particles, Adv. Colloid Interface Sci. 48 (1994) 93–120.

[32] R. Pugh, Experimental techniques for studying the structure of foams and froths, Adv. Colloid Interface Sci. 114 (2005) 239–251.

[33] Y. Zhao, M.B. Brown, S.A. Jones, Pharmaceutical foams: are they the answer to the dilemma of topical nanoparticles?, Nanomed. Nanotech. Biol. Med. 6 (2010) 227–236.

[34] H. Komatsu, H. Yamada, S.F. Shiseido, Rheological properties of soap foam, J. Soc. Cosmet. Chem. 29 (1978) 237–246.

[35] H. Zhang, C.A. Miller, P.R. Garrett, K.H. Raney, Mechanism for defoaming by oils and calcium soap in aqueous systems, J. Colloid Interface Sci. 263 (2003) 633–644.

[36] M. Breuer, H. Tsai, Measuring the viscoelastic properties of aerosol shaving foams, 35 (1984) 59–71.

[37] R.K. Prud'homme, Foams: theory, measurements and applications, CRC Press, New York, 1995.

[38] M.J. Rosen, J.T. Kunjappu, Surfactants and interfacial phenomena, John Wiley & Sons, New York, 2012.

[39] J.L. Joye, G.J. Hirasaki, C.A. Miller, Dimple formation and behavior during axisymmetrical foam film drainage, Langmuir 8 (1992) 3083–3092.

[40] F. Vardar-Sukan, Foaming: consequences, prevention and destruction, Biotechnol. Adv. 16 (1998) 913–948.

[41] N. Schelero, G. Hedicke, P. Linse, R.v. Klitzing, Effects of counterions and co-ions on foam films stabilized by anionic dodecyl sulfate, J. Phys. Chem. B 114 (2010) 15523–15529.

[42] S. Rouimi, C. Schorsch, C. Valentini, S. Vaslin, Foam stability and interfacial properties of milk protein–surfactant systems, Food Hydrocoll. 19 (2005) 467–478.

[43] M. Simjoo, T. Rezaei, A. Andrianov, P. Zitha, Foam stability in the presence of oil: effect of surfactant concentration and oil type, Colloids Surf. A 438 (2013) 148–158.

[44] Q. Sun, Z. Li, S. Li, L. Jiang, J. Wang, P. Wang, Utilization of surfactant-stabilized foam for enhanced oil recovery by adding nanoparticles, Energy Fuels 28 (2014) 2384–2394.

[45] W. Drenckhan, A. Saint-Jalmes, The science of foaming, Adv. Colloid Interface Sci. 222 (2015) 228–259.

[46] S.I. Karakashev, M.V. Grozdanova, Foams and antifoams, Adv. Colloid Interface Sci. 176 (2012) 1–17.

[47] M.R. Behera, S.R. Varade, P. Ghosh, P. Paul, A.S. Negi, Foaming in micellar solutions: effects of surfactant, salt, and oil concentrations, Ind. Eng. Chem. Res. 53 (2014) 18497–18507.

[48] N. Yekeen, M.A. Manan, A.K. Idris, A.M. Samin, Influence of surfactant and electrolyte concentrations on surfactant adsorption and foaming characteristics, J. Pet. Sci. Technol. 149 (2017) 612–622.

[49] K. Osei-Bonsu, N. Shokri, P. Grassia, Foam stability in the presence and absence of hydrocarbons: from bubble-to bulk-scale, Colloids Surf. A 481 (2015) 514–526.

[50] A.K. Vikingstad, A. Skauge, H. Høiland, M. Aarra, Foam–oil interactions analyzed by static foam tests, Colloids Surf. A 260 (2005) 189–198.

[51] P. Grassia, S. Ubal, M.D. Giavedoni, D. Vitasari, P.J. Martin, Surfactant flow between a Plateau border and a film during foam fractionation, Chem. Eng. Sci. 143 (2016) 139–165.

[52] D. Vitasari, P. Grassia, P. Martin, Surfactant transport onto a foam lamella, Chem. Eng. Sci. 102 (2013) 405–423.

[53] J. Wang, A.V. Nguyen, S. Farrokhpay, A critical review of the growth, drainage and collapse of foams, Adv. Colloid Interface Sci. 228 (2016) 55–70.

[54] L. Wang, R.-H. Yoon, Effects of surface forces and film elasticity on foam stability, Int. J. Miner. Process. 85 (2008) 101–110.

[55] B. Derjaguin, Experimental investigations on solvation of surfaces with application to the development of a mathematical theory of the stability of lyophobic colloids, Bull. Acad. Sci. URSS Phys. Ser. 5 (1937) 1153–1164.

[56] B. Derjaguin, On the repulsive forces between charged colloid particles and on the theory of slow coagulation and stability of lyophobe sols, J. Chem. Soc. Faraday Trans. 35 (1940) 203–215.

[57] B. Derjaguin, N. Churaev, On the question of determining the concept of disjoining pressure and its role in the equilibrium and flow of thin films, J. Colloid Interface Sci. 66 (1978) 389–398.

[58] A. Nguyen, H.J. Schulze, Colloidal science of flotation, CRC Press, New York, 2003.

[59] K.J. Mysels, S. Frankel, K. Shinoda, Soap films: studies of their thinning and a bibliography, Pergamon Press, London, 1959.

[60] V. Bergeron, Forces and structure in thin liquid soap films, J. Phys. Condens. Matter 11 (1999) R215–R238.

[61] C. Stubenrauch, R. Von Klitzing, Disjoining pressure in thin liquid foam and emulsion films–new concepts and perspectives, J. Phys. Condens. Matter 15 (2003) R1197–R1232.

[62] N. Churaev, Derjaguin's disjoining pressure in the colloid science and surface phenomena, Adv. Colloid Interface Sci. 104 (2003) XV–XX.

[63] J.N. Israelachvili, Intermolecular and surface forces, Academic Press, London, 2011.

[64] R.J. Hunter, Foundations of colloid science, Oxford University Press, Oxford, 2001.

[65] J. Lyklema, Fundamentals of interface and colloid science: soft colloids, Academic Press, San Diego, 2005.

[66] H.C. Hamaker, The London–van der Waals attraction between spherical particles, Physica 4 (1937) 1058–1072.

[67] A. Scheludko, D. Exerowa, Über den elektrostatischen und van der Waalsschen zusätzlichen Druck in wässerigen Schaumfilmen, Kolloid-Zeitschrift 168 (1960) 24–28.

[68] A. Sheludko, Thin liquid films, Adv. Colloid Interface Sci. 1 (1967) 391–464.

[69] D. Möbius, R. Miller, Proteins at liquid interfaces, Elsevier, Amsterdam, 1998.

[70] I. Ivanov, Thin liquid films, Marcel Dekker, New York, 1988.

[71] J. Angarska, B. Dimitrova, K. Danov, P. Kralchevsky, K. Ananthapadmanabhan, A. Lips, Detection of the hydrophobic surface force in foam films by measurements of the critical thickness of the film rupture, Langmuir 20 (2004) 1799–1806.

[72] R. Sedev, Z. Németh, R. Ivanova, D. Exerowa, Surface force measurement in foam films from mixtures of protein and polymeric surfactants, Colloids Surf. A 149 (1999) 141–144.

[73] V. Carrier, A. Colin, Coalescence in draining foams, Langmuir 19 (2003) 4535–4538.

[74] D. Langevin, Influence of interfacial rheology on foam and emulsion properties, Adv. Colloid Interface Sci. 88 (2000) 209–222.

[75] G. Narsimhan, E. Ruckenstein, Hydrodynamics, enrichment, and collapse in foams, Langmuir 2 (1986) 230–238.

[76] A. Nikolov, D. Wasan, N. Denkov, P. Kralchevsky, I. Ivanov, Drainage of foam films in the presence of nonionic micelles, 82 (1990) 87–98.

[77] P. Ghosh, V. Juvekar, Analysis of the drop rest phenomenon, Chem. Eng. Res. Des. 80 (2002) 715–728.

[78] P. Kruglyakov, S. Karakashev, A. Nguyen, N. Vilkova, Foam drainage, Curr. Opin. Colloid Interface Sci. 13 (2008) 163–170.

[79] A. Saint-Jalmes, Physical chemistry in foam drainage and coarsening, Soft Matter 2 (2006) 836–849.

[80] A. Saint-Jalmes, D. Langevin, Time evolution of aqueous foams: drainage and coarsening, J. Phys. Condens. Matter 14 (2002) 9397.

[81] S.A. Koehler, S. Hilgenfeldt, H.A. Stone, A generalized view of foam drainage: experiment and theory, Langmuir 16 (2000) 6327–6341.

[82] P. Stevenson, On the forced drainage of foam, Colloids Surf. A 305 (2007) 1–9.

[83] E. Rio, W. Drenckhan, A. Salonen, D. Langevin, Unusually stable liquid foams, Adv. Colloid Interface Sci. 205 (2014) 74–86.

[84] D. Weaire, R. Phelan, The physics of foam, J. Phys. Condens. Matter 8 (1996) 9519–9524.

[85] R. Lemlich, A theory for the limiting conductivity of polyhedral foam at low density, J. Colloid Interface Sci. 64 (1978) 107–110.

[86] Y.S. Cho, J.S. Laskowski, Bubble coalescence and its effect on dynamic foam stability, Can. J. Chem. Eng. 80 (2002) 299–305.

[87] S. Samanta, P. Ghosh, Coalescence of bubbles and stability of foams in aqueous solutions of Tween surfactants, Chem. Eng. Res. Des. 89 (2011) 2344–2355.

[88] D. Langevin, Bubble coalescence in pure liquids and in surfactant solutions, Curr. Opin. Colloid Interface Sci. 20 (2015) 92–97.

[89] P. Ghosh, Coalescence of air bubbles at air–water interface, Chem. Eng. Res. Des. 82 (2004) 849–854.

[90] P. Ghosh, Colloid and interface science, PHI Learning Pvt. Ltd., New Delhi, 2009.

[91] K. Giribabu, M. Reddy, P. Ghosh, Coalescence of air bubbles in surfactant solutions: role of salts containing mono-, di-, and trivalent ions, Chem. Eng. Commun. 195 (2007) 336–351.

[92] M. Kumar, P. Ghosh, Coalescence of air bubbles in aqueous solutions of ionic surfactants in presence of inorganic salt, Chem. Eng. Res. Des. 84 (2006) 703–710.

[93] T. Mitra, P. Ghosh, Binary coalescence of water drops in organic media in presence of ionic surfactants and salts, J. Dispersion Sci. Technol. 28 (2007) 785–792.

[94] S. Samanta, P. Ghosh, Coalescence of bubbles and stability of foams in Brij surfactant systems, Ind. Eng. Chem. Res. 50 (2011) 4484–4493.

[95] S. Samanta, P. Ghosh, Coalescence of air bubbles in aqueous solutions of alcohols and nonionic surfactants, Chem. Eng. Sci. 66 (2011) 4824–4837.

[96] A. Srinivas, P. Ghosh, Coalescence of bubbles in aqueous alcohol solutions, Ind. Eng. Chem. Res. 51 (2012) 795–806.

[97] B. Burghoff, Foam fractionation applications, J. Biotechnol. 161 (2012) 126–137.

[98] A. Šonc, V. Grilc, Batch foam fractionation of surfactants from aqueous solutions, Acta Chim. Slov. 51 (2004) 687–698.

[99] S. Boonyasuwat, S. Chavadej, P. Malakul, J.F. Scamehorn, Anionic and cationic surfactant recovery from water using a multistage foam fractionator, Chem. Eng. J. 93 (2003) 241–252.

[100] S. Boonyasuwat, S. Chavadej, P. Malakul, J.F. Scamehorn, Surfactant recovery from water using a multistage foam fractionator: part I effects of air flow rate, foam height, feed flow rate and number of stages, Sep. Sci. Technol. 40 (2005) 1835–1853.

[101] S. Boonyasuwat, S. Chavadej, P. Malakul, J.F. Scamehorn, Surfactant recovery from water using a multistage foam fractionator: effect of surfactant type, Sep. Sci. Technol. 44 (2009) 1544–1561.

[102] Z. Zhang, Z. Wu, G. Liu, Interfacial adsorption of methyl orange in liquid phase of foam fractionation using dodecyl dimethyl betaine as the collector, J. Ind. Eng. Chem. 28 (2015) 184–189.

[103] W. Bae, H. Won, B. Hwang, R.A. de Toledo, J. Chung, K. Kwon, H. Shim, Characterization of refractory matters in dyeing wastewater during a full-scale Fenton process following pure-oxygen activated sludge treatment, J. Hazard. Mater. 287 (2015) 421–428.

[104] A. Lopez, G. Ricco, R. Ciannarella, A. Rozzi, A. Di Pinto, R. Passino, Textile wastewater reuse: ozonation of membrane concentrated secondary effluent, Water Sci. Technol. 40 (1999) 99–105.

[105] C.-H. Tung, S.-Y. Shen, J.-H. Chang, Y.-M. Hsu, Y.-C. Lai, Treatment of real printing wastewater with an electrocatalytic process, Sep. Purif. Technol. 117 (2013) 131–136.

[106] S.S. Srinet, A. Basak, P. Ghosh, J. Chatterjee, Separation of anionic surfactant in paste form from its aqueous solutions using foam fractionation, J. Environ. Chem. Eng. 5 (2017) 1586–1598.

[107] R. Lemlich, Adsorptive bubble separation methods – foam fractionation and allied techniques, Ind. Eng. Chem. 60 (1968) 16–29.

[108] P. Stevenson, Foam fractionation: principles and process design, CRC Press, Boca Raton, 2019.

[109] G. Morgan, U. Wiesmann, Single and multistage foam fractionation of rinse water with alkyl ethoxylate surfactants, Sep. Sci. Technol. 36 (2001) 2247–2263.

[110] A.K. Kumar, N. Rawat, P. Ghosh, Removal and recovery of a cationic surfactant from its aqueous solution by foam fractionation, J. Environ. Chem. Eng. 8 (2020) 103555.

[111] R. Lemlich, Adsorptive bubble separation techniques, Academic Press, New York, 1972.

[112] D. Jenkins, Application of foam fractionation to wastewater treatment, J (Water Pollut. Control Fed.) (1966) 1737–1766.

[113] R. Grieves, R. Wood, Continuous foam fractionation: the effect of operating variables on separation, AlChE J. 10 (1964) 456–460.

[114] P. Somasundaran, Foam separation methods, Sep. Purif. Methods. 1 (1972) 117–198.

[115] N. Tharapiwattananon, J.F. Scamehorn, S. Osuwan, J.H. Harwell, K.J. Haller, Surfactant recovery from water using foam fractionation, Sep. Sci. Technol. 31 (1996) 1233–1258.

[116] K. Kumpabooth, J.F. Scamehorn, S. Osuwan, J.H. Harwell, Surfactant recovery from water using foam fractionation: effect of temperature and added salt, Sep. Sci. Technol. 34 (1999) 157–172.

[117] E. Rubin, J. Jorne, Foam separation of solutions containing two ionic surface-active solutes, Ind. Eng. Chem. Fundam. 8 (1969) 474–483.

[118] Y.H. Qu, G.M. Zeng, J.H. Huang, K. Xu, Y.Y. Fang, X. Li, H.L. Liu, Recovery of surfactant SDS and Cd^{2+} from permeate in MEUF using a continuous foam fractionator, J. Hazard. Mater. 155 (2008) 32–38.

[119] K. Tadakamalla, K. Marathe, Hydrodynamic study and optimization strategy for the surfactant recovery from aqueous solutions, Desalination 266 (2011) 98–107.

[120] P. Stevenson, R. Shaw, J. Tulloch, G.M. Evans, The influence of stirring upon the adsorption of a cationic surfactant onto activated carbon particles, Adsorpt. Sci. Technol. 29 (2011) 99–116.

[121] F. Marrakchi, W. Khanday, M. Asif, B. Hameed, Cross-linked chitosan/sepiolite composite for the adsorption of methylene blue and reactive orange 16, Int. J. Biol. Macromol. 93 (2016) 1231–1239.

[122] P. Gupta, W.A. Khanday, S.A. Majid, V. Kushwa, S. Tomar, R. Tomar, Study of sorption of metal oxoanions from waste water on surfactant modified analog of laumontite, J. Environ. Chem. Eng. 1 (2013) 510–515.

[123] W.A. Khanday, S.A. Majid, S.C. Shekar, R. Tomar, Synthesis and characterization of various zeolites and study of dynamic adsorption of dimethyl methyl phosphate over them, Mater. Res. Bull. 48 (2013) 4679–4686.

[124] W. Khanday, F. Marrakchi, M. Asif, B. Hameed, Mesoporous zeolite–activated carbon composite from oil palm ash as an effective adsorbent for methylene blue, J. Taiwan Inst. Chem. Eng. 70 (2017) 32–41.

[125] I.D. Kamalanathan, P.J. Martin, Competitive adsorption of surfactant–protein mixtures in a continuous stripping mode foam fractionation column, Chem. Eng. Sci. 146 (2016) 291–301.

[126] J. Eastoe, S. Nave, A. Downer, A. Paul, A. Rankin, K. Tribe, J. Penfold, Adsorption of ionic surfactants at the air−solution interface, Langmuir 16 (2000) 4511–4518.

[127] C.-H. Chang, E.I. Franses, Adsorption dynamics of surfactants at the air/water interface: a critical review of mathematical models, data, and mechanisms, Colloids Surf. A 100 (1995) 1–45.

[128] A.J. Prosser, E.I. Franses, Adsorption and surface tension of ionic surfactants at the air–water interface: review and evaluation of equilibrium models, Colloids Surf. A 178 (2001) 1–40.

[129] L. Wang, R.-H. Yoon, Hydrophobic forces in the foam films stabilized by sodium dodecyl sulfate: effect of electrolyte, Langmuir 20 (2004) 11457–11464.

[130] X. Dong, D. Sun, G. Liu, C. Cao, X. Jiang, Aqueous foam stabilized by hydrophobically modified cellulose and alkyl polyoxyethyl sulfate complex in the presence and absence of electrolytes, Colloids Surf. A 345 (2009) 58–64.

[131] E. Ruckenstein, A. Bhakta, Effect of surfactant and salt concentrations on the drainage and collapse of foams involving ionic surfactants, Langmuir 12 (1996) 4134–4144.

[132] E. Dutkiewicz, A. Jakubowska, Effect of electrolytes on the physicochemical behaviour of sodium dodecyl sulphate micelles, Colloid. Polym. Sci. 280 (2002) 1009–1014.

[133] J. Isrealachvili, Intermolecular and surface forces, Academic Press, San Diego, 1991.

Chapter 2

Materials and Experimental Methods

CHAPTER 2

MATERIALS AND EXPERIMENTAL METHODS

2.1. Materials

The detailed list of chemicals used in this work, including their source and purity, is given in Table 2.1. All chemicals were of analytical grade, and they were used as received from their respective manufacturers. Milli-Q water [make: Millipore (USA), model: Elix-3] having a conductivity of 5.5 μS m^{-1} (at 298 K) was used to prepare the stock solutions for the analysis. These solutions were diluted further as per the requirements.

Table 2.1 Chemicals used in this work

Chemicals	*Purity (%)*	*Source*
Acetonitrile	99.9	Spectrochem (India)
Benzene	99.7	Merck (India)
Calcium chloride	98.0	Merck (India)
Cetyltrimethylammonium bromide	99.0	Sigma-Aldrich (India)
Chloroform	99.0	Merck (India)
Dimidium bromide and disulfine blue	99.0	Loba Chemie (India)
Disulfine blue VN	99.0	Loba Chemie (India)
Ethanol	99.9	Changshu Yangyuan (China)
Hexane	99.7	Merck (India)
Hyamine	99.0	Loba Chemie (India)
Methanol	99.9	Spectrochem (India)
Sodium chloride	99.5	Merck (India)

Sodium dodecyl benzene sulfonate	99.0	Sigma-Aldrich (India)
Sodium dodecyl sulfate	99.0	Sigma-Aldrich (India)
Sodium sulfate	99.0	Merck (India)
Toluene	99.9	Merck (India)

2.2. Experimental setup

The experimental setup is shown in Figure 2.1. It consisted of an air compressor, control valve, rotameter, drain valve, sparger, sample collection port, liquid solution container (made of transparent polypropylene sheet, 25 cm height, 5.5 cm inside diameter, and 3 mm wall thickness), frustum (to prevent the formation of eddies), air diffuser, and a cylindrical column (made of transparent Perspex®, 52 cm height, 29 cm inside diameter, and 5 mm wall thickness). The rectangular air diffuser was inserted at the base of the liquid solution container and the air was introduced by using a compressor [make: Tarsons (India), model: Rockyvac 320] to generate the foam. A rotameter was installed before the sparger to measure the airflow rate.

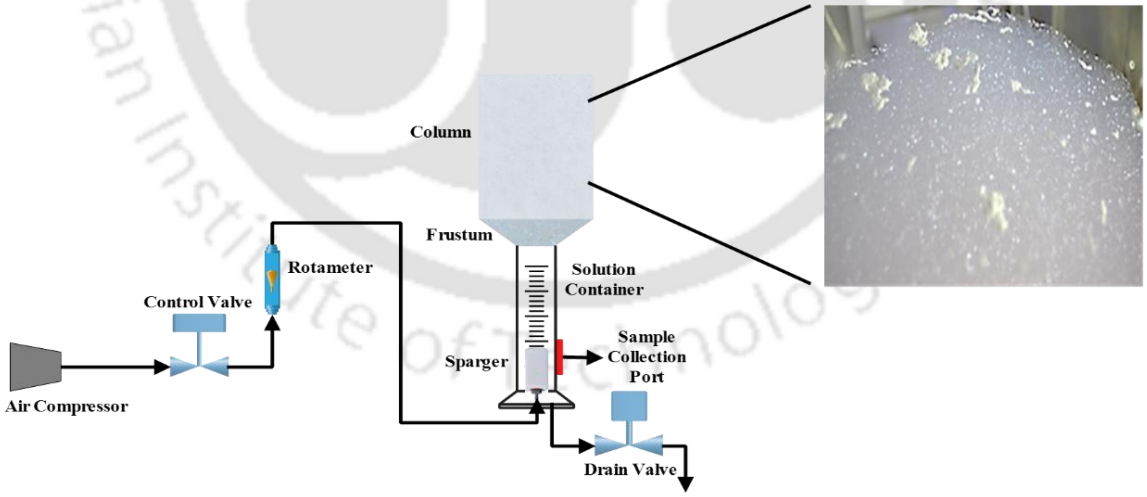

Figure 2.1 Foam fractionation setup.

The feed solution was introduced from the top of the column. Samples were collected by using a syringe through a sample collection port located at 6 cm height from the base of the

solution container. For each experiment, 500 cm^3 of the surfactant solution was used. The test was carried out until the surfactant concentration in the aqueous phase was reduced by 85–95%. The samples (about 5 cm^3) were collected at 30 min time intervals. After ~1 h of sparging, solid flakes of the surfactant began to form at the top of the column. They were skimmed and collected in a petri dish. The flakes obtained from each experiment were dried for 24 h at 323 K in a hot air oven [make: IKON Instruments (India), model: Memmert oven], and their weight was measured by a digital balance [make: Mettler Toledo (India), model: ME204]. At the end of the experiment, the foam was left in the column to collapse spontaneously, and the volume of liquid remaining in the container was measured. The surfactant stuck to the column wall was cleaned with a known amount of water. The concentration of this solution was measured, which was termed as the *foamate concentration*. Subsequently, the column was thoroughly washed using Millipore water before the beginning of the next experiment. The accuracy of the experimental data was verified by performing an overall material balance.

2.3. Measurement of surfactant concentration

2.3.1. Measurement of CTAB concentration

The CTAB concentration was measured by using a two-phase titration method [1]. SDS was used as the anionic titrant, and disulfine blue VN (an anionic dye) was used as the indicator [2]. For each analysis, 5 cm^3 sample was taken in a conical flask, and an equal amount of chloroform was added to it. The sample and chloroform separated into an aqueous phase (i.e., the upper phase) and an organic phase (i.e., the lower phase). Both of these phases were visible inside the flask. Next, a few drops of the indicator were added to this mixture. The cationic surfactant and the anionic indicator reacted and produced a non-polar blue complex, which was soluble in chloroform and insoluble in the aqueous phase. Then, this solution was titrated by

adding the titrant (i.e., 0.004 mol dm^{-3} SDS solution) dropwise to this two-phase mixture. After each drop of the titrant was added, the mixture was vigorously shaken and then allowed to separate. SDS displaced the anionic dye (i.e., disulfine blue VN) during the titration, and the blue color slowly disappeared from the chloroform phase. The dye passed into the aqueous phase. The decolorization of the chloroform phase indicated the endpoint of the titration. The concentration of the CTAB solution was determined by using equation 2.1 [1] given below.

$$\text{CTAB concentration} = \frac{a \times M \times \text{Mol. wt. of CTAB}}{\text{Volume of the sample } \left(\text{cm}^3\right)} \qquad (2.1)$$

where a is the volume (cm^3) of SDS required for the titration and M is the concentration of the SDS solution. The molecular weight of CTAB is 364.45 g mol^{-1}. The foamate concentration was also measured using equation 2.1.

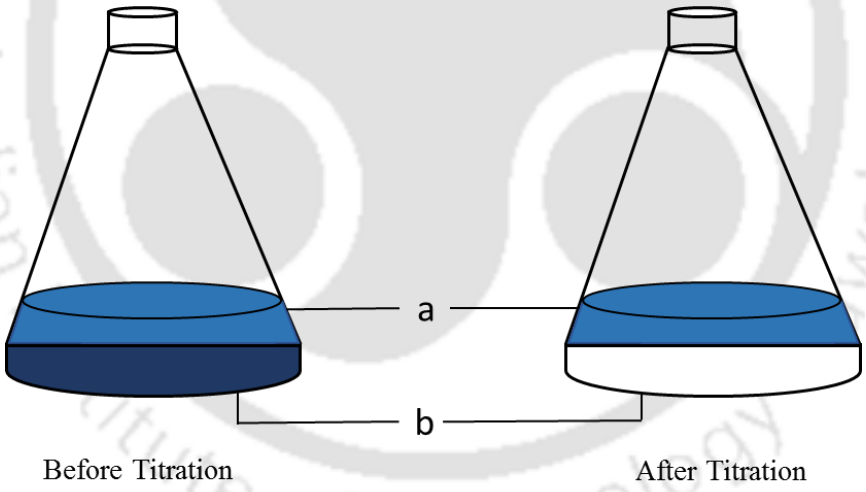

Figure 2.2 Schematic diagram showing the two-phase titration for determining the concentration of CTAB (before and after): (a) aqueous phase and (b) organic phase.

2.3.2. Measurement of SDS concentration

SDS concentration in the aqueous phase was measured by a two-phase titration method [3]. Benzethonium chloride was used as the titrant. The indicator was an acidic mixture of a

cationic dye (i.e., dimindium bromide) and an anionic dye (i.e., disulphine blue VN). The titration was performed in a water−chloroform two-phase medium.

The concentration of the surfactant in a 5 cm^3 sample was measured. The sample was collected in a flask. After that, the same volume of chloroform (i.e., 5 cm^3) was added to the flask. Separation of the organic (i.e., lower) and the aqueous phase (i.e., top) in the container was clearly visible. A few droplets of the indicator were applied to the solution, and the same was stirred. The SDS and the cationic dye reacted and generated a pink complex, which was non-polar. This complex was miscible in the chloroform phase and immiscible in water (Fig. 2.3). Then this solution was titrated by Hyamine 1622. After the addition of every droplet of the titrant (i.e., Hyamine 1622), the solution was stirred and then permitted to separate into the two phases. The titrant displaced the cationic dye during titration, the pink complex slowly faded from the organic phase, and the dye went into the aqueous solution. The pink color vanished at the endpoint, the chloroform phase became colorless, and the excess titrant formed a non-polar blue complex with the anionic dye in the chloroform phase. The surfactant concentration was computed from equation 2.2.

$$\text{Surfactant concentration} = \frac{a \times c \times \mathrm{M}}{V} \tag{2.2}$$

where a is the volume of benzethonium chloride necessary for titration (in cm^3), c is the concentration of benzethonium chloride (in mol dm^{-3}), M is the molecular weight of SDS (i.e., 288.38 g mol^{-1}), and V is the volume of the sample (in cm^3).

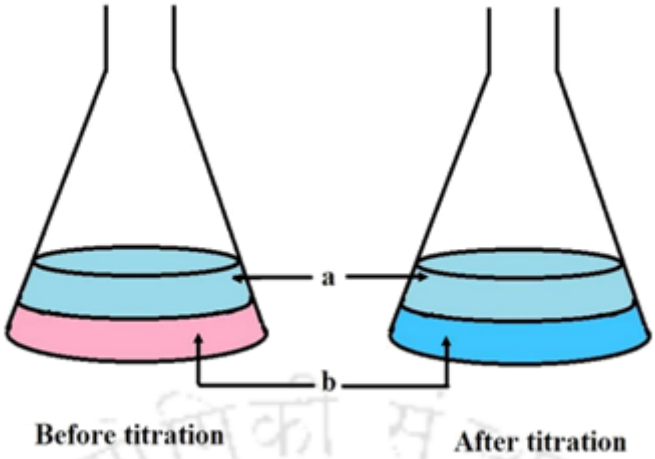

Figure 2.3 Illustration of the titration for determining the concentration of SDS: (a) aqueous solution and (b) chloroform phase.

2.3.3. Measurement of SDBS concentration

The SDBS concentration was measured by using a UV-Vis spectrophotometer (Make: Shimadzu (Singapore), Model No.: UV-2600). The absorbance versus concentration profiles at various SDBS concentrations is shown in Fig. 2.4. The spectra matched well with that reported in the literature [4]. The SDBS has a well-defined peak at 261 nm, and the absorbance was measured at this wavelength. A calibration curve of absorbance versus concentration was plotted to determine the SDBS concentration. The concentrations were varied in the range of 0–100 mg dm^{-3} due to the linear range in this concentration. The calibration plot was linear, and a zero-intercept equation was fitted to it.

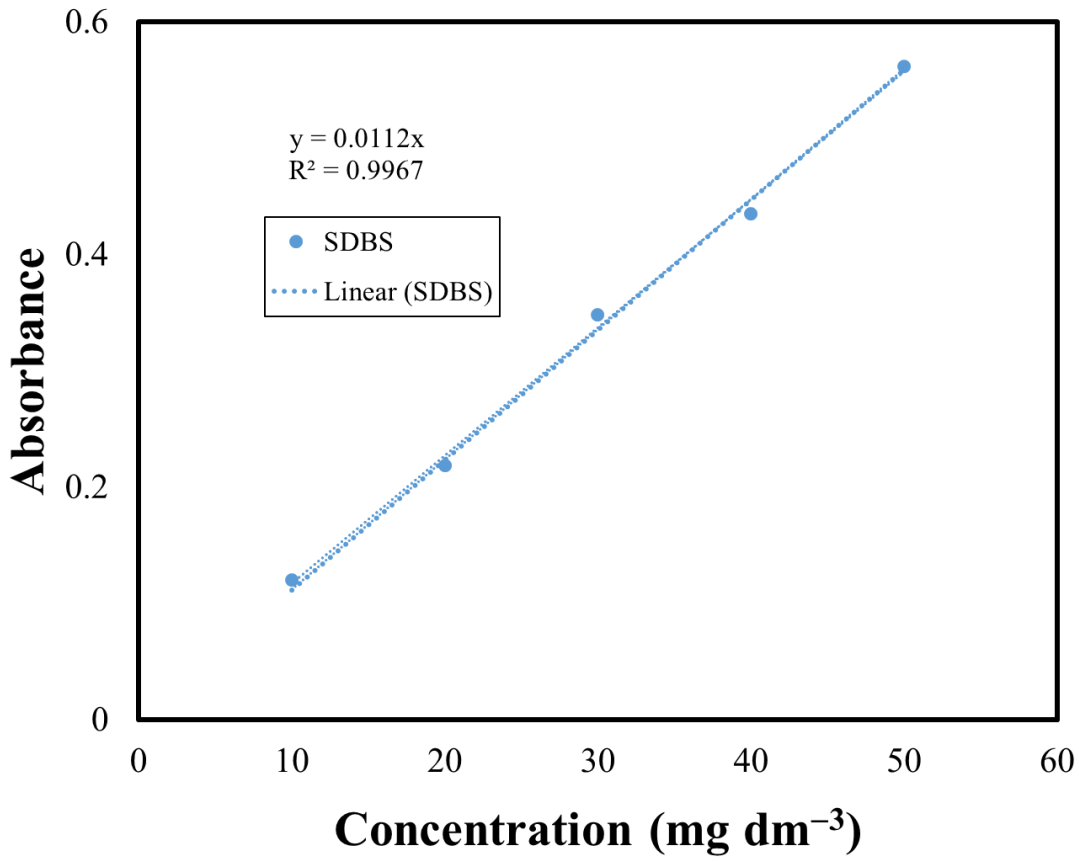

Figure 2.4 Absorption versus concentration calibration curve for UV–Vis spectrophotometry.

5 cm^3 sample was collected through the collection port for determining the concentration of SDBS in the aqueous phase. To ensure that the concentration of SDBS in the sample would fall within the range covered by the calibration curve, the sample was diluted with a known amount of water. The sample was placed in the measuring cuvette, and the absorbance was measured by UV–Vis spectrophotometry. The calibration equation was used to calculate the concentration of SDBS. The concentration of SDBS in the original sample was determined by using the dilution factor.

2.4. Measurement of surface and interfacial tension

The surface and interfacial tension data are required for estimating the adsorption of surfactant at the fluid–fluid interfaces. A tensiometer (see Fig. 2.5) [make: Kyowa Interface Science (Japan), model: DY–300] was used to measure the surface and interfacial tension. The optimal method depends upon the nature of the liquid, the stability of its surface when it is deformed, and the conditions under which the tension is to be measured. The du Noüy ring and the Wilhelmy plate methods are employed in this tensiometer.

Figure 2.5 A photograph of the tensiometer used for the measurement of surface and interfacial tension.

2.4.1. Wilhelmy plate method

It is similar to the du Noüy ring method. However, it does not require correction. In this method, a thin platinum plate is used. The measurement of the surface tension by the plate was done as per the procedure described in the ASTM standard D1331-14 (2014). The plate was dipped into the liquid whose surface tension was to be measured. The vessel containing the liquid was gradually lowered, and the force measured by the balance at the point of detachment (F) was noted. This force was used to calculate the surface tension by using the Wilhelmy equation, given by [5],

$$\gamma = \frac{F}{P\cos\theta} \tag{2.6}$$

A plate made of platinum and iridium was used for measuring the surface tension. The plate was cleaned by burning it in the flame of the Bunsen burner before each experiment. The contact angle of such a plate with water is close to zero, and therefore, $\cos\theta \approx 1$, and the liquid wets the plate completely. The Wilhelmy plate method is not recommended for interfacial tension measurements because the zero contact angle with another liquid is not ensured when the plate is wetted with one liquid.

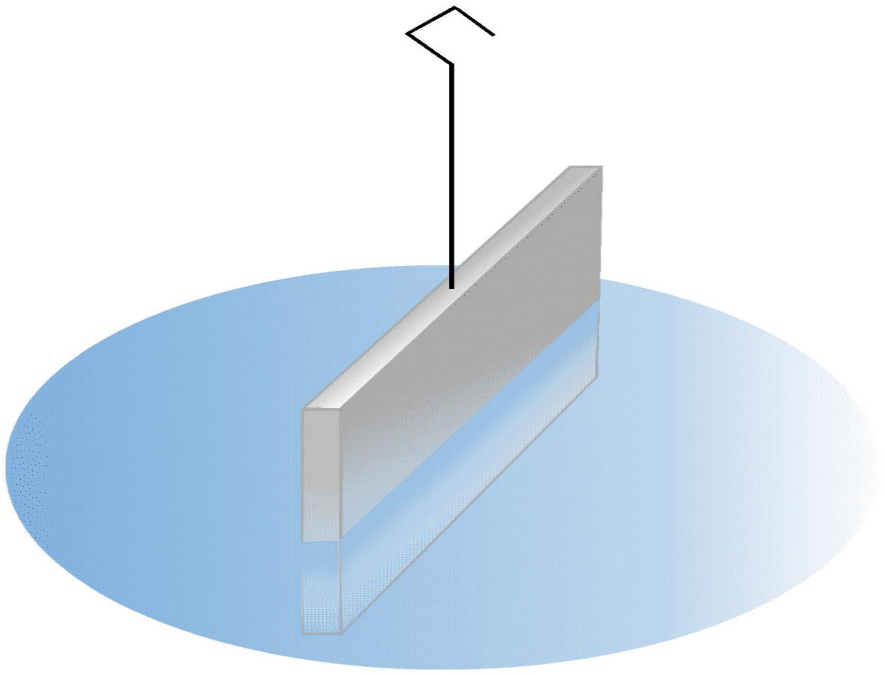

Figure 2.6 Schematic illustration of the Wilhelmy plate method.

The Wilhelmy plate method does not need any correction because the weight of the film hanging from the plate is negligibly small. Hence, for the surfactant solutions, it can be placed right at the surface and not moved while the surface tension is measured. Therefore, the surfactants are given a sufficiently long time to reach equilibrium. For this advantage, the plate method often gives superior accuracy in the measurement.

2.4.2. du Noüy ring method

The du Noüy ring method is an accurate method for measuring the interfacial tension. The measurement of interfacial tension by the ring was done as per the procedure described in the ASTM (American Society for Testing and Materials) Standard D1331–14 (2014). In this method, the platinum ring is first cleaned thoroughly. Then it is dipped into the surfactant solution completely. The equilibrated oil phase is gently poured over the aqueous phase. After the equilibrium is reached between the two phases, the glass vessel containing the sample is slowly

lowered until the ring detaches from the oil–water interface. The detachment force, *F*, is equal to the interfacial tension, γ, multiplied by the periphery of the detached surface. Therefore, the equation for calculating the interfacial tension is given by [5]

$$\gamma = \frac{F}{4\pi R_r} \tag{2.3}$$

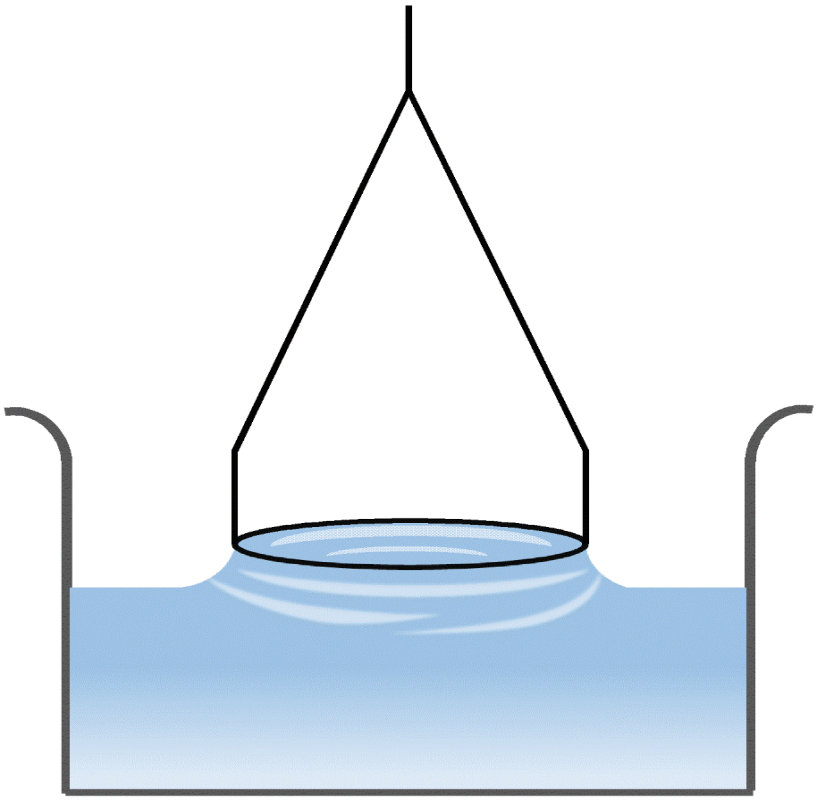

Figure 2.7 Schematic illustration of the du Noüy ring method.

The Zuidema–Waters correction [6] was applied to obtain the final value of the interfacial tension. This correction factor appears due to the weight of the liquid film immediately beneath the ring, which is also raised when the ring is pulled up. It depends upon the complex shape of the meniscus during the detachment of the ring, the density of the liquid, the radius of the ring (R_r), and the radius of the wire (r_w) of which the ring is made. The correct interfacial tension can be obtained by the equation

$$\gamma = \left(\frac{F}{4\pi R_r} \right) f \tag{2.4}$$

The Zuidema–Waters correction [6] for f is given by

$$f = 0.725 + \left[\frac{0.00363\gamma_{\text{Expt}}}{\pi^2 R_r{}^2 \Delta\rho} + 0.04534 - 1.679\left(\frac{r_w}{R_r} \right) \right]^{1/2} \tag{2.5}$$

Equations (2.4) and (2.5) assume that the contact angle is zero. To ensure this, the platinum ring is cleaned by burning it in the blue flame of a Bunsen burner. Distortions of the ring must be avoided, and the ring should be cleaned thoroughly after every use. The advantage of the ring method is that it is rapid, straightforward, and does not need to be calibrated by using solutions of known surface tension.

2.5. Measurement of zeta potential

The zeta potential at the air−water interface was measured using a zeta potentiometer [make: Beckman Coulter (Switzerland), model: Delsa Nano C]. An ultrasonic water bath [make: Telsonic Ultrasonics (Switzerland), model: TPC 15 H] was used for the sonication of the sample for 15–30 min to generate the micronanobubbles in the aqueous solution [7]. Next, the dispersion (~1 cm^3) containing the micronanobubbles was immediately transferred to the flow cell of the zeta potentiometer. The micronanobubbles traveled through a confined capillary channel in the flow cell under an electric field. The Doppler frequency shifts of the scattered light were used for measuring the electrophoretic mobility of these micronanobubbles. The Smoluchowski equation was used for the estimation of zeta potential at the air−water interface.

$$\zeta = \left(\frac{\mu}{\varepsilon\varepsilon_0} \right) U \tag{2.7}$$

Figure 2.8 A photograph of the zeta potentiometer.

2.6 Experimental conditions

All the experiments were carried out in an air-conditioned room where the temperature was maintained at 298±1 K. The temperature fluctuation was so slight that it did not affect the experiment results.

References

[1] C. Das, S. Dasgupta, S. De, Simultaneous separation of mixture of metal ions and aromatic alcohol using cross flow micellar-enhanced ultrafiltration and recovery of surfactant, Sep. Sci. Technol. 43 (2008) 71–92.

[2] M. Idouhar, A. Tazerouti, Spectrophotometric determination of cationic surfactants using patent blue V: application to the wastewater industry in Algiers, J. Surfactants Deterg. 11 (2008) 263–267.

[3] S.R. Epton, A new method for the rapid titrimetric analysis of sodium alkyl sulphates and related compounds, J. Chem. Soc. Faraday Trans. 44 (1948) 226–230.

[4] S.S. Srinet, A. Basak, P. Ghosh, J. Chatterjee, Separation of anionic surfactant in paste form from its aqueous solutions using foam fractionation, J. Environ. Chem. Eng. 5 (2017) 1586–1598.

[5] P. Ghosh, Colloid and interface science, PHI Learning Pvt. Ltd., New Delhi, 2009.

[6] H. Zuidema, G. Waters, Ring method for the determination of interfacial tension, Ind. Eng. Chem. Anal. Ed. 13 (1941) 312–313.

[7] M. Banik, P. Ghosh, The electroviscous effect at fluid–fluid interfaces, Ind. Eng. Chem. Res. 52 (2013) 1581–1590.

Chapter 3

Removal and Recovery of a Cationic Surfactant from its Aqueous Solution by Foam Fractionation

Published article: A.K. Kumar, N. Rawat, P. Ghosh, Removal and recovery of a cationic surfactant from its aqueous solution by foam fractionation, J. Environ. Chem. Eng. 8 (2020) 103555.

CHAPTER 3

REMOVAL AND RECOVERY OF A CATIONIC SURFACTANT FROM ITS AQUEOUS SOLUTION BY FOAM FRACTIONATION

3.1. Introduction

The human society has been facing an increasing pollution of surface and ground waters during the last few decades. There are several sources of pollution, with industry being one of the most significant. Surfactants are found in a variety of industries and manufactured products including the detergents [1], personal care products [2], food [3], firefighting [4], ore flotation [5], paints, and many others [6]. Surfactant-based separation methods, which are increasingly being utilzed to remove pollutants from wastewater and groundwater, constitute one important source of pollution. Large-scale use of the surfactants helps the development of many consumer products, but it contaminates water in many cases. The surfactant concentration in the effluent streams is becoming more of a concern as the environmental pollution rules become more stringent. Since, the surfactant is the main consumable item in these processes, it is beneficial to collect and reuse it as much as possible. Thus, the removal and recovery of these surfactants has become essential.

In this study, a cationic surfactant (i.e., cetyltrimethylammonium bromide, CTAB) was recovered from its aqueous solution by employing the foam fractionation method in batch mode in a cylindrical column. The surfactant concentration was five times its critical micellar concentration (i.e., 1822 mg dm^{-3}). The effects of three salts (i.e., NaCl, $CaCl_2$, and Na_2SO_4)

and airflow rate on the surfactant recovery were studied. The salt concentration was varied from 10 to 100 mol m^{-3}, and the airflow rate was varied from 0.4 to 1.6 dm^3 min^{-1}.

3.2. Results and Discussion

3.2.1. Effect of surfactant and salt concentrations

The volume of foam generated mainly depended on the airflow rate, and the type of salt and its concentration. Although the formation of foam appears like a simple macroscopic process, it is, in fact, a complex process, which involves several phenomena occurring simultaneously. During foam formation, the CTAB molecules adsorb on the surface of the foam bubbles. It causes a reduction in the concentration of surfactant in the bulk solution. The interaction between the surfactant molecules governs their adsorption at the air–water interface. The surface tension of the surfactant solution plays a major role in the generation of foam. An aqueous surfactant solution with a low surface tension is most suitable for foam generation. Thus, the surfactant, which lowers the surface tension significantly, and generates a good amount of foam is suitable for recovery by foam fractionation. The surfactant solution used in this work had these favorable characteristics.

In the foam fractionation experiment, the rate of foam generation and its volume is governed by the airflow rate. Foam formation involves the dynamic adsorption of the surfactant molecules at the air–water interface. In our foam fractionation experiments, two types of foam structures were observed. Wet foams having spherical bubbles occupied the bottom of the fractionation column, whereas, the top section of the column was occupied by the dry polyhedral bubbles. The wet foams usually have liquid content greater than 36% whereas, the dry foams have < 5% liquid content [7]. The foam generated from an aqueous surfactant solution has three distinct interrelated structural elements, i.e., film, Plateau border, and node,

which have simple and precise geometry. These were discussed in Section 1.3.1. The structure and stability of the foam depend mostly on the surfactant concentration in the bulk solution and the ability of the surfactant molecules to stabilize the foam films. The foam film stability depends upon the gravity drainage, electrostatic double layer (EDL) repulsion, van der Waals (vdW) attraction, steric repulsion, capillary suction, surface elasticity, and surface and bulk viscosities [8].

Foams generated in the fractionation column have bubbles of a broad size range. The pressure inside the smaller bubbles is higher than that inside the larger bubbles (see Equation 1.2). The air inside the smaller bubble diffuses into the bigger bubbles due to the pressure gradient. Subsequently, smaller air bubbles disappear and the larger bubbles coarsen, leading to the expansion of the bubbles. When a foam bubble is surrounded by its neighbor bubbles, the number of nodes increases with the expansion of the bubble. This causes the structure of the foam bubble to change from spherical to polyhedral, and increases its facial area. Gradually the bubbles containing five (or fewer) sides contract and those with at least seven or more sides grow [9]. Enlargement of the foam causes the films to expand. In a typical foam network, the foam surfaces are curved at the edges and the foam films connect at the Plateau borders. The pressure is smaller at the Plateau borders than at the center of the film, and thus, a radial flow is induced, which initiates the drainage of the liquid out of the foam film [10].

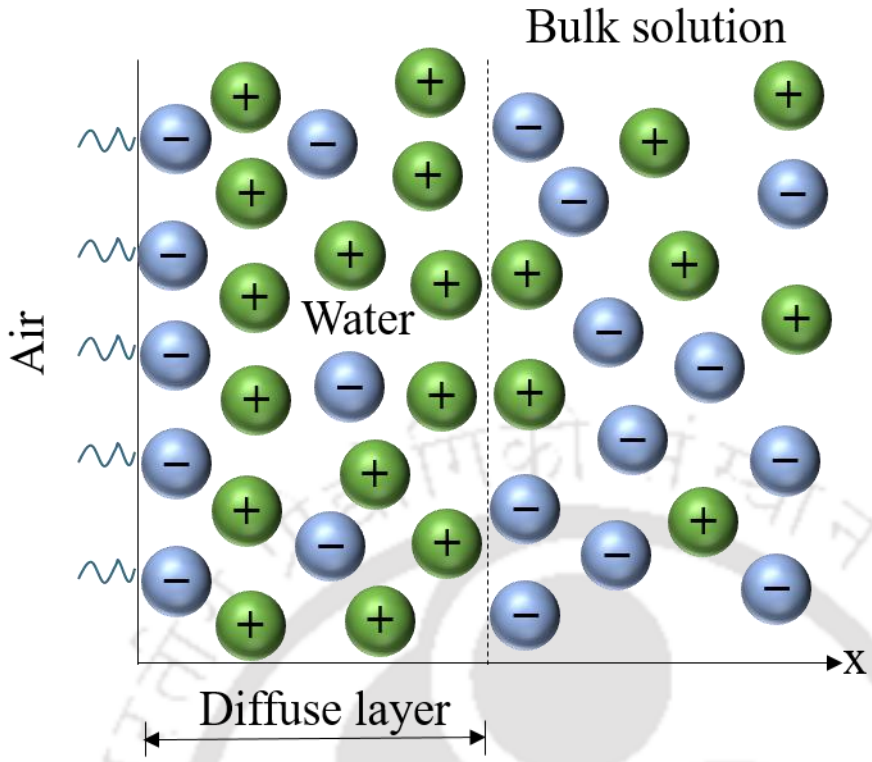

Figure 3.1 The EDL when a cationic surfactant is adsorbed at a flat air–water interface in the presence of salt.

The drainage has several intermediate stages until the foam film ruptures. Hydrodynamic interaction occurs between the bubbles when they approach each other, and a thick lamella is developed. A "dimple" is formed due to the distortion of the two bubble surfaces. The dimple vanishes progressively, leaving behind a plane-parallel film [11]. The surfactant concentration and its physical characteristics (e.g., structure and charge) affect the reduction in foam film thickness beyond the critical value. This critical film thickness is defined as the mean thickness of the foam film at the point of rupture in a foam network. The van der Waals, EDL, and short-range repulsive forces begin to impact its stability when the thickness of the foam film approaches ~50 nm [12]. The net disjoining pressure (Π) acting on the thin foam film is given by [13]

$$\Pi = \Pi_{EDL} + \Pi_{Sr} + \Pi_{vdW} \tag{3.1}$$

where Π_{EDL}, Π_{Sr}, and Π_{vdW} are the disjoining pressures due to the EDL, short-range hydration forces, and van der Waals forces, respectively. The balance between the capillary pressure and the disjoining pressure, i.e., $\left(\gamma/r_p - \Pi\right)$ (where r_p is the radius of curvature at the Plateau border) may decrease the drainage rate and restrict coalescence of the bubbles. Based on the concentration of the electrolyte and surfactant, bubbles may burst at a critical thickness lying in the range of 10–50 nm [12, 14]. Film thinning is hindered when Π is positive, while its negative value quickens it. The repulsive EDL force, generated from the positively-charged head-groups of the CTAB, repels the air–water interfaces in the thin foam film, but the attractive van der Waals force reduces the thickness of the film [15], leading to its rupture. When two air bubbles approach one another, the EDL force is adequately large due to the overlap of the double layers. The higher surfactant concentration in the foam film prompts an osmotic attraction for transferring the water molecules from the bulk liquid into the film, thereby stabilizing the film [16]. The short-range hydration force arises when the water molecules are actively associated with the head-groups (i.e., quaternary ammonium groups) of the surfactant. In the foam lamellae, the repulsive hydration force between the air–water interfaces arises due to the overlap of the hydrated head-groups [16]. This force prevents the interfaces from coming nearer than ~5 nm [17]. The strength of this force depends upon the energy needed to disrupt the hydrogen-bonding network of water and dehydrate the interfaces.

The salts of sodium, calcium, and magnesium usually exist in surface and groundwater in varied quantities [13]. The cationic surfactant (i.e., CTAB) is resistant to precipitation in the presence of most of these salts. However, these salts reduce the foam volume substantially. The experiments were run for 3–4 h. The concentration profiles of CTAB depicting the effects of NaCl, $CaCl_2$, and Na_2SO_4 are shown in Figures 3.2–3.4.

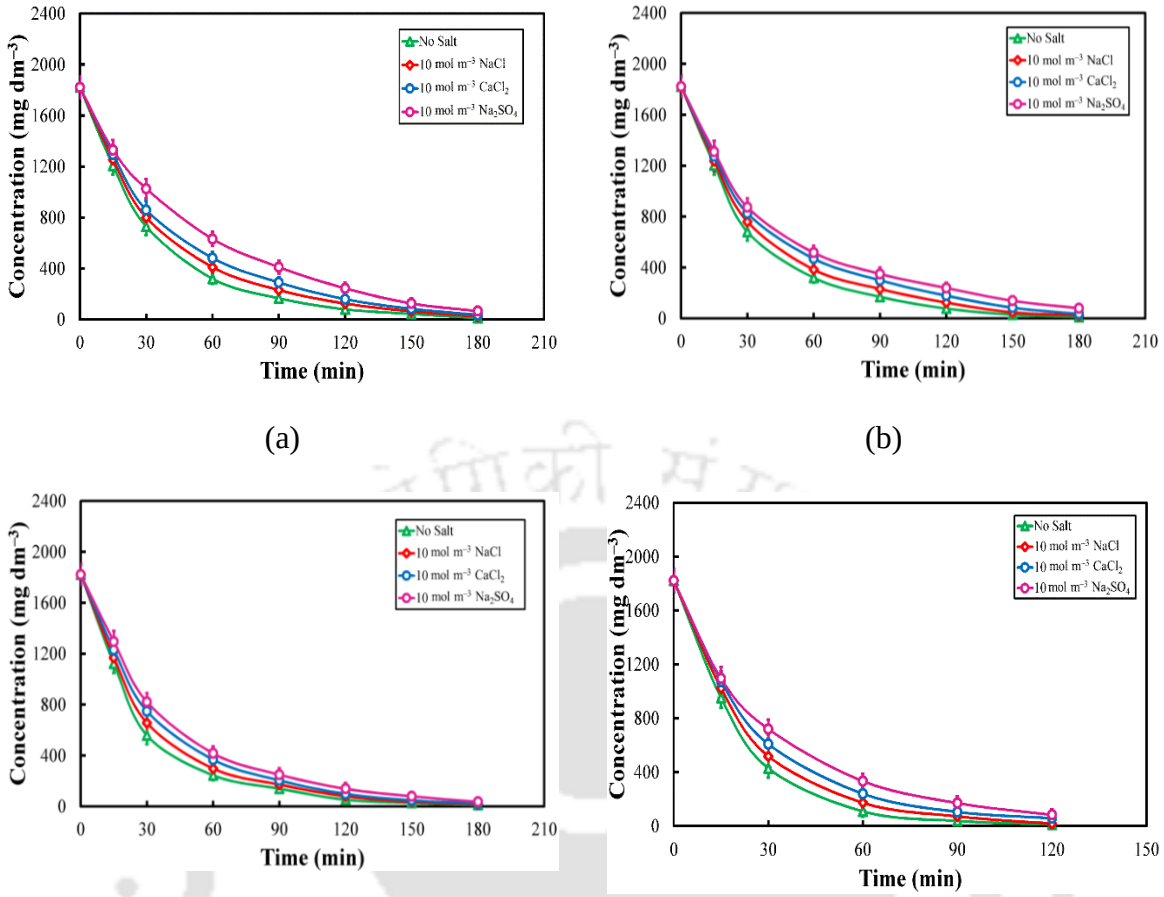

Figure 3.2 A comparison of the effects of 10 mol m^{-3} NaCl, $CaCl_2$, and Na_2SO_4 on the surfactant concentration profiles at different airflow rates: (a) 0.4, (b) 0.8, (c) 1.2, and (d) 1.6 dm^3 min^{-1}.

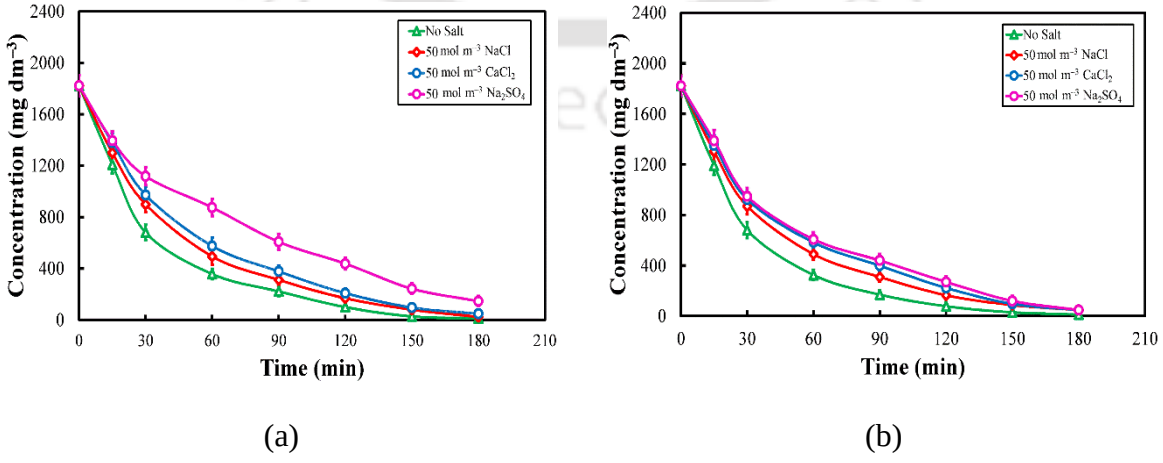

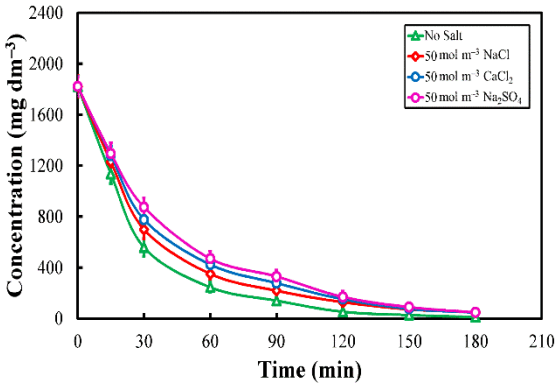

(c)

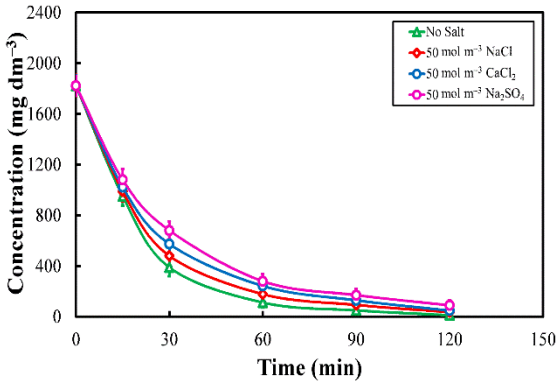

(d)

Figure 3.3 A comparison of the effects of 50 mol m^{-3} NaCl, $CaCl_2$, and Na_2SO_4 on the surfactant concentration profiles at different airflow rates: (a) 0.4, (b) 0.8, (c) 1.2, and (d) 1.6 dm^3 min^{-1}.

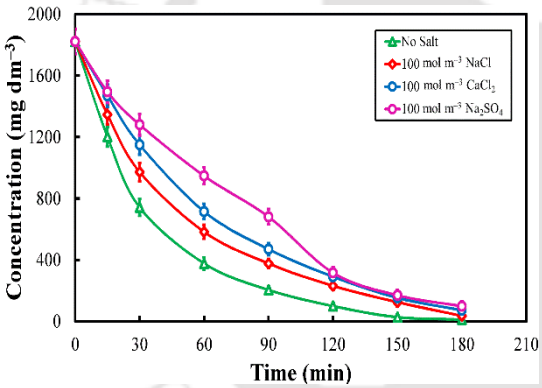

(a)

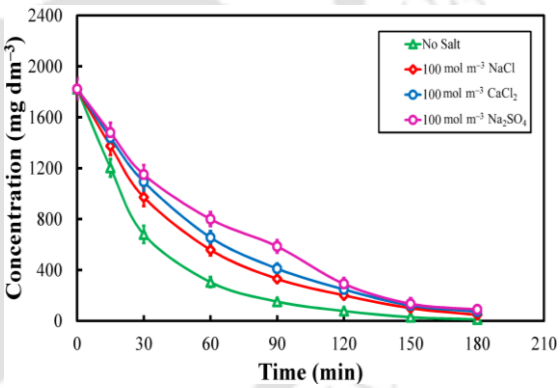

(b)

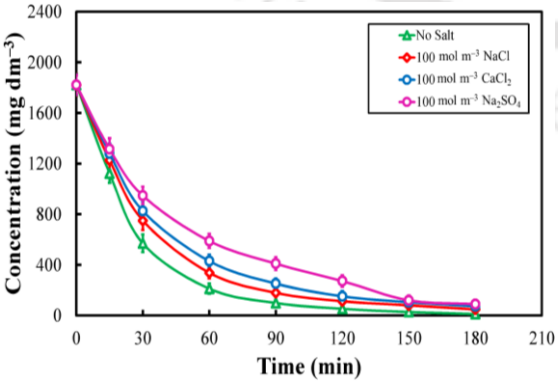

(c)

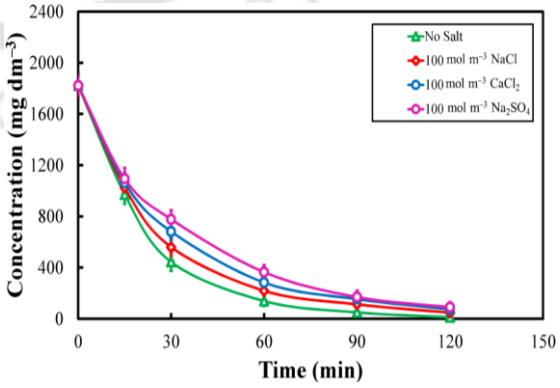

(d)

Figure 3.4 A comparison of the effects of 100 mol m^{-3} NaCl, $CaCl_2$, and Na_2SO_4 on the surfactant concentration profiles at different airflow rates: (a) 0.4, (b) 0.8, (c) 1.2, and (d) 1.6 dm^3 min^{-1}.

The concentration of the surfactant in the aqueous phase decreased with increasing airflow rate. This phenomenon occurred due to the generation of more foam, which stripped the surfactant from the aqueous phase. The surface tensions of the feed solutions are shown in Table 3.1. Since the concentration of CTAB in the solution was much higher than its CMC, the addition of salt did not reduce the surface tension further. At the low surfactant concentrations, the air–water interface was not saturated. The repulsion between the charged head-groups of the surfactant molecules decreased with the addition of salt, which caused more adsorption of the surfactant molecules at the air–water interface [10]. Similar results have been reported in a few other works [18, 19].

Table 3.1 Effect of salt on surface tension of the feed solutions

Salt	*Salt concentration (mol m^{-3})*	*Surface tension (mN m^{-1})*
NaCl	10	36.0
	50	36.0
	100	36.0
$CaCl_2$	10	37.0
	50	36.0
	100	36.0
Na_2SO_4	10	39.0
	50	38.0
	100	38.0

It has been reported that the wetness of foams is increased by the addition of salt [20]. However, with the increasing concentration of the salt, the disjoining pressure in the foam film due to EDL (i.e., Π_{EDL}) decreased. The Debye length $\left(\kappa^{-1}\right)$ (see Section 1.4.3) depends on the concentration of salt and the valence of the ions. It decreases with increasing salt concentration. The effect of salt containing divalent ions differs from the same containing monovalent ions in two ways. Firstly, the ionic strength of the solution containing the divalent ions is higher, and hence, they are more effective in electrostatic screening. At equal concentrations, the presence of divalent ions leads to a smaller Debye length. Secondly, the surface potential is lower in the presence of the divalent ions than their monovalent counterparts [21]. It has been observed that the zeta potential decreases with the increasing valence of the ions [22]. Therefore, salts containing the divalent ions destabilize the foam films more effectively than the monovalent ions.

The sulfate ions adsorb at the Stern layer more favorably than the chloride ions [22]. Therefore, the zeta potential was less in the presence of the sulfate ions as compared to the chloride ions, which was corroborated from the experimental data. Thus, Na_2SO_4 was more effective in reducing the Π_{EDL}. The zeta potential was higher in the presence of NaCl as compared to $CaCl_2$ and Na_2SO_4.

For a symmetric *z*:*z* electrolyte, the surface potential depends on the concentration of electrolyte, which is given by the Grahame equation (based on the Gouy–Chapman theory of EDL) [16],

$$\zeta \approx \psi_0 = \left(\frac{2kT}{ze}\right)\sinh^{-1}\left[\sigma\left(8RT\varepsilon\varepsilon_0 c^{\infty}\right)^{-1/2}\right] \tag{3.2}$$

In equation (7), the surface potential $\left(\psi_0\right)$ has been approximated by the zeta potential $\left(\zeta\right)$. The latter signifies the electric potential at the surface of shear, which is located a few

molecular diameters away from the Stern layer. The stability of the foams significantly depends on the electrical charge on the air–water interfaces. Therefore, the zeta potential reflects the stability of the foam to a significant extent. A low value of the zeta potential predicts a lower stability of the foam. The zeta potential was measured with and without the salts. Equation (7) shows that the zeta potential would decrease with increasing salt concentration and valence. The experimental data are shown in Table 3.2.

Table 3.2 Effect of salt on the zeta potential at the air–water interface

Salt	*Salt concentration (mol m^{-3})*	*Zeta potential (mV)*
NaCl	10	20.0
	50	17.0
	100	13.0
$CaCl_2$	10	16.0
	50	14.0
	100	11.0
Na_2SO_4	10	15.0
	50	12.0
	100	8.0

3.2.2. Surfactant recovery

To reuse the surfactant, its recovery is essential. The recovery (ρ) is defined as the ratio of the amount of surfactant recovered to the amount of surfactant present in the feed solution. Therefore,

$$\rho(\%) = \left(\frac{\text{Recovered quantity of surfactant as solid}}{\text{Quantity of surfactant present in the feed solution}} \right) \times 100 \qquad (3.3)$$

A significant quantity of CTAB was recovered as solid from the dry foam at the top portion of the column. A small amount of surfactant stayed in the foam lamellae, which could not be recovered. Figure 3.5 shows that nearly 65% of the surfactant was recovered in the absence of NaCl, whereas the recovery was approximately 60% in its presence. The surfactant recovery decreased with increasing salt concentration. Since the stability of the foam was reduced in the presence of the salt (see Section 3.3), the recovery of CTAB from the aqueous phase was decreased. The recovery of surfactant increased with increasing airflow rate. The surfactant recovery was more when the airflow rate was in the range of 1.2 to 1.6 dm^3 min^{-1}. Similar trends were observed for $CaCl_2$ and Na_2SO_4, which are shown in Figures 3.6 and 3.7, respectively. Increase in the airflow rate generated more bubbles, and more surfactant molecules were adsorbed on the surface of the bubbles. Therefore, a higher rate of bubble generation led to a greater recovery of the surfactant at the higher airflow rates. This effect of airflow rate agrees with the previous studies reported [30]. However, when the airflow rate was very high, the foam was unstable. The foam collapsed suddenly resulting in a decrease in the surface area. This collapse caused more wetness in the foam, which led to a reduction in the surfactant recovery. The effectiveness of the salts in reducing the surfactant recovery followed the sequence: NaCl < $CaCl_2$ < Na_2SO_4.

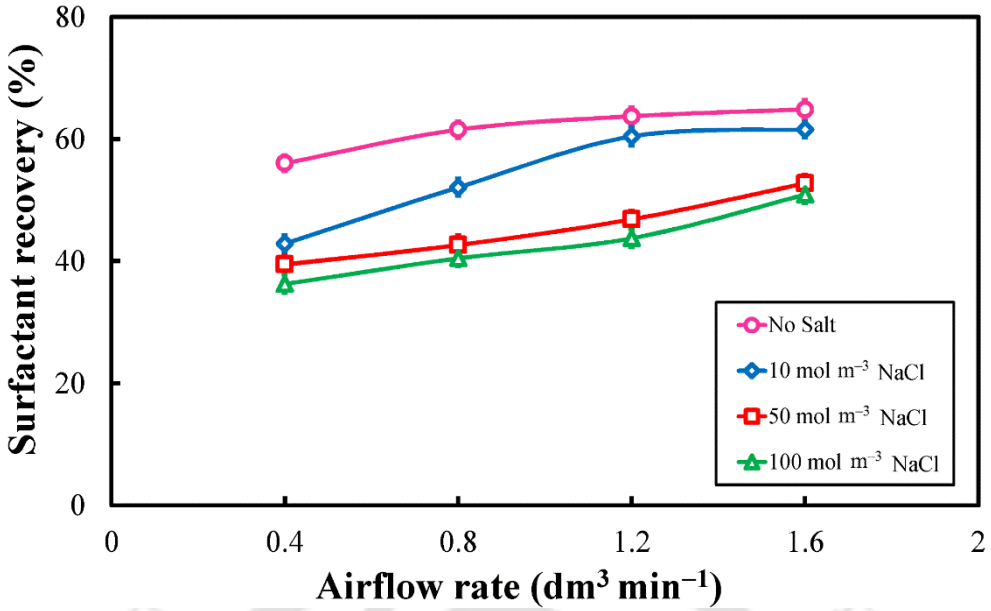

Figure 3.5 Variation of surfactant recovery with airflow rate at different NaCl concentrations.

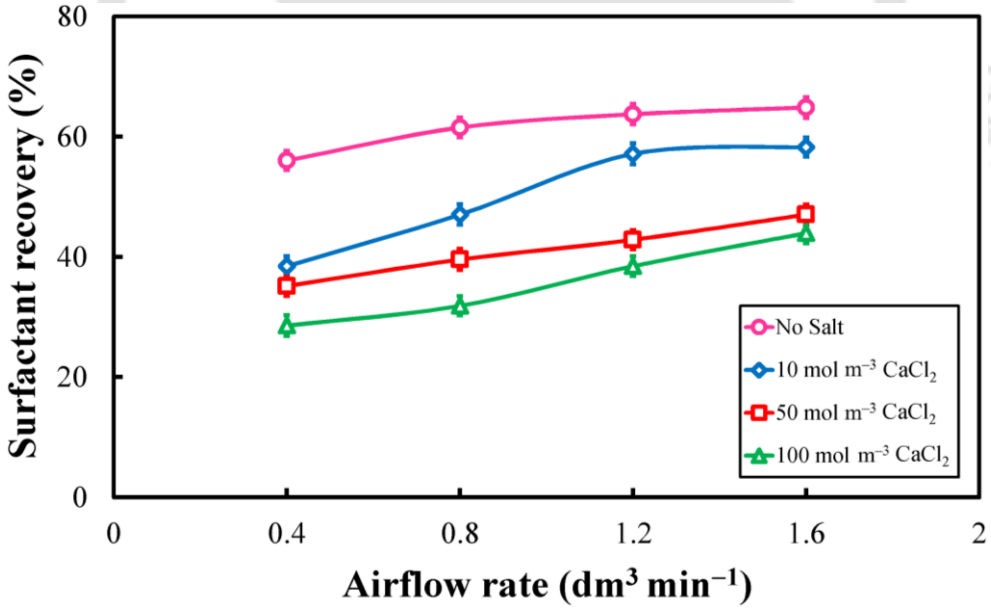

Figure 3.6 Variation of surfactant recovery with airflow rate at different $CaCl_2$ concentrations.

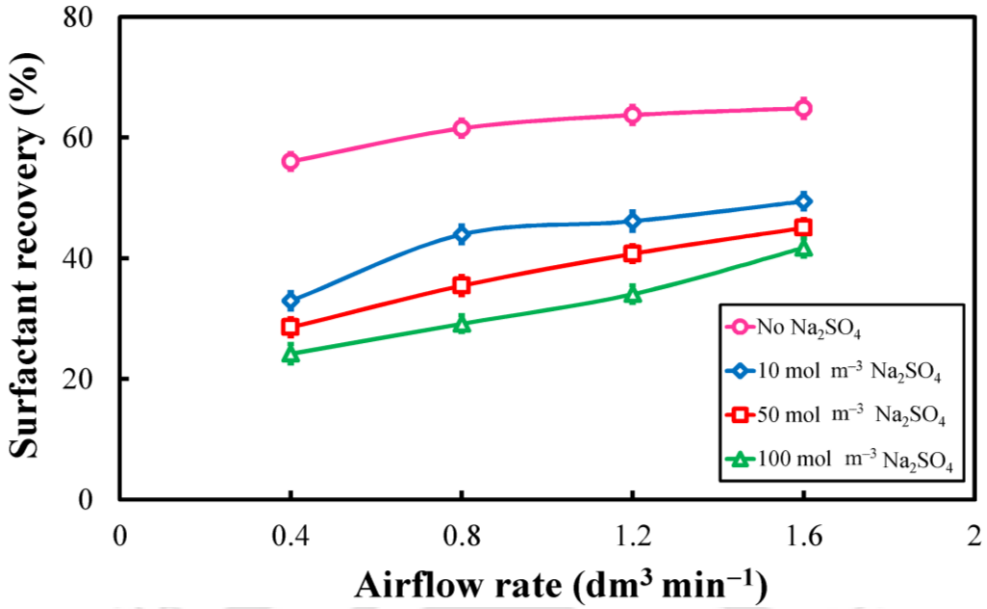

Figure 3.7 Variation of surfactant recovery with airflow rate at different Na_2SO_4 concentrations.

3.2.3. Foam volume

The foams were wet near the base of the column, which indicates a higher water content. On the other hand, the upper portion of the foam was rather dry, with a much smaller water content. Since the air was continuously sparged from the bottom of the column into the surfactant solution, the foam expanded into the entire column. The air could escape from the foam fractionation column only if the foam collapsed at the highest point. In the initial stage, the foam volume increased with time due to the availability of a large number of surfactant molecules in the aqueous solution. However, at the later stages, the aqueous solution became lean with the surfactant and foam stability decreased. As a result, the foam volume decreased. After some time, the top portion of the foam was very dry, and the foam began to distort. Solid flakes of CTAB were formed at this stage.

The variation in the foam volume with time in the presence of salts at different airflow rates is shown in Figures 3.8–3.10. The volume of foam increased with increasing airflow rate.

The foam volume was higher in the absence of the salts. However, with increasing salt concentration, the foam volume decreased, due to the reduction in their stability, as discussed in Section 3.1. At the low airflow rates, the foam volume increased slowly. This ensured that the foam, close to the highest point of the column, had an adequate time to dry and ultimately distort when its age exceeded 1 h. The effectiveness of the salts in reducing the foam volume followed the sequence: NaCl < $CaCl_2$ < Na_2SO_4.

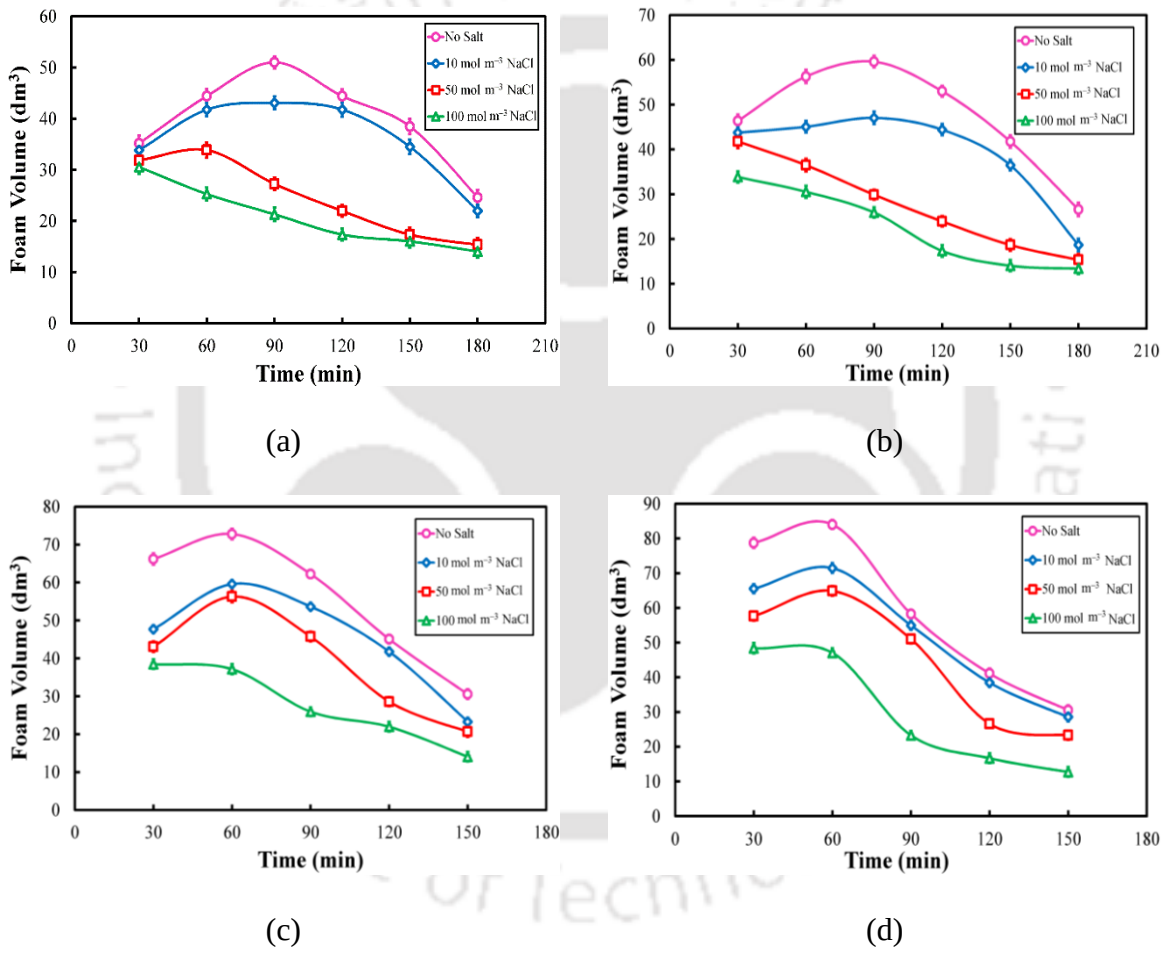

Figure 3.8 The effect of NaCl on foam volume at different airflow rates: (a) 0.4, (b) 0.8, (c) 1.2, and (d) 1.6 dm^3 min^{-1}.

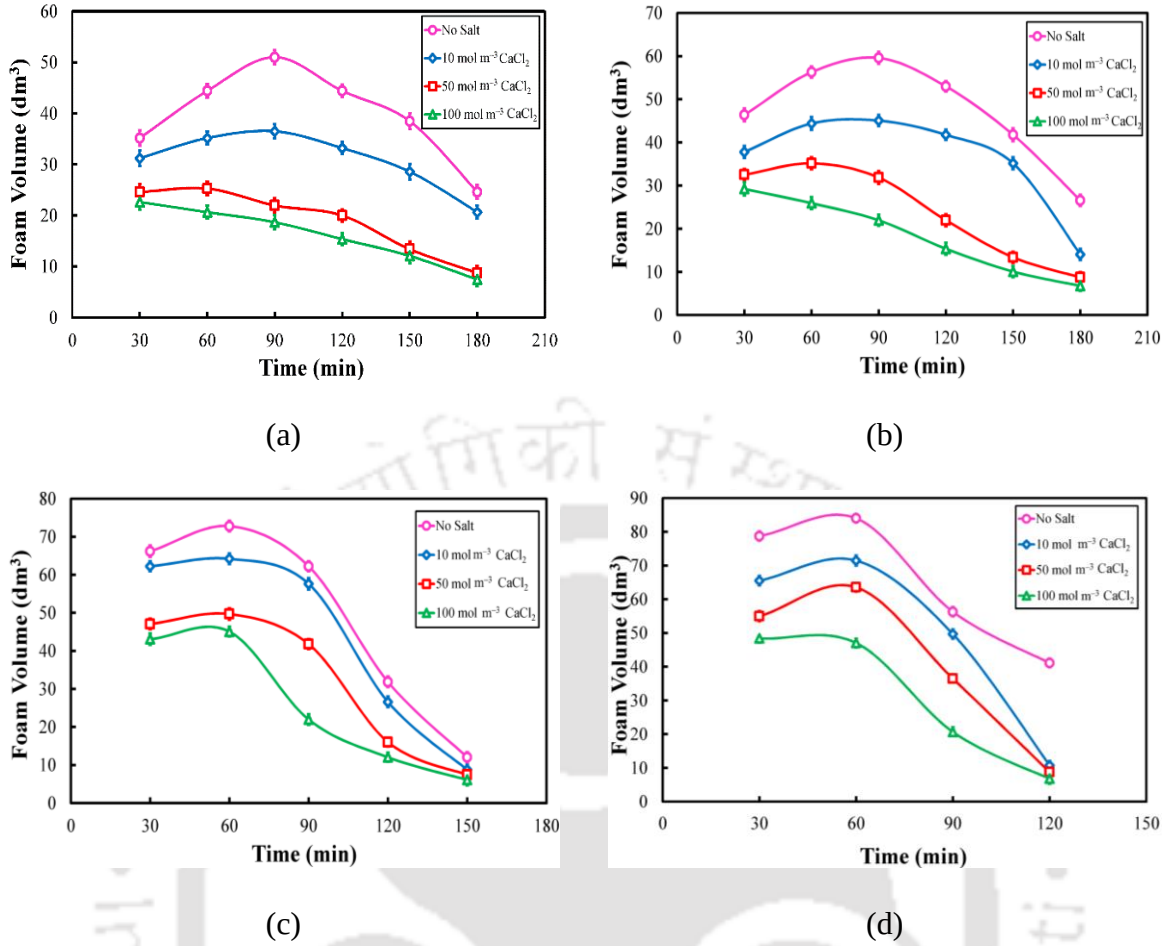

Figure 3.9 The effect of $CaCl_2$ on foam volume at different airflow rates: (a) 0.4, (b) 0.8, (c) 1.2, and (d) 1.6 dm^3 min^{-1}.

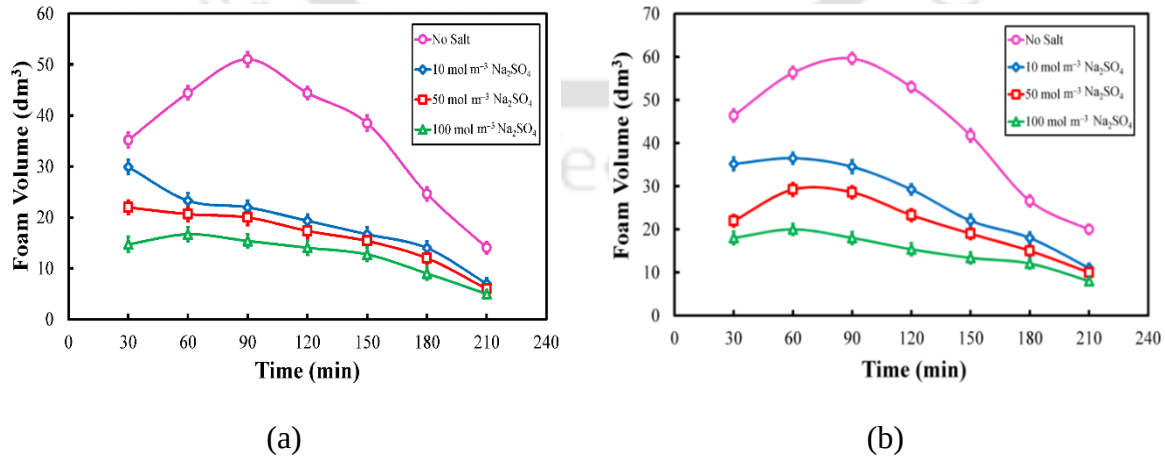

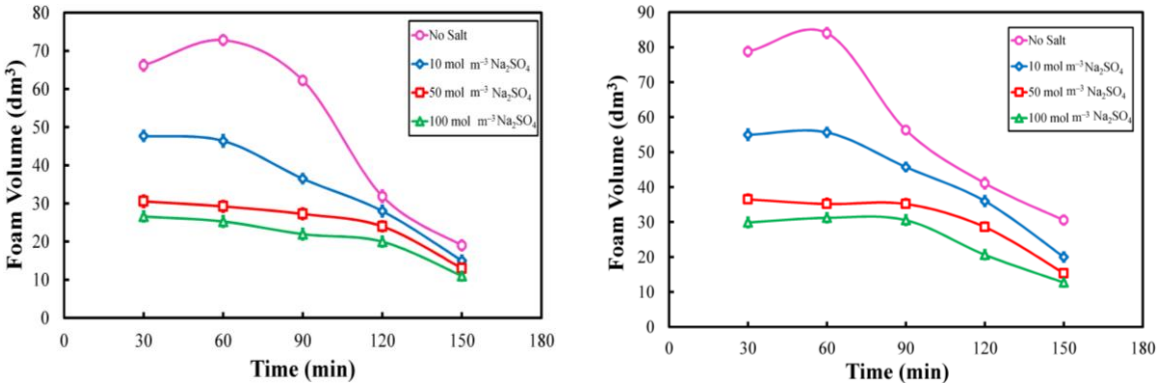

(c) (d)

Figure 3.10 The effect of Na_2SO_4 on foam volume at different airflow rates: (a) 0.4, (b) 0.8, (c) 1.2, and (d) 1.6 dm^3 min^{-1}.

3.2.4. Water recovery

Water recovery is an important aspect of foam fractionation. The recovery of water facilitates its reuse. Just a small amount of water was lost in this process. Overall, the water recovery was good. The feed solution subjected to foam fractionation was 500 cm^3. About 495 cm^3 water was recovered in the absence of salt at the lowest airflow rate. The formation of foam was more at the higher flow rates, which caused a slightly higher water loss. It was observed that the water recovery was almost similar in the presence of all three salts (i.e., NaCl, $CaCl_2$, and Na_2SO_4).

3.3. Conclusions

The present work demonstrates the removal and recovery of a cationic surfactant (i.e., CTAB) from the aqueous medium by using foam fractionation. The concentration of CTAB in the solution was very high (i.e., five times its CMC). It was recovered as a wet solid paste. Based on the experimental findings, the following conclusions have been reached:

- The CTAB concentration in the aqueous phase steadily decreased with time.

- The surfactant recovery and foam volume increased with increasing airflow rate.
- The recovery of the surfactant decreased in the presence of salt due to the collapse of the foam.
- The foam volume and surfactant recovery both decreased with increasing salt concentration. The effectiveness of the salts in reducing the surfactant recovery followed the sequence: $NaCl < CaCl_2 < Na_2SO_4$.
- Since the surfactant concentration was far above its CMC, the addition of salt did not have much effect on the surface tension.
- The zeta potential decreased with increasing salt concentration. The zeta potential was highest in the presence of NaCl, and lowest for Na_2SO_4.
- The water recovery was excellent in all systems studied in this work.

Nomenclature

Symbols

r	radius of the bubble, m
R	gas constant, J mol^{-1} K^{-1}
T	temperature, K
k	Boltzmann's constant, J K^{-1}
z	valence of ion

Greek letters

γ	surface tension, N m^{-1}
γ_0	surface tension of pure water, N m^{-1}
ε	dielectric constant of the medium
ε_0	permittivity of free space, C^2 J^{-1} m^{-1}
κ	Debye–Hückel parameter, m^{-1}
Π	disjoining pressure in the thin liquid film, Pa
Π_{vdW}	disjoining pressure due to the van der Waals force, Pa
Π_{EDL}	disjoining pressure due to electrostatic double layer force, Pa
Π_{SR}	disjoining pressure due to the short-range repulsive forces (e.g., the hydration force), Pa
ψ_0	potential at the surface (or interface), V
ρ	recovery

References

[1] Y. Yangxin, Z. Jin, A.E. Bayly, Development of surfactants and builders in detergent formulations, Chin. J. Chem. Eng. 16 (2008) 517–527.

[2] L.D. Rhein, M. Schlossman, A. O'Lenick, P. Somasundaran, Surfactants in personal care products and decorative cosmetics, CRC Press, Boca Raton, 2006.

[3] I. Kralova, J. Sjöblom, Surfactants used in food industry: a review, J. Dispersion Sci. Technol. 30 (2009) 1363–1383.

[4] C. Hill, A. Czajka, G. Hazell, I. Grillo, S.E. Rogers, M.W. Skoda, N. Joslin, J. Payne, J. Eastoe, Surface and bulk properties of surfactants used in fire-fighting, J. Colloid Interface Sci. 530 (2018) 686–694.

[5] M.C. Brum, J.F. Oliveira, Removal of humic acid from water by precipitate flotation using cationic surfactants, Miner. Eng. 20 (2007) 945–949.

[6] F. Aloui, S. Kchaou, S. Sayadi, Physicochemical treatments of anionic surfactants wastewater: effect on aerobic biodegradability, J. Hazard. Mater. 164 (2009) 353–359.

[7] A. Saint-Jalmes, Physical chemistry in foam drainage and coarsening, Soft Matter 2 (2006) 836–849.

[8] J.L. Joye, G.J. Hirasaki, C.A. Miller, Dimple formation and behavior during axisymmetrical foam film drainage, Langmuir 8 (1992) 3083–3092.

[9] P. Stevenson, Foam engineering: fundamentals and applications, John Wiley & Sons, West Sussex, 2012.

[10] A. Bhakta, E. Ruckenstein, Decay of standing foams: drainage, coalescence and collapse, Adv. Colloid Interface Sci. 70 (1997) 1–124.

[11] L.L. Schramm, Foams: fundamentals and applications in the petroleum industry, American Chemical Society, Washington DC, 1994.

[12] R.G. Horn, L.A. Del Castillo, S. Ohnishi, Coalescence map for bubbles in surfactant-free aqueous electrolyte solutions, Adv. Colloid Interface Sci. 168 (2011) 85–92.

[13] S.S. Srinet, A. Basak, P. Ghosh, J. Chatterjee, Separation of anionic surfactant in paste form from its aqueous solutions using foam fractionation, J. Environ. Chem. Eng. 5 (2017) 1586–1598.

[14] T.O. Oolman, H.W. Blanch, Bubble coalescence in stagnant liquids, Chem. Eng. Commun. 43 (1986) 237–261.

[15] P. Ghosh, Colloid and interface science, PHI Learning Pvt. Ltd., New Delhi, 2009.

[16] J.N. Israelachvili, Intermolecular and surface forces, Academic Press, London, 2011.

[17] J.N. Israelachvili, H. Wennerstroem, Hydration or steric forces between amphiphilic surfaces?, Langmuir 6 (1990) 873–876.

[18] M.J. Rosen, J.T. Kunjappu, Surfactants and interfacial phenomena, John Wiley & Sons, New York, 2012.

[19] M. Kumar, P. Ghosh, Coalescence of air bubbles in aqueous solutions of ionic surfactants in presence of inorganic salt, Chem. Eng. Res. Des. 84 (2006) 703–710.

[20] K. Kumpabooth, J.F. Scamehorn, S. Osuwan, J.H. Harwell, Surfactant recovery from water using foam fractionation: effect of temperature and added salt, Sep. Sci. Technol. 34 (1999) 157–172.

[21] G. Trefalt, T. Palberg, M. Borkovec, Forces between colloidal particles in aqueous solutions containing monovalent and multivalent ions, Curr. Opin. Colloid Interface Sci. 27 (2017) 9–17.

[22] G. Trefalt, S.H. Behrens, M. Borkovec, Charge regulation in the electrical double layer: ion adsorption and surface interactions, Langmuir 32 (2015) 380–400.

Chapter 4

Removal and Recovery of an Anionic Surfactant from its Aqueous Solution by Foam Fractionation

Published article: A.K. Kumar, P. Ghosh, Recovery of an anionic surfactant in the presence of benzene, toluene, and hexane by foam fractionation, Int. J. Environ. Sci. Technol. (2021). Doi:10.1007/s13762-021-03796-z

CHAPTER 4

REMOVAL AND RECOVERY OF AN ANIONIC SURFACTANT FROM ITS AQUEOUS SOLUTION BY FOAM FRACTIONATION

4.1. Introduction

Anionic surfactants are widely used in enhanced oil recovery due to their low cost, ability to reduce the interfacial tension (IFT) between the trapped crude oil and water and adsorb on the oil-wet surface [1]. One of the biggest issues in wastewater treatment is dealing with new pollutants like the surfactants. Surfactants are a particularly challenging group of pollutants to deal with. This is due to their widespread use and variety, as well as their harmful impact on the environment.

With people realizing the great importance of environmental protection, the treatment and reuse of industrial wastewater have become an essential issue. Treatment of contaminated water for its recycling is essential because clean water is the basic need of human life. Oil mixed with surfactants is a major concern for wastewater treatment. The proficient removal of toxic surfactants and oil is difficult because of the high cost and complication involved in the removal techniques. The main objective of this research was to examine the removal and recovery of an anionic surfactant (i.e., sodium dodecyl sulfate, SDS) in the presence of benzene, toluene, and hexane. This study also investigates the adsorption of the surfactant at the air–water interface, which was analyzed through the surface tension measurements. The effects of oil on surfactant recovery were also studied. The foam stability was analyzed by zeta potential and the entering, spreading, and bridging coefficients. A rigorous study of the impacts of several parameters such as airflow rate, foam volume of the surfactant solution, oil type, and time on the removal and recovery of the surfactant has been performed.

4.2. Results and Discussion

4.2.1. Foam volume

The experiments were conducted at a concentration of SDS (i.e., 3000 mg dm^{-3}) that was above its CMC (i.e., 2364.7 mg dm^{-3}). The volume of foam was primarily controlled by the airflow rate and the oil's physicochemical properties. Oils and surfactants are generally present in the groundwater in varied quantities. Oils such as benzene, toluene, and hexane come to wastewater from the industrial effluents, whereas surfactants usually appear in the wastewater from domestic as well as industrial effluents. These oils-based SDS solutions are resilient to precipitation. However, these oils decrease the volume of foam significantly [2].

The formation of foam depends on the adsorption of the surfactant molecules at the air–water interface. In the present study, the dry polyhedral bubbles was present at the upper part of the column, whereas wet foam containing spherical bubbles was present at the base of the column. The foam was spread over the column due to the continuous flow of the air through the surfactant solution. In the beginning, the volume of foam increased with time, caused by a higher concentration of the surfactant in the solution. Nevertheless, after some time, the surfactant concentration was depleted, resulting in decreased stability of the foam film. Consequently, the volume of foam was reduced. After approximately 60 min, the foam column's highest stage became very dry, and it started to shrink. Solid flakes of SDS started to appear at this time.

Figure 4.1 shows the effect of benzene, toluene, and hexane on foam volume at various airflow rates. As the airflow rate increased, the foam volume also increased. The foam film's stability has a profound impact on the foam volume. It mainly depends on the SDS concentration, its capability to stabilize the foam film, and the antifoaming effect of the oil. The strength of the foam film is controlled by the van der Waals (vdW), electrostatic double layer (EDL), hydrophobic, and hydration forces as its thickness become ~50 nm [3]. The net

disjoining pressure (Π) developed in the thin foam film has been described in Section 3.2.1. The films drain under the combined effect of disjoining pressure and the pull at the Plateau borders. Consequently, the film thinning relies on the concentration of the surfactant and the presence of oil. At the higher concentration of the surfactant, ions in the film impart an osmotic pull to transfer the molecules of water from the bulk to the film, which stabilizes the foam film [4]. The attractive hydrophobic force, in the presence of the oils, tries to merge the two interfaces, leading to the rupture of the film.

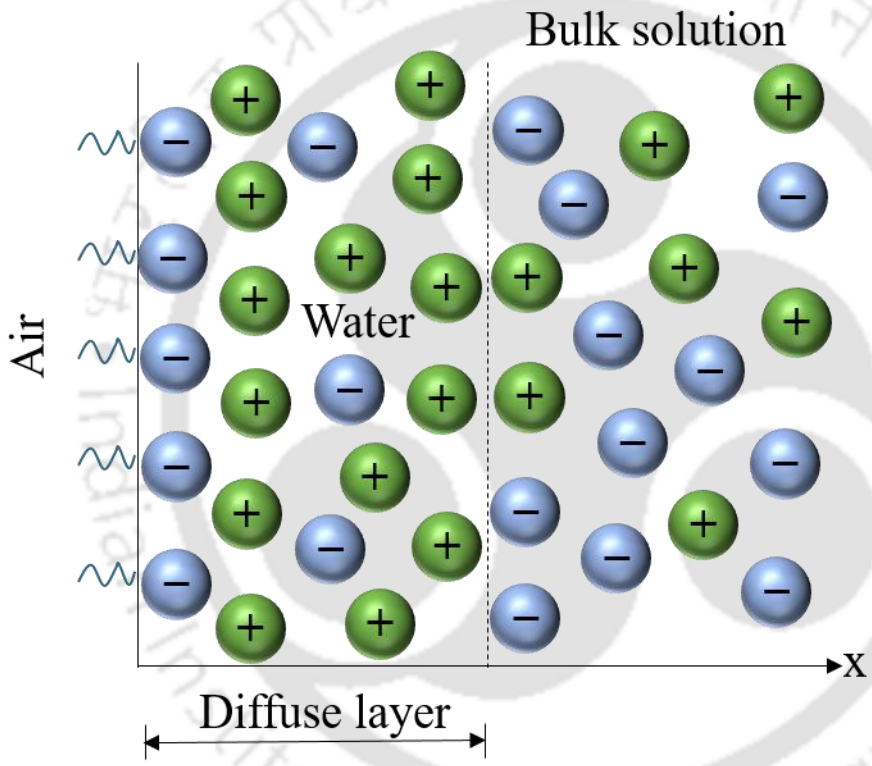

Figure 4.1 The EDL when an anionic surfactant is adsorbed at a flat air–water interface.

The initial volume of foam significantly decreased in the oil-based surfactant solutions due to the reduction in their stability. The most stable foam was formed in the absence of the oils. However, in their presence, the foams collapsed rapidly after generation. The success of foam fractionation is adversely affected by this phenomenon [5]. The stability of the foam in the oil-based surfactant solution relies on the pseudoemulsion film developed between the oil and the air [6]. The oil droplet enters the film during the formation of foam. This entering point

has a crucial role in film stability. Firstly, the droplet of oil enters the lamella and the Plateau border of the foam film. After that, it spreads simultaneously on the foam lamella and disrupts the capability of the surfactant to stabilize the foam film [7]. The spreading of oil in the foam lamella removes the surfactant molecules and leads to the Marangoni effect. It appears due to the mass transfer along the interface due to a gradient of interfacial tension. According to spreading mechanism, the oil spreads quickly across the foam film surface and enhances its thinning and subsequently leads to its rupture [8]. Capillary waves of large amplitude and wavelength are developed due to the spreading of the oil, leading to the shrinkage of the thin film. The spreading of oil decreases the surface tension of the liquid. It increases the radius of curvature while altering the surface viscosity and surface elasticity, triggering the foam film to reduce its strength [9]. The foam film ruptures when a few droplets of oil are trapped in the Plateau border of the film. These droplets obstruct the flow of the aqueous solution near the Plateau border, resulting in the reduction of the film thickness. Due to this, the pseudoemulsion film's radius increases, which causes the collapse of the foam film. Thus, the oil droplets present in the Plateau border and foam lamella play a key role in determining the stability of the foam. Damage to the foam film in the presence of oil can also take place due to the bridging–dewetting [10]. Penetration of the oil produces an oil channel between the foam lamellae. The hydrophobic oil leads to dewetting, leading to the rupture of the thin foam film [8].

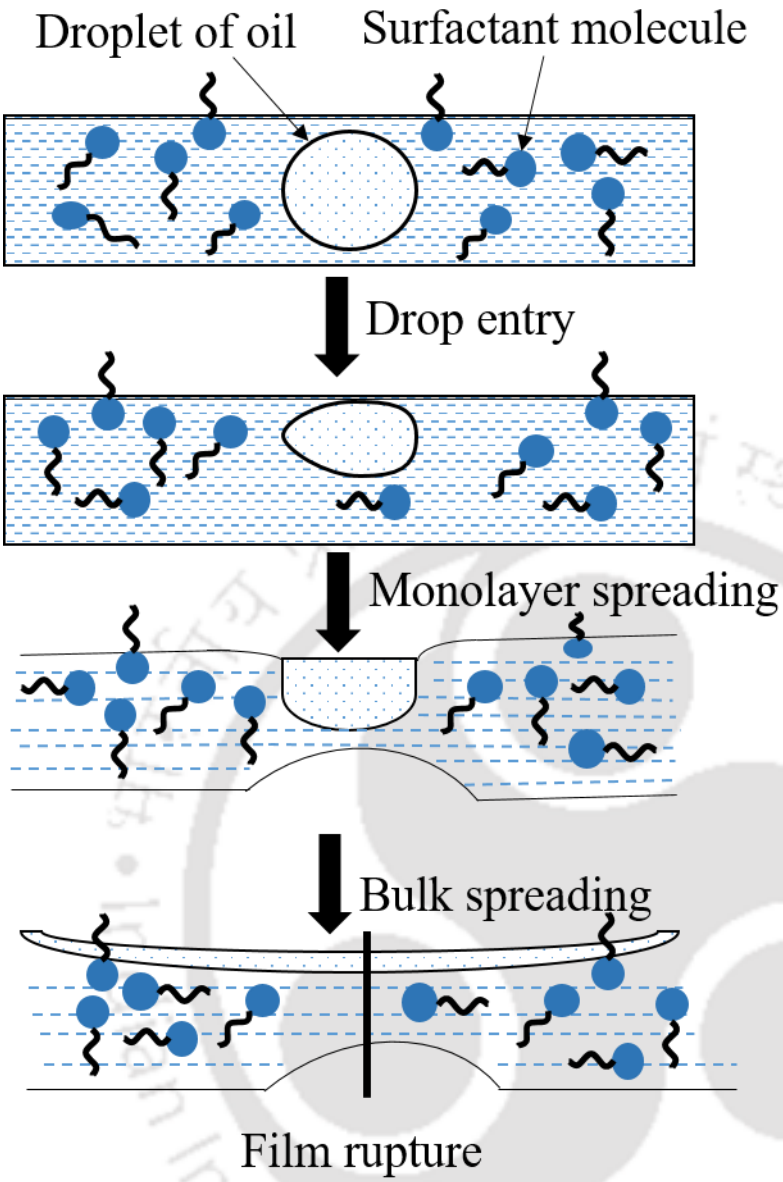

Figure 4.2 Schematic presentation of the spreading-oil entrainment mechanism of foam film rupture.

There are three main mechanisms, which govern the destabilization of the foam film in the presence of oil [5], i.e., (a) weakening of aqueous film caused by the entry of the oil droplet into the air–water interface, (b) spreading of the oil on the air–water interface, and (c) development of an unstable bridge across the foam lamella. The stability of foam in the presence of oil can be analyzed by the entering (*E*), spreading (*S*), and bridging (*B*) coefficients [11]. *E*, *S*, and *B* are defined in terms of the surface and interfacial tensions as follows:

$$E = \sigma_{aw} + \sigma_{wo} - \sigma_{oa} \tag{4.1}$$

$$S = \sigma_{aw} - \sigma_{wo} - \sigma_{oa} \tag{4.2}$$

$$B = \sigma_{aw}^2 + \sigma_{wo}^2 - \sigma_{oa}^2 \tag{4.3}$$

where σ_{aw} is the surface tension between air and water, σ_{wo} is the interfacial tension between water and oil, and σ_{oa} is the surface tension between oil and air. These three coefficients determine the thermodynamic stability of the foam film in the presence of oil [12]. The foam film's stability reduces with the increasing values of all three coefficients.

Table 4.1 Entering, spreading, and bridging coefficients in the presence of oil

Oil	*E* ($mN\ m^{-1}$)	*S* ($mN\ m^{-1}$)	*B* ($mN^2\ m^{-2}$)
Benzene	11.8	1.4	427.8
Toluene	12.7	1.6	508.0
Hexane	18.3	12.7	805.9

The entry of the oil droplet into the air–water interface is essential for shrinking the foam lamella. Equation (4.1) indicates that a positive value of the entering coefficient will lead to the diffusion of oil into the air–water interface. Equation (4.2) indicates that a positive spreading coefficient leads to the spread of the oil droplet on the air–water interface. If both these equations are satisfied in such a way that the droplets of oil can occupy the air–water interface, the shrinkage of the film may occur. Once the droplet of oil enters the air–water interface, it must be spread easily on the film's surface. The spreading of the droplet of oil over the surface of the film pushes the liquid from the foam film into the Plateau borders, and then the film becomes thin, which may lead to its rupture [5]. Equation (4.3) defines the bridging coefficient. If *B* is positive, then it will be unstable, and the rupture of foam film will occur. In case of no spreading (i.e., $S < 0$), a lens between the air–water interfaces will develop by the

droplet of oil, which will rupture the foam film eventually [13]. Therefore, a positive value of *B* predicts an unstable film, whereas a negative value of *B* predicts a stable film.

The values of *E*, *S*, and *B* were positive for the surfactant solutions containing oil (Table 4.1). These values clearly justify the results that the presence of oil destabilized the foam film, reduced its volume in the foam fractionation column, and eventually led to a lower surfactant recovery. Hexane has the largest values of all three coefficients (i.e., *E*, *S*, and *B*). Therefore, it showed a substantial destabilizing effect on the foam. The foam volume in the presence of oil was in the following order: benzene < toluene < hexane.

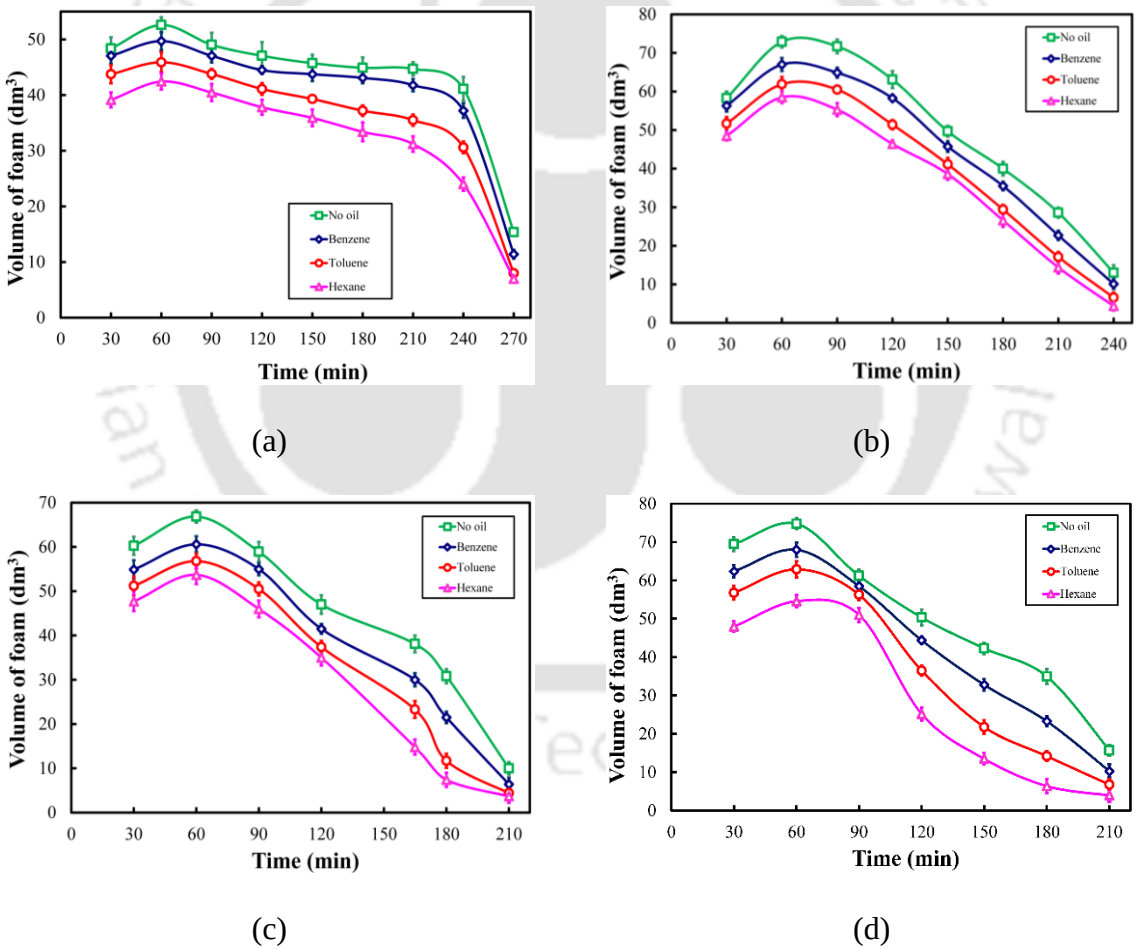

Figure 4.3 The effects of benzene, toluene, and hexane on foam volume at various airflow rates: (a) 0.4, (b) 0.8, (c) 1.2, and (d) 1.6 dm^3 min^{-1}.

4.2.2. Surfactant concentration profiles

The SDS concentration profiles showing the effects of benzene, toluene, and hexane are shown in Figure 4.4. The study was done without oil also. The SDS molecules adsorbed on the surface of the foam bubbles at the time of foam generation. The surfactant was stripped from the aqueous phase as the bubbles carried them upward [14]. It caused a gradual drop in the surfactant concentration in the aqueous solution with time. The foam at the top of the column had sufficient drying time, and surfactant flakes formed there. The foam finally collapsed once its age surpassed ~1 h. The concentration of SDS in the aqueous phase was reduced more with increasing airflow rate. This apparently happened because of more foam formation and adsorption of an increasing number of SDS molecules at the air–water interface.

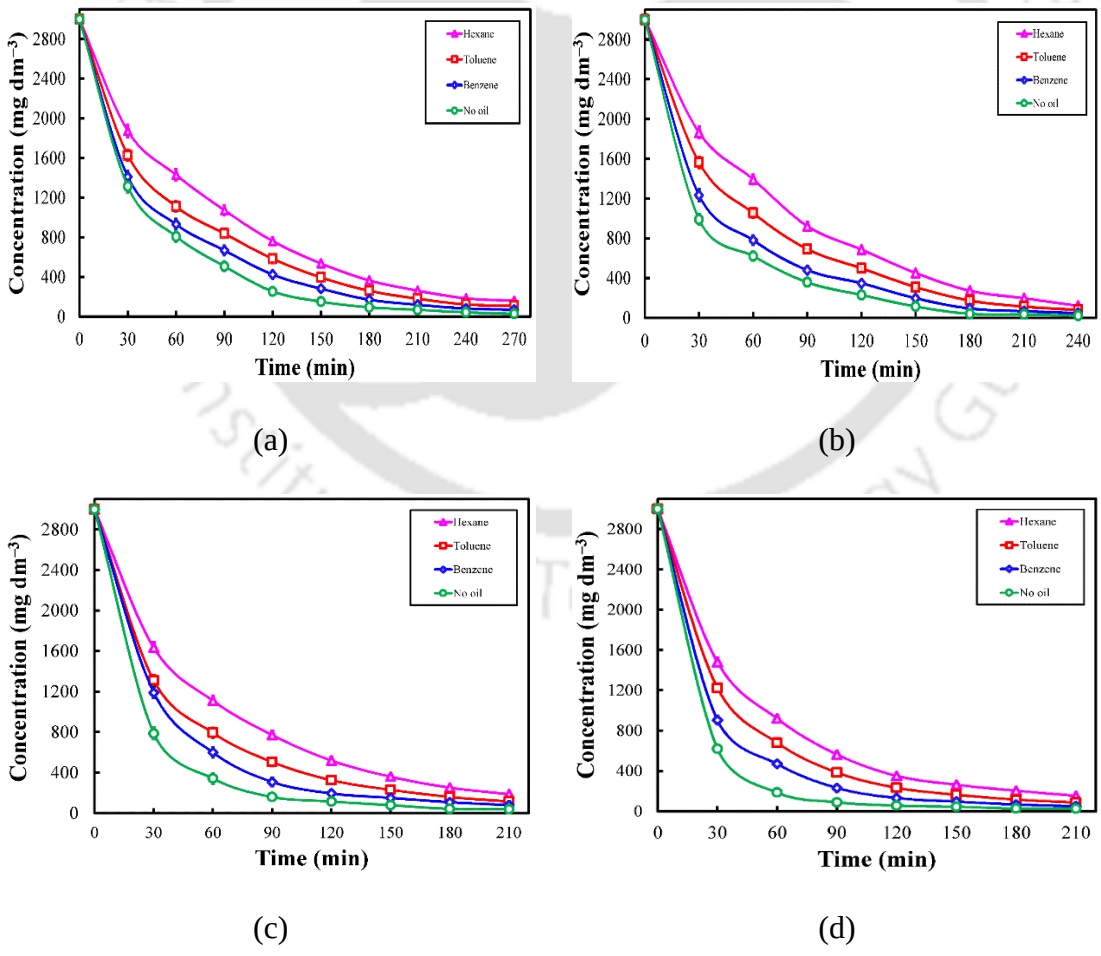

Figure 4.4 The effects of benzene, toluene, and hexane on the SDS concentration at various airflow rates: (a) 0.4, (b) 0.8, (c) 1.2, and (d) 1.6 dm^3 min^{-1}.

The concentration profiles of the oil-based surfactant systems were similar. However, the foam was less stable in the presence of oils. With the addition of oil, the stability of foam decreased. The concentration profiles of benzene and toluene decreased more with time as compared to hexane. The SDS concentration in the solution increased in the following order: benzene < toluene < hexane. These results are directly related to the foam volume and stability, as explained in the section titled "Foam volume".

4.2.3. Surface tension of the aqueous solutions

The surface tension of the aqueous surfactant solution plays a significant role during foam generation. In general, an aqueous surfactant solution having a lower surface tension is more suitable for foam generation. Consequently, a surfactant that reduces the surface tension considerably and produces more foam is ideal for recovery using the foam fractionation technique. The surface tension of the feed solution was monitored before the start of the experiment. It was 33.3 mN m^{-1} for aqueous SDS solution in the absence of oil, and 34.6, 36.2, and 36.8 mN m^{-1} in the presence of benzene, toluene, and hexane, respectively. The surface tension of the surfactant solutions (with and without oil) after the experiments are reported in Table 4.2. The effect of the oils followed a similar trend inasmuch as the highest surface tension reduction was observed in the presence of hexane. The effect of the oils followed a similar trend inasmuch as the highest surface tension reduction was observed in the presence of hexane. The surface tension increased with increasing airflow rate. This occurred because of the increase in the stripping of the SDS molecules from the aqueous phase. The adsorption of the SDS molecules at the air–water interface was reduced due to the presence of oil. The ability of the oils to reduce the surface tension followed the sequence: benzene < toluene < hexane.

Table 4.2 Surface tension of the oil-based surfactant solutions at different airflow rates (after the experiments)

Oil	*Airflow rate ($dm^3\ min^{-1}$)*	*Surface tension ($mN\ m^{-1}$)*
No oil	0.4	37.5
	0.8	38.9
	1.2	41.0
	1.6	43.1
Benzene	0.4	38.4
	0.8	39.2
	1.2	41.0
	1.6	43.2
Toluene	0.4	39.2
	0.8	41.1
	1.2	43.7
	1.6	47.3
Hexane	0.4	40.1
	0.8	42.5
	1.2	47.9
	1.6	49.5

4.2.4. Zeta potential at the air–water interface

The zeta potential is a key parameter for the stability of the foam stabilized by an ionic surfactant. It is a measure of the charge developed at the air–water interface. A higher degree of electrostatic repulsion between the two air–water interfaces that constitute the foam lamellae results in higher foam stability. The zeta potential at the interface for the SDS solution in the

absence of oil, measured at the beginning of the experiment, was –98.8 mV. It was –84.7, –81.5, and –71.9 mV in the presence of benzene, toluene, and hexane, respectively. Evidently, the zeta potential decreased in the presence of oil.

The zeta potentials of the oil-based surfactant solutions after the experiments are reported in Table 4.3. It reduced with increasing airflow rate due to the increase in the removal of SDS from the aqueous phase. The zeta potential was high in the absence of oil, which signifies the better stability (and higher volume) of the foam. The zeta potentials in the aqueous systems in the presence of oil were in the following sequence: benzene > toluene > hexane.

Table 4.3 Zeta potential of the oil-based surfactant solutions at different airflow rates (after the experiments)

Oil	*Airflow rate (dm^3 min^{-1})*	*Zeta potential (mV)*
No oil	0.4	–62.9
	0.8	–56.2
	1.2	–48.5
	1.6	–39.7
Benzene	0.4	–44.1
	0.8	–36.3
	1.2	–23.0
	1.6	–18.4
Toluene	0.4	–34.0
	0.8	–26.4
	1.2	–19.4
	1.6	–15.5

Hexane	0.4	–23.7
	0.8	–18.3
	1.2	–16.7
	1.6	–11.6

4.2.5. Surfactant recovery

The recovery of the surfactant is crucial for reusing it. It is described in Section 3.2.2. As mentioned in the section titled "Surfactant concentration profiles", a substantial amount of wet solid flakes of SDS was recovered at the column's top section. An insignificant amount of surfactant remained in the lamellae of foam that could not be recovered. Figure 4.5 depicts that approximately 72% of the surfactant was recovered in the absence of oil. The surfactant recovery decreased in the presence of oil, which was due to the reduction in the stability of the foam. The recovery was significantly increased at the higher airflow rates (i.e., 1.2 and 1.6 dm^3 min^{-1}). The larger volume of foam produced at the higher airflow rates caused more surfactant molecules to adsorb on their surface, which led to higher recovery. The effect of the oil in decreasing the surfactant's recovery followed the order: benzene < toluene < hexane.

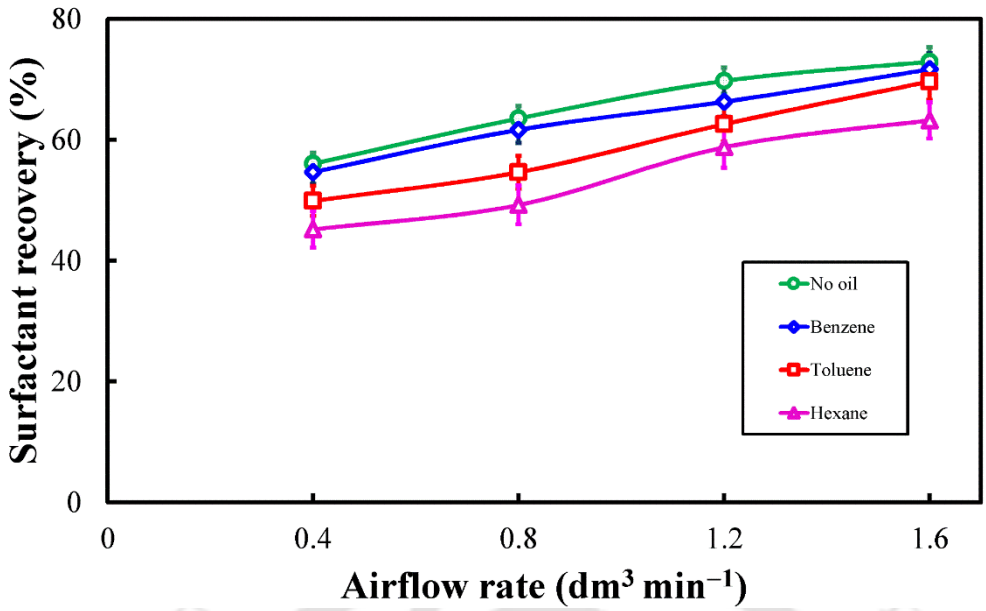

Figure 4.5 The effect of different airflow rates on the recovery of surfactant in the presence of benzene, hexane, and toluene.

4.2.6. Water recovery

Water recovery is a significant parameter in foam fractionation. The water recovery can ensure its reuse. Only a slight amount of water was lost during the experiment. The feed used in the experiments contained 400 cm^3 water and 10 cm^3 oil. About 385 cm^3 (i.e., ~97.5%) water was recovered in the process. The presence of oil did not have a significant influence on water recovery. It was noticed that the recovery of water was nearly equal in the presence of benzene, toluene, and hexane. At the high airflow rates (e.g., 1.6 dm^3 min^{-1}), the formation of foam was more effective, which triggered a slightly higher loss of water.

4.3. Conclusions

The present study reports the removal and recovery of SDS from its aqueous solution in the presence and absence of oil using foam fractionation. The SDS concentration in the aqueous solution was well-above its CMC. The recovered SDS was in the solid paste form. The following conclusions have been drawn based on the experimental findings:

- SDS showed good foamability in the absence of the oils. The foam volume reduced in the presence of oil in the following sequence: benzene < toluene < hexane. The entering, spreading, and bridging coefficients were positive. These values indicate that the oils had a destabilizing effect on the foam.
- The foam volume increased with increasing airflow rate because of the formation of more air bubbles.
- The SDS concentration in the aqueous solution decreased with time. The effect of oil on SDS concentration in the aqueous phase was in the following sequence: benzene < toluene < hexane.
- The surface tension of the surfactant solution was measured before the start of the experiments, as well as after their completion. The surface tension increased with increasing airflow rate.
- The zeta potential at the air–water interface was measured before and after the completion of the experiment. It decreased with increasing airflow rate. It was highest in the presence of benzene and lowest for hexane.
- A good amount of surfactant was recovered by this process. The oil's effect in the surfactant recovery was in the following sequence: benzene < toluene < hexane.
- The recovery of water was good in all the experiments performed in this study.

Nomenclature

Symbols

E	entering coefficient, mN m^{-1}
S	spreading coefficient, mN m^{-1}
B	bridging coefficient, mN^2 m^{-2}

Greek letters

σ_{aw}	the surface tension between air and water, mN m^{-1}
σ_{wo}	the interfacial tension between water and oil, mN m^{-1}
σ_{oa}	the surface tension between oil and air, mN m^{-1}

References

[1] N. Saxena, A. Kumar, A. Mandal, Adsorption analysis of natural anionic surfactant for enhanced oil recovery: the role of mineralogy, salinity, alkalinity and nanoparticles, J. Pet. Sci. Technol. 173 (2019) 1264–1283.

[2] M.R. Behera, S.R. Varade, P. Ghosh, P. Paul, A.S. Negi, Foaming in micellar solutions: effects of surfactant, salt, and oil concentrations, Ind. Eng. Chem. Res. 53 (2014) 18497–18507.

[3] R.G. Horn, L.A. Del Castillo, S. Ohnishi, Coalescence map for bubbles in surfactant-free aqueous electrolyte solutions, Adv. Colloid Interface Sci. 168 (2011) 85–92.

[4] J.N. Israelachvili, Intermolecular and surface forces, Academic Press, London, 2011.

[5] K. Osei-Bonsu, N. Shokri, P. Grassia, Foam stability in the presence and absence of hydrocarbons: from bubble-to bulk-scale, Colloids Surf. A 481 (2015) 514–526.

[6] D. Exerowa, P.M. Kruglyakov, Foam and foam films: theory, experiment, application, Elsevier, Amsterdam, 1997.

[7] L.L. Schramm, Emulsions, foams, and suspensions: fundamentals and applications, John Wiley & Sons, Weinheim, 2006.

[8] E.S. Basheva, D. Ganchev, N.D. Denkov, K. Kasuga, N. Satoh, K. Tsujii, Role of betaine as foam booster in the presence of silicone oil drops, Langmuir 16 (2000) 1000–1013.

[9] L.L. Schramm, Surfactants: fundamentals and applications in the petroleum industry, Cambridge University Press, New York, 2000.

[10] P. Garrett, J. Davis, H. Rendall, An experimental study of the antifoam behaviour of mixtures of a hydrocarbon oil and hydrophobic particles, Colloids Surf. A 85 (1994) 159–197.

[11] J. Lee, A. Nikolov, D. Wasan, Stability of aqueous foams in the presence of oil: on the importance of dispersed vs solubilized oil, Ind. Eng. Chem. Res. 52 (2013) 66–72.

[12] C. Wang, H. Fang, Q. Gong, Z. Xu, Z. Liu, L. Zhang, L. Zhang, S. Zhao, Roles of catanionic surfactant mixtures on the stability of foams in the presence of oil, Energy Fuels 30 (2016) 6355–6364.

[13] R. Farajzadeh, A. Andrianov, R. Krastev, G. Hirasaki, W.R. Rossen, Foam–oil interaction in porous media: implications for foam assisted enhanced oil recovery, Adv. Colloid Interface Sci. 183 (2012) 1–13.

[14] M. Simjoo, T. Rezaei, A. Andrianov, P. Zitha, Foam stability in the presence of oil: effect of surfactant concentration and oil type, Colloids Surf. A 438 (2013) 148–158.

Chapter 5

Removal and Recovery of an Anionic Surfactant in the Presence of Alcohol by Foam Fractionation

Published article: A.K. Kumar, P. Ghosh, Removal and recovery of an anionic surfactant in the presence of alcohol by foam fractionation, Ind. Eng. Chem. Res. (2022). Doi: 10.1021/acs.iecr.2c00372

CHAPTER 5

REMOVAL AND RECOVERY OF AN ANIONIC SURFACTANT IN THE PRESENCE OF ALCOHOL BY FOAM FRACTIONATION

5.1. Introduction

Anionic surfactants are used in the production of a wide range of consumer goods. Their widespread domestic and industrial use and discharge into the waterbodies result in significant water contamination [1]. Foaming, the toxicity of the aquatic species, increased solubilization of pesticides, disruption in the auto-remediation of aqueous culture, and the absorption of oxygen into the waterbodies are some of the detrimental effects of their presence in the aqueous environments [2-4]. Organic solvents like alcohols and oils are the most popular additives in aqueous micellar solutions to generate diverse solubilized systems or microemulsions for a variety of chemical, medicinal, industrial, and technical applications [5, 6]. Oil, alcohol, and different types of impurities combined with the surfactants create a big concern for wastewater treatment due to the high cost and complexity of the removal methods.

The alcohol industry is one of the most popular among all industries and a key contributor in the world's economic growth. Unfortunately, these industries are also considered as one of the major sources of water and environmental pollution. It is one of the most alarming dangers that faces living beings including humans [7, 8]. Distillery industries produce a large volume of dark-colored effluent and large quantities of high-strength liquid effluents with high concentrations of organic matter due to ethanol fermentation. The major pollutant from distillery industries includes spent wash, fermenter cleaning, fermenter cooling, condenser

cooling, floor wash, and bottling plant. The presence of alcohol in the wastewater is highly toxic for the aquatic and the terrestrial eco-system. In aquatic resources, it reduces the penetration power of sunlight, causing a reduction in the photosynthetic activity of aquatic plants, and dissolved oxygen content in the water bodies. In the terrestrial regions, it causes genotoxic and phytotoxic effects on animal and plants, respectively.

In the present work, the effects of methanol and ethanol on the removal and recovery of an anionic surfactant [i.e., sodium dodecyl benzene sulfonate (SDBS)] by foam fractionation are presented. The effects of these alcohols on surfactant recovery were investigated. The adsorption of the surfactant was studied by surface tension measurements. The charge on the air–water interface was determined from the zeta potential measurements to assess the foam stability. The results were analyzed in terms of the airflow rate, foam volume, type of alcohol, and time.

5.2. Results and discussion

5.2.1. Foam volume

The experiments were carried out at 500, 1000, 2000, and 3000 mg dm^{-3} concentrations of SDBS. The CMC of the SDBS used in this work was 500 mg dm^{-3}. Therefore, the surfactant concentration ranged from the CMC to far above it. Methanol and ethanol were used to study the effect of alcohol at different surfactant concentrations. Experiments were also performed without the alcohols. The airflow rates were varied from 0.4 to 1.6 dm^3 min^{-1}. The run time of the experiment was in the range of 2 – 4 h. The foam volume mainly depended upon the concentration and type of the alcohols used. The interaction between the alcohol and surfactant molecules controls their adsorption at the air–water interface.

At the beginning of the experiment, the foam volume was high due to the high concentration of the surfactant molecules in the aqueous solution. The foam volume increased with the airflow rate as shown in Figure 5.1 for 500 mg dm^{-3} surfactant solution. The foam volume became almost constant after ~2 h of the runs at the lower airflow rates (i.e., 0.4 and 0.8 dm^3 min^{-1}). However, at the higher airflow rates (i.e., 1.2 and 1.6 dm^3 min^{-1}), the foam volume quickly reached its maximum. Thereafter, the foam volume decreased with time. After ~90 min, the decrease in foam volume with time was rather small. The foam fractionation experiments were conducted for 5 h, and the surfactant concentration decreased with time. The initial rate of foam formation was high, as shown by the foam volume profiles. During the foam fractionation experiments, the foam spread to fill the entire column. Although the foams were wet at the bottom of the column, the top portion of the foam became very dry after a while. The lamella of the foams drained and eventually ruptured. The foam began to crumble, leaving behind the slightly-wet flakes of the surfactant. A constant steady foam volume, as shown in Figure 5.1, confirms this fact. The foam volume profiles for 1000, 2000, and 3000 mg dm^{-3} SDBS solutions were similar, as depicted in Figures 5.2–5.4.

The volume of the foam increased in the presence of the alcohols. Alcohols are amphiphilic compounds (with an amphipathic structure). Like the surfactants, the alcohols are pushed to the interface from the bulk of the solution due to the hydrophobic effect. They are significantly adsorbed at the air–water interface. Due to the presence of a polar hydroxyl group (–OH) and a short non-polar hydrophobic aliphatic chain in their molecules, ethanol and methanol possess surface active properties. As a result, they reduce the surface tension of the aqueous phase. Alcohols are well-known for producing foams in beverages and flotation cells [9-11]. The use of alcohols in the food and minerals flotation industries confirms this fact [12]. The alcohols produce a ‘protective’ monolayer around the foam bubbles, preventing their coalescence [13]. Several water molecules are stacked in concentric hydration shells around

the polar groups of the alcohol molecules adsorbed at the air–water interfaces in the foam lamella [14]. The overlap of the hydration shells between the two interacting air–water interfaces originates the repulsion between them. To make room for the shrinking region, the hydrating water molecules need to escape as the surfaces approach closer, which is energetically unfavorable. This repulsion resulting from the hydration force is believed to play a major role in stabilizing foams in the alcohol solutions.

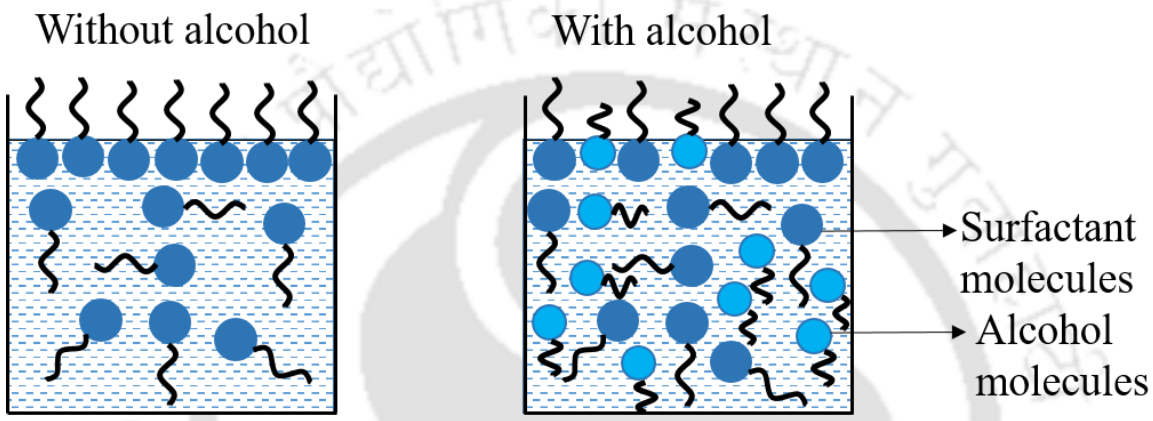

Figure 5.1 Adsorption of surfactant/alcohol molecules at air–water interface.

As the SDBS concentration increased, the amount of foam generation increased due to the availability of more surfactant molecules at the air–water interface. In Figure 5.2, ethanol increased the foam volume more than methanol due to the higher reduction of the surface tension [15]. In addition, ethanol has a higher molecular weight than methanol, which leads to its stronger adsorption [16]. The foam was destroyed when the lamella drained and eventually ruptured. As a result, the rate of foam formation at the bottom of the foam column equaled the rate of foam loss at the top after a certain period, thereby reaching a steady state operation. This was confirmed by a constant steady foam volume. In Figure 5.2 (c) and (d), the foam volume increased sharply within 30 min due to the high airflow rate. A similar phenomenon was observed in Figures 5.3 – 5.5.

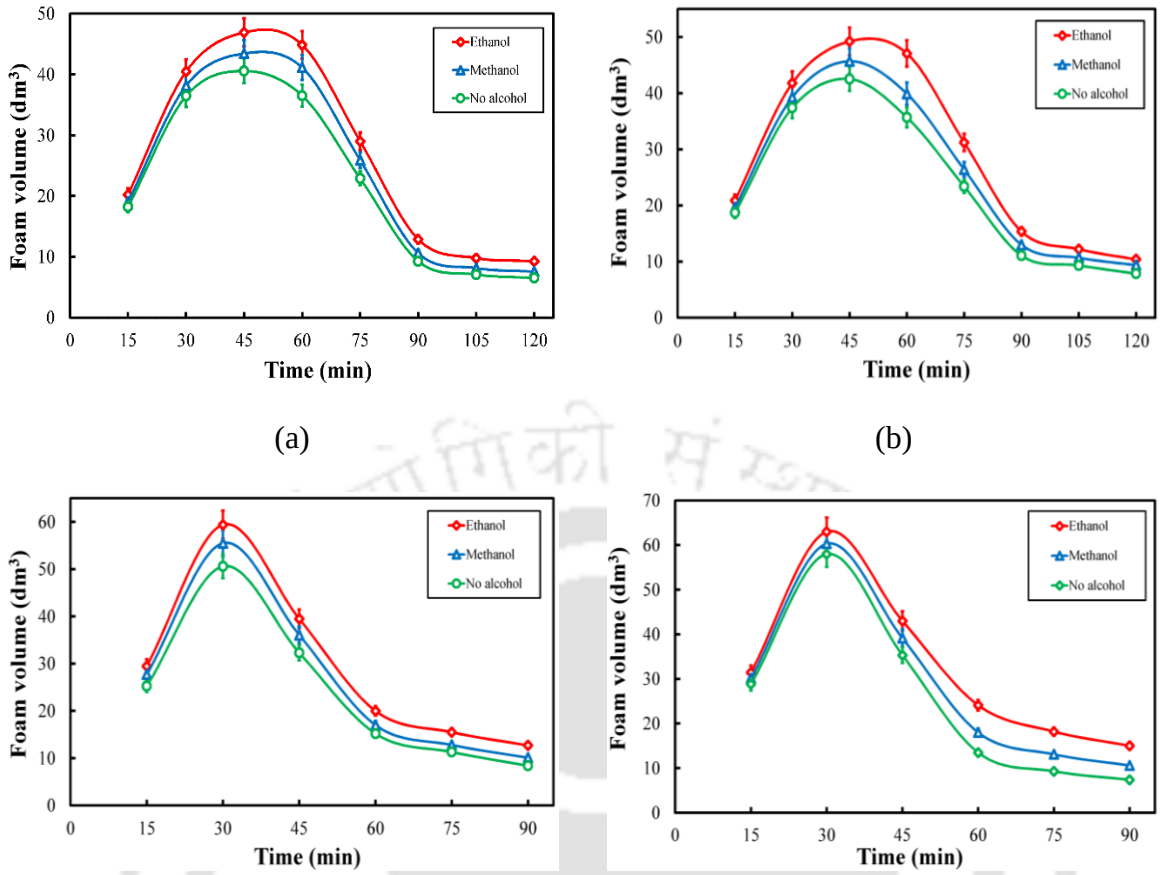

Figure 5.2 Variation of foam volume with time at different airflow rates at 500 mg dm^{-3} SDBS: (a) 0.4, (b) 0.8, (c) 1.2, and (d) 1.6 dm^3 min^{-1}.

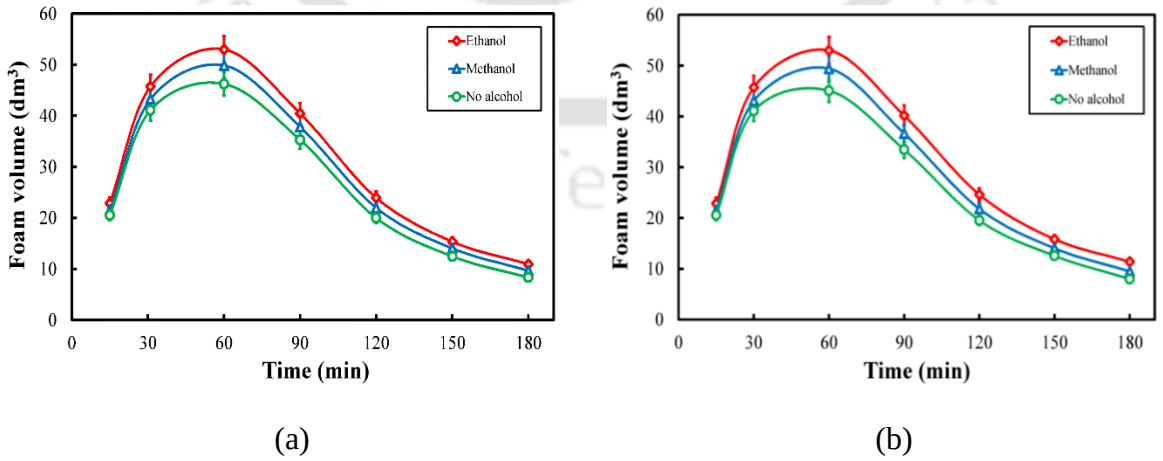

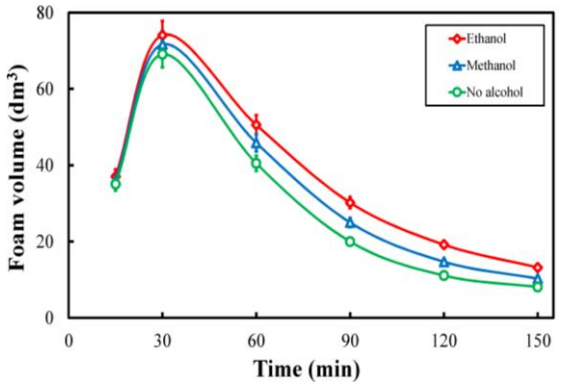

(c)

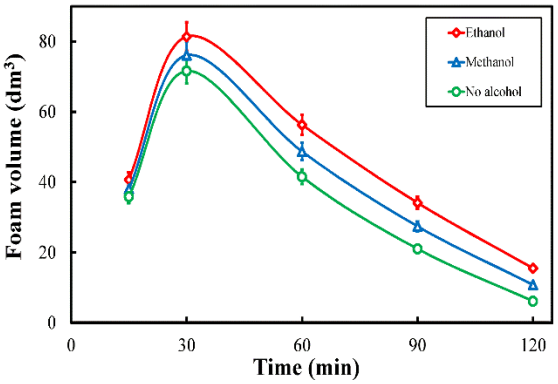

(d)

Figure 5.3 Variation of foam volume with time at different airflow rates at 1000 mg dm^{-3} SDBS: (a) 0.4, (b) 0.8, (c) 1.2, and (d) 1.6 dm^3 min^{-1}.

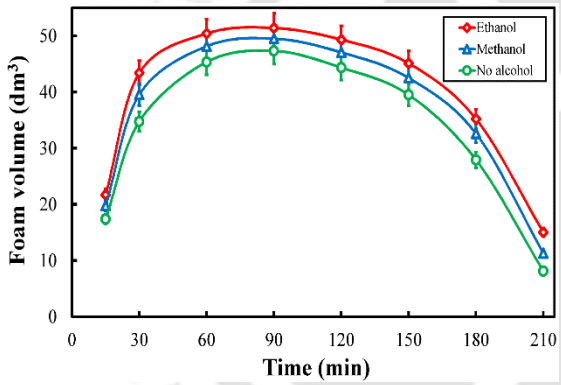

(a)

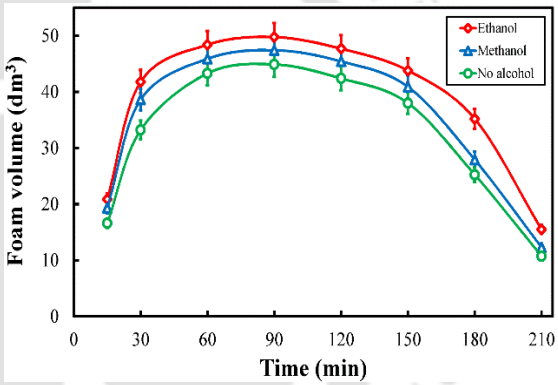

(b)

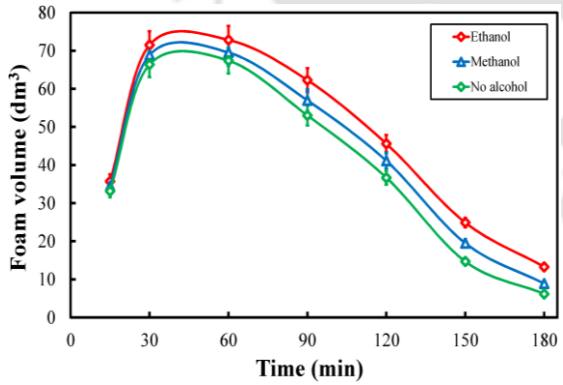

(c)

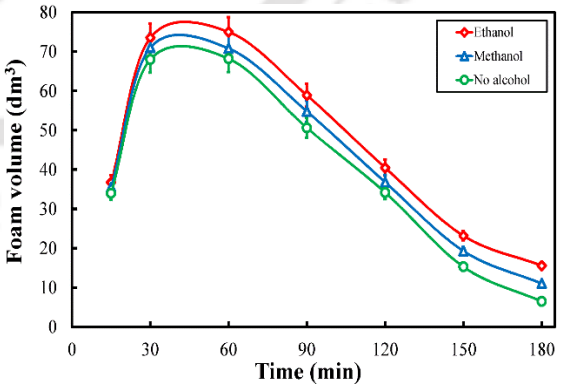

(d)

Figure 5.4 Variation of foam volume with time at different airflow rates at 2000 mg dm^{-3} SDBS: (a) 0.4, (b) 0.8, (c) 1.2, and (d) 1.6 dm^3 min^{-1}.

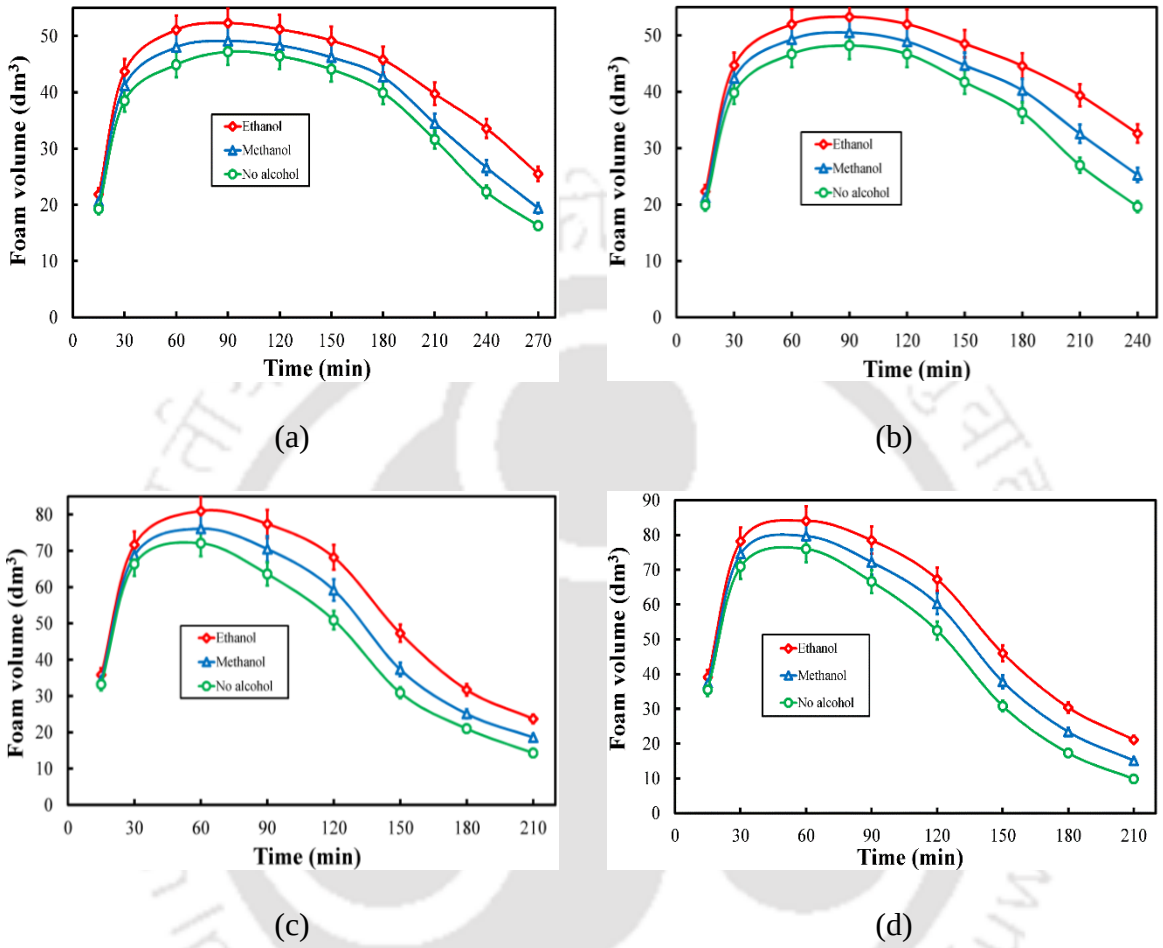

Figure 5.5 Variation of foam volume with time at different airflow rates at 3000 mg dm^{-3} SDBS: (a) 0.4, (b) 0.8, (c) 1.2, and (d) 1.6 dm^3 min^{-1}.

The variation in foam height over time, obtained from the Ross–Miles test [as per the ASTM Standard D1173–07 (2015)] at various surfactant concentrations is shown in Figure 5.6. Because the foam formed by this method is a dynamic phenomenon requiring rapid entrainment of air, the initial foam height (or volume) is an important parameter of foam production. The initial foam height increased with increasing surfactant concentration, as observed in Figure 5.6. This clearly demonstrated that the production of foam and its stability increased with the

surfactant concentration and the presence of alcohol. The effect of alcohol on foam height followed the sequence: ethanol > methanol > no alcohol. During the initial period, the foam height declined rapidly with time. Thereafter, the foam height decreased slowly with time.

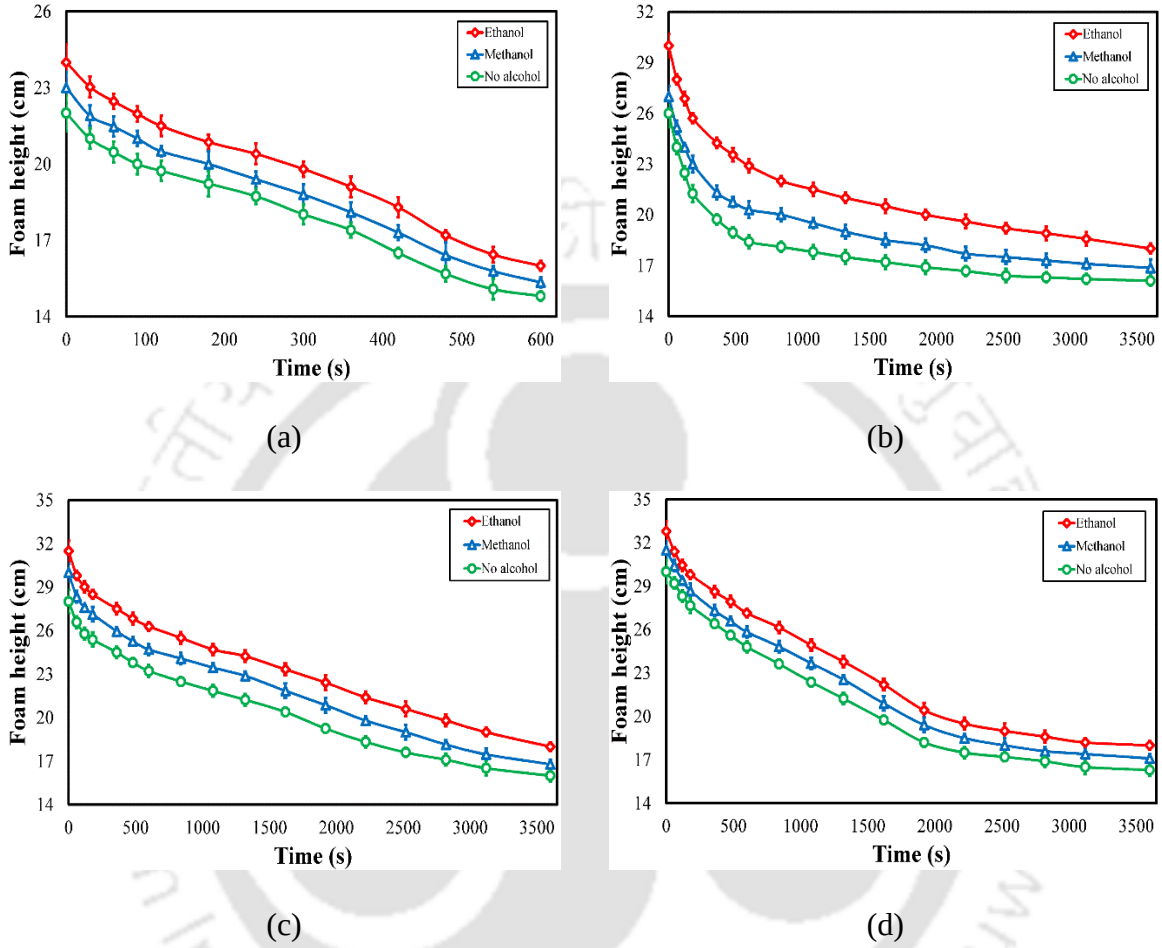

Figure 5.6 Variation of foam height with time at different surfactant concentrations: (a) 500, (b) 1000, (c) 2000, and (d) 3000 mg dm^{-3}.

5.2.2. Surfactant concentration profiles

It has been mentioned in Section 3.1 that small amounts of ethanol dissolved in water inhibit the coalescence of bubbles [13]. The effects of ethanol and methanol at various SDBS concentrations are shown in Figure 5.7. The SDBS concentration in the aqueous solution had a substantial impact on the performance of the foam fractionator. At the time of foam

generation, SDBS molecules adsorbed on the surface of the foam bubbles. As the bubbles moved upward, the SDBS molecules were stripped from the aqueous phase. This resulted in a steady decrease in the concentration of the surfactant in the aqueous phase over time. It was found that the foam at the top of the column had enough time to dry and had eventually collapsed after 1 h. With the rising airflow rate, the concentration of SDBS in the aqueous solution decreased further. This occurred as a result of more SDBS molecules adsorbing at the air–water interface and thereby forming more foam. With the addition of alcohol, the surface tension of the liquid decreased, allowing the formation of smaller bubbles, which were more stable. The increased stability of foam with small bubbles could be due to the reduction in the film drainage [17].

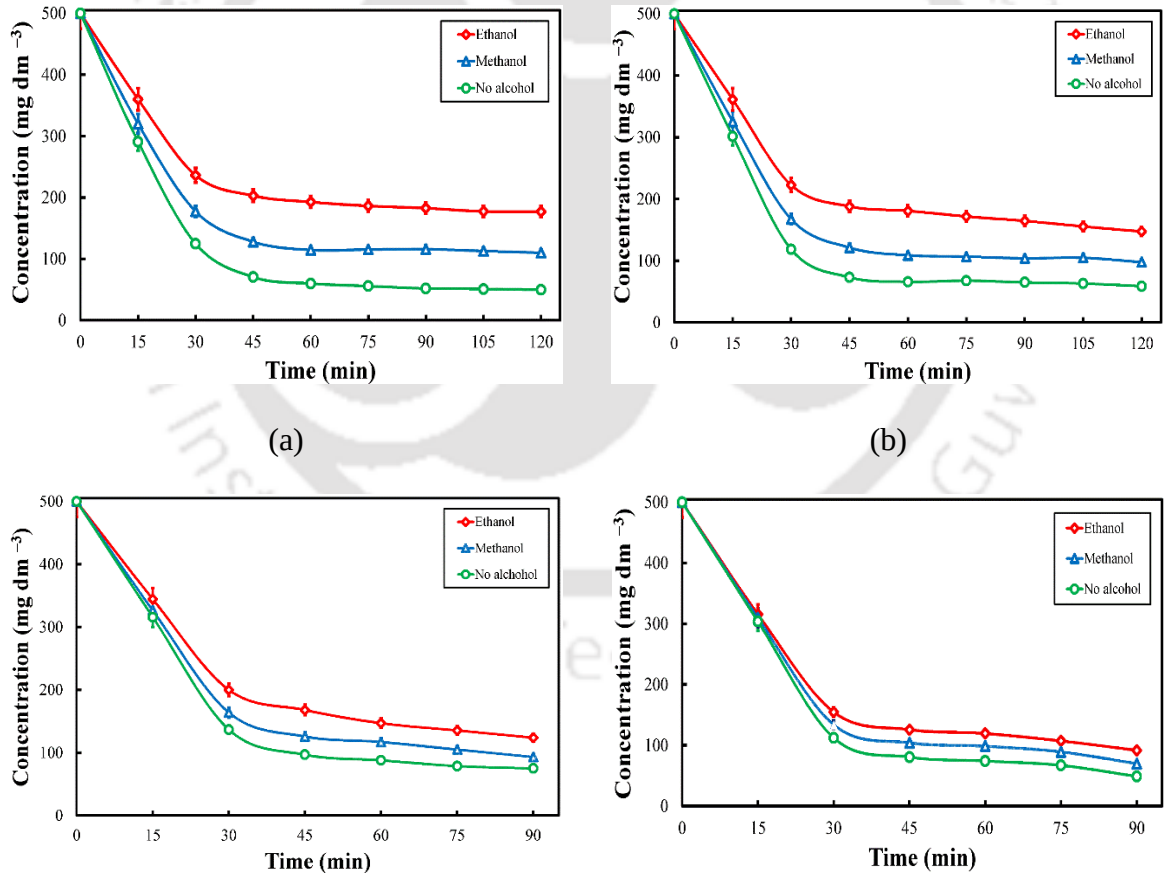

Figure 5.7 Effect of airflow rate on the concentration profiles at 500 mg dm^{-3} of SDBS with time: (a) 0.4, (b) 0.8, (c) 1.2, and (d) 1.6 dm^3 min^{-1}.

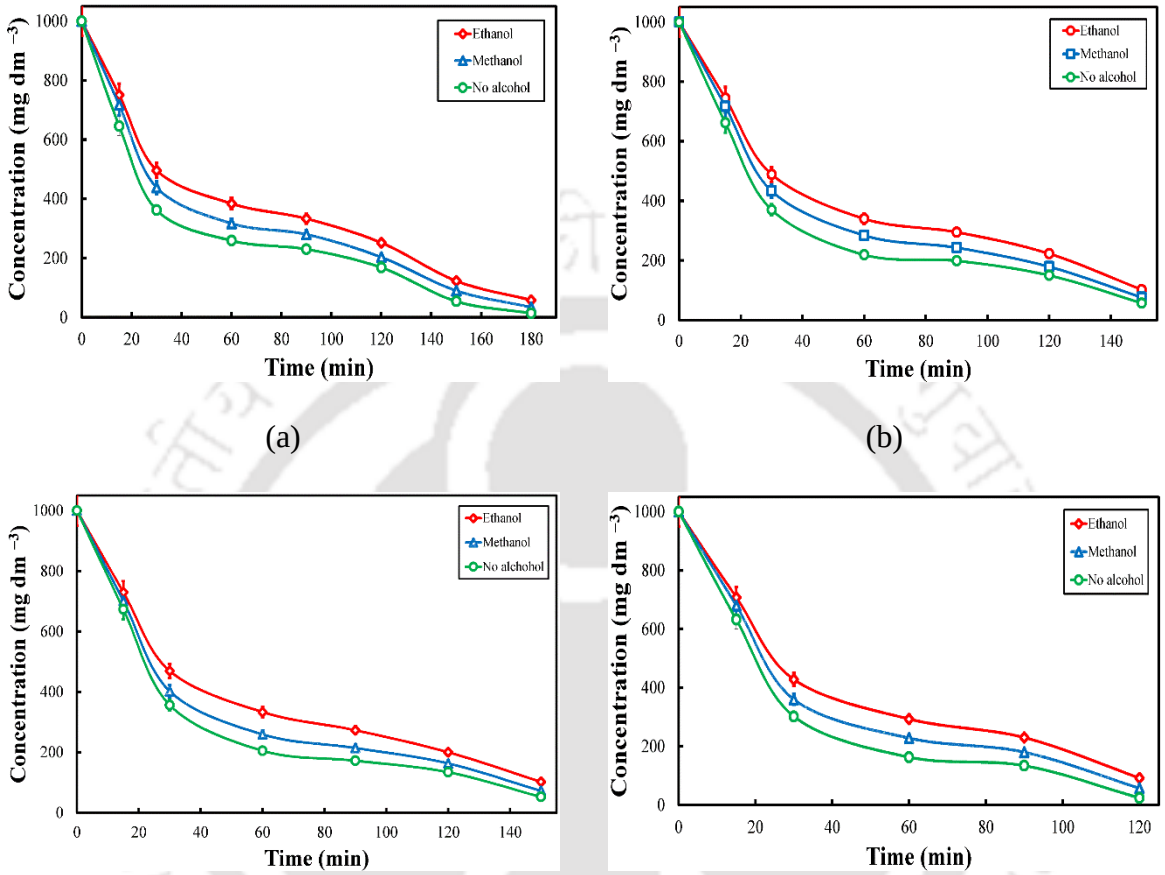

Figure 5.8 Effect of airflow rate on the concentration profiles at 1000 mg dm^{-3} of SDBS with time: (a) 0.4, (b) 0.8, (c) 1.2, and (d) 1.6 dm^3 min^{-1}.

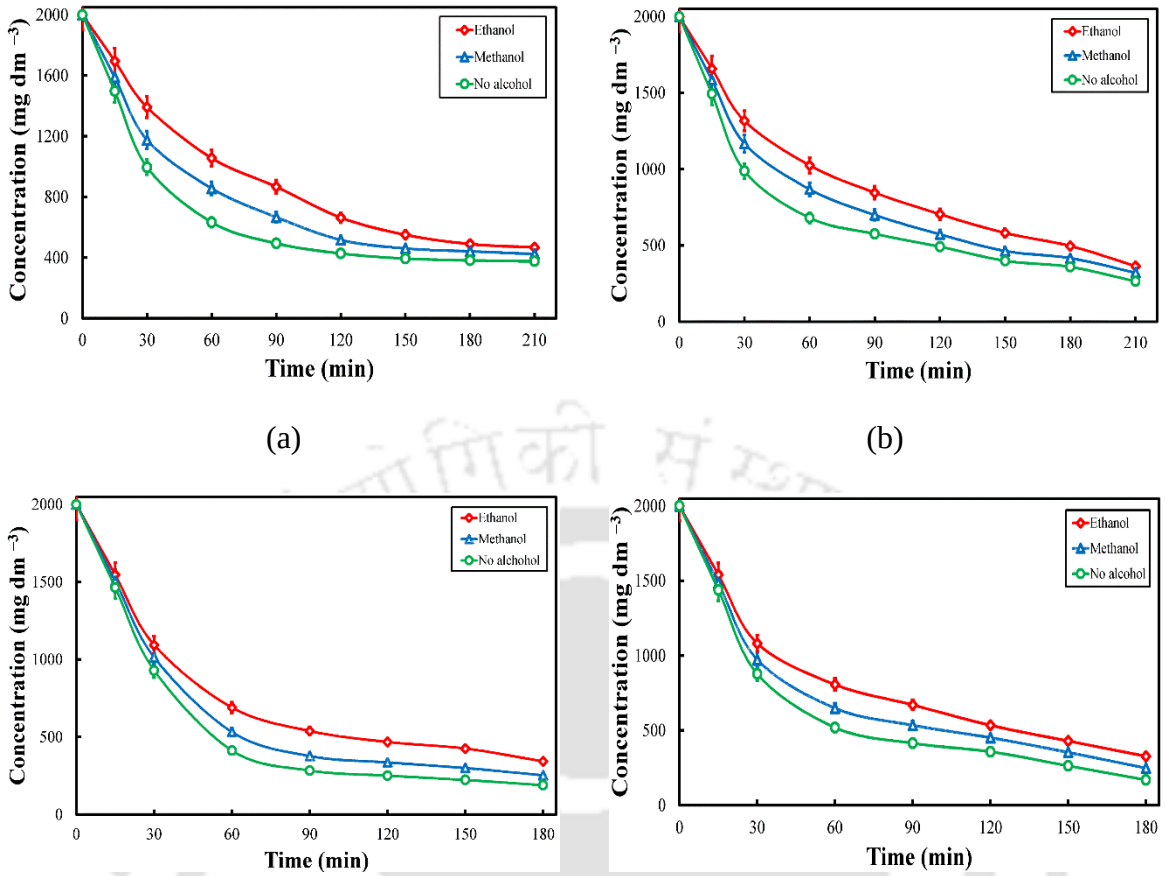

Figure 5.9 Effect of airflow rate on the concentration profiles at 2000 mg dm^{-3} of SDBS with time: (a) 0.4, (b) 0.8, (c) 1.2, and (d) 1.6 dm^3 min^{-1}.

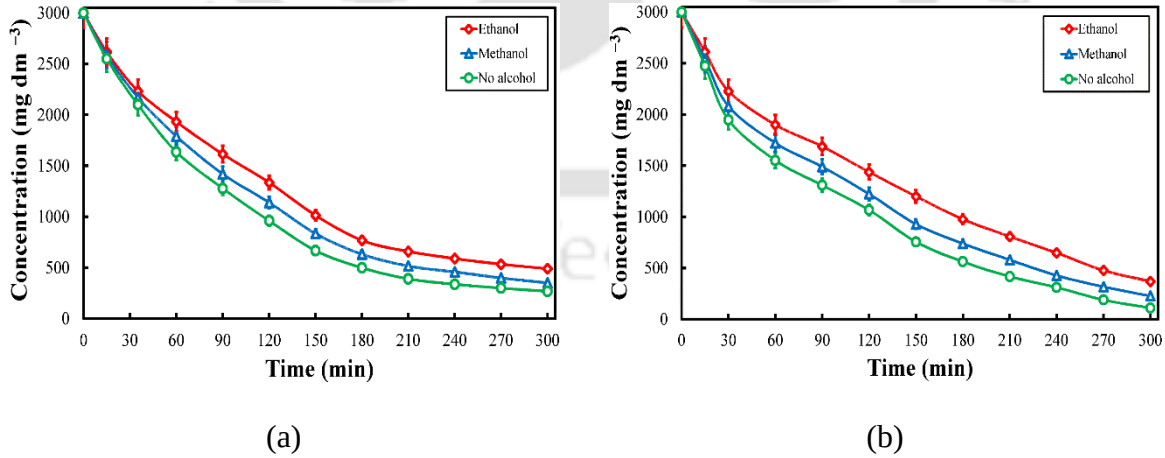

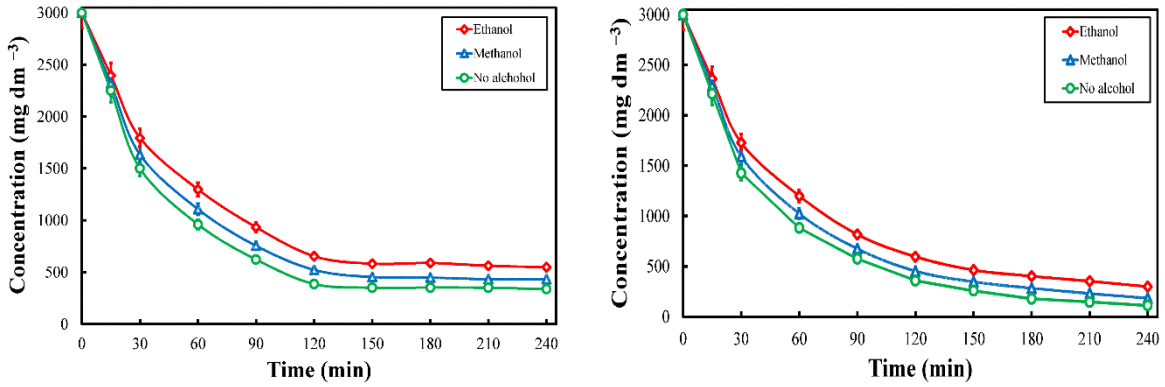

(c) (d)

Figure 5.10 Effect of airflow rate on the concentration profiles at 3000 mg dm^{-3} of SDBS with time: (a) 0.4, (b) 0.8, (c) 1.2, and (d) 1.6 $dm^3\ min^{-1}$.

The alcohol-based surfactant systems had identical concentration profiles. The rate of foam collapse increased with the rising concentration of SDBS. This may be due to the decrease in the Gibbs elasticity (E) of the foam film with the increasing concentration of SDBS. E is defined as

$$E = 2A\frac{d\gamma}{dA} \tag{5.1}$$

The value of E can be calculated by combining the Langmuir and Gibbs adsorption equations [18], i.e.,

$$E = \frac{4RT\Gamma_\infty^2 K_L^2 c_s}{h\left(1+K_L c_s\right)^2 + 2\Gamma_\infty K_L} \tag{5.2}$$

A film with a high degree of elasticity is more stable [19]. The elasticity of film increases as the concentration of SDBS increases, reaches a maximum, and then reduces at the high concentrations of the surfactant, resulting in a rapid collapse of the foam.

5.2.3. Surface tension of the aqueous solutions

The surface tension of the aqueous solution is a critical parameter in foam generation. In general, an aqueous surfactant solution with a lower surface tension is more effective for foam

generation. As a result, a surfactant that considerably lowers the surface tension is suitable for its recovery by using the foam fractionation technique. The surface tension of the feed solutions was measured prior to the start of the experiment, and these are reported in Table 5.1. The surface tensions of the aqueous solutions at the end of the experiments were also measured, and these values reported in the Tables 5.2 – 5.5. As the airflow rate increased, the surface tension increased as well. This was due to the increase in the amount of SDBS molecules stripped from the aqueous phase by foam fractionation. The ability of the alcohols to reduce the surface tension followed the sequence: ethanol > methanol > no alcohol.

Table 5.1 Surface tensions of the feed solutions at different concentrations of SDBS

SDBS concentration *(mg dm^{-3})*	*No alcohol* *(mN m^{-1})*	*Methanol* *(mN m^{-1})*	*Ethanol* *(mN m^{-1})*
500	36.6	36.2	34.5
1000	36.1	35.5	34.2
2000	35.9	34.7	33.7
3000	35.7	34.2	33.0

Table 5.2 Surface tensions of the alcohol-based surfactant solutions at 500 mg dm^{-3} after the experiments at different airflow rates

Alcohol	*Airflow rate (dm^3 min^{-1})*	*Surface tension (mN m^{-1})*
No alcohol	0.4	64.4
	0.8	66.5
	1.2	67.2
	1.6	67.9

Methanol	0.4	62.3
	0.8	65.2
	1.2	65.9
	1.6	67.2
Ethanol	0.4	55.5
	0.8	64.7
	1.2	65.7
	1.6	66.5

Table 5.3 Surface tensions of the alcohol-based surfactant solutions at 1000 mg dm^{-3} after the experiments at different airflow rates

Alcohol	*Airflow rate (dm^3 min^{-1})*	*Surface tension (mN m^{-1})*
No alcohol	0.4	58.4
	0.8	60.2
	1.2	62.8
	1.6	64.7
Methanol	0.4	55.8
	0.8	59.1
	1.2	61.9
	1.6	63.2
Ethanol	0.4	54.5
	0.8	57.5
	1.2	61.1
	1.6	62.8

Table 5.4 Surface tensions of the alcohol-based surfactant solutions at 2000 mg dm^{-3} after the experiments at different airflow rates

Alcohol	*Airflow rate (dm^3 min^{-1})*	*Surface tension (mN m^{-1})*
No alcohol	0.4	60.0
	0.8	61.6
	1.2	64.5
	1.6	66.2
Methanol	0.4	53.9
	0.8	59.7
	1.2	63.7
	1.6	65.2
Ethanol	0.4	53.1
	0.8	56.4
	1.2	61.2
	1.6	63.1

Table 5.5 Surface tensions of the alcohol-based surfactant solutions at 3000 mg dm^{-3} after the experiments at different airflow rates

Alcohol	*Airflow rate (dm^3 min^{-1})*	*Surface tension (mN m^{-1})*
No alcohol	0.4	60.0
	0.8	61.2
	1.2	63.5
	1.6	64.7

Methanol	0.4	58.9
	0.8	61.5
	1.2	63.2
	1.6	64.5
Ethanol	0.4	51.5
	0.8	55.0
	1.2	60.4
	1.6	62.1

5.2.4. Zeta potential at the air–water interface

The zeta potential is an important parameter for the stability of the foams. It is a measure of the charge that develops at the air–water interface. High electrostatic repulsion between the two air–water interfaces of the foam lamellae results in a more stable foam. The values of the zeta potential in the absence of alcohols are reported in Table 5.6. The zeta potential of the aqueous solutions at the end of the experiments were also measured, and these values reported in the Tables 5.7 – 5.10. The results indicate that the addition of alcohol increased the negative charge at the air–water interface (i.e., zeta potential increased in the presence of alcohol). The reduction of charge at the interface is due to the competitive displacement of the hydroxide ions by the more surface-active alcohol molecules. It decreased as the airflow rate increased due to the removal of SDBS from the aqueous phase. The zeta potentials in the aqueous systems were in the following sequence: ethanol > methanol > no alcohol.

Table 5.6 Zeta potential at the air–water interfaces at different concentrations of SDBS

SDBS concentration (mg dm^{-3})	*No alcohol (mV)*	*Methanol (mV)*	*Ethanol (mV)*
500	–4.4	–10.8	–15.6
1000	–8.5	–14.5	–20.2
2000	–12.5	–16.7	–24.5
3000	–13.9	–18.8	–27.4

Table 5.7 Zeta potentials after the experiments at different airflow rates at 500 mg dm^{-3} surfactant concentration

Alcohol	*Airflow rate (dm^3 min^{-1})*	*Zeta potential (mV)*
No alcohol	0.4	–4.3
	0.8	–4.1
	1.2	–3.7
	1.6	–3.2
Methanol	0.4	–9.7
	0.8	–8.9
	1.2	–8.5
	1.6	–7.6
Ethanol	0.4	–15.0
	0.8	–13.7
	1.2	–11.5
	1.6	–10.2

Table 5.8 Zeta potentials after the experiments at different airflow rates at 1000 mg dm^{-3} surfactant concentration

Alcohol	*Airflow rate (dm^3 min^{-1})*	*Zeta potential (mV)*
No alcohol	0.4	–8.1
	0.8	–7.4
	1.2	–7.1
	1.6	–5.8
Methanol	0.4	–13.7
	0.8	–12.5
	1.2	–10.6
	1.6	–9.9
Ethanol	0.4	–18.4
	0.8	–16.5
	1.2	–13.7
	1.6	–10.9

Table 5.9 Zeta potentials after the experiments at different airflow rates at 2000 mg dm^{-3} surfactant concentration

Alcohol	*Airflow rate (dm^3 min^{-1})*	*Zeta potential (mV)*
No alcohol	0.4	–12.2
	0.8	–11.7
	1.2	–7.5
	1.6	–4.0

Methanol	0.4	–15.5
	0.8	–12.7
	1.2	–8.3
	1.6	–5.8
Ethanol	0.4	–23.4
	0.8	–20.4
	1.2	–18.4
	1.6	–15.1

Table 5.10 Zeta potentials after the experiments at different airflow rates at 3000 mg dm^{-3} surfactant concentration

Alcohol	*Airflow rate (dm^3 min^{-1})*	*Zeta potential (mV)*
No alcohol	0.4	–11.8
	0.8	–10.7
	1.2	–8.3
	1.6	–6.6
Methanol	0.4	–18.0
	0.8	–16.2
	1.2	–13.7
	1.6	–10.2
Ethanol	0.4	–26.5
	0.8	–25.4
	1.2	–18.4

	1.6	−11.5

5.2.5. Surfactant recovery

The recovery of the surfactant is essential for reusing it. It is described in Section 3.2.2. The top portion of the column yielded a significant amount of wet solid flakes of SDBS. In the lamellae of foam, a small number of surfactant molecules remained that could not be retrieved. Without the alcohol, approximately 75% of the surfactant molecules were recovered (see Figure 5.11). Therefore, in the presence of alcohol, surfactant recovery decreased. Due to the shorter residence time of the growing foam bubbles, some surfactant remained in the lamellae liquid, which was eventually drained off, causing a lower recovery. The addition of ethanol disturbed the hydrophobic interaction between the surfactant molecules, reducing their binding strength [20]. With increasing airflow rate, the recovery of SDBS increased. The recovery was substantially improved at the higher airflow rates (i.e., 1.2 and 1.6 dm^3 min^{-1}). At the higher airflow rates, more bubbles were created, causing more surfactant molecules to adsorb on their surface, resulting in a higher recovery. A lower recovery was observed in the presence of ethanol than methanol due to the presence of more SDBS molecules in the aqueous surfactant solution after the experiment was completed. It may also be due to the decrease in the micellization of surfactant in the presence of ethanol [21]. The effect of alcohol in reducing the recovery of surfactant followed the order: ethanol > methanol > no alcohol.

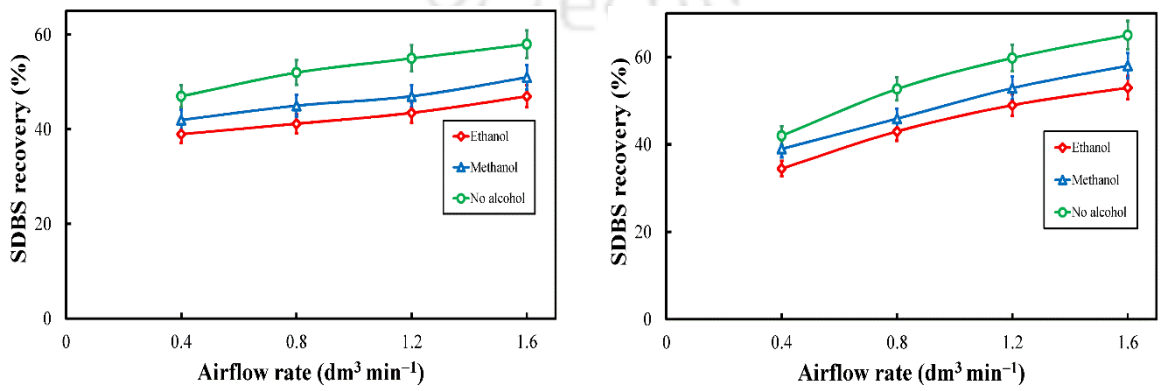

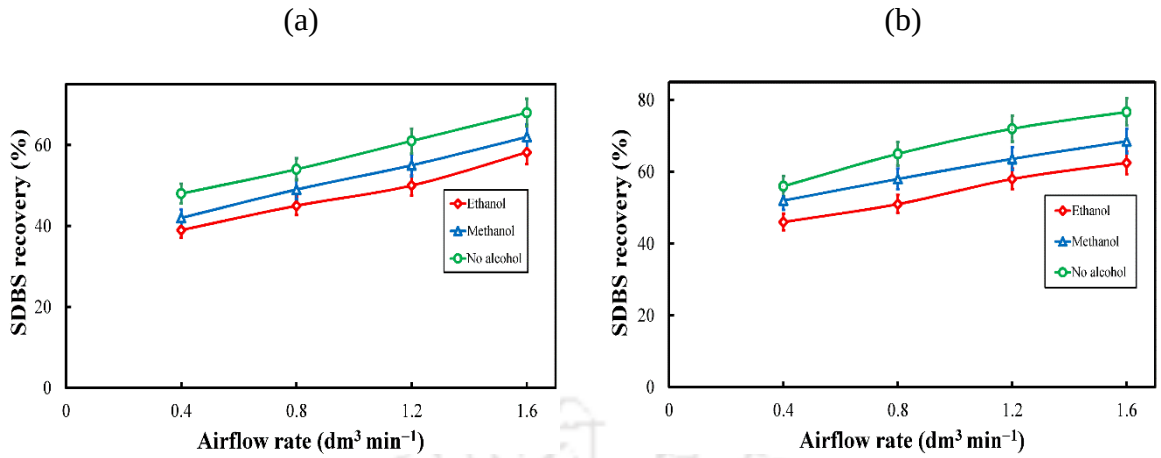

Figure 5.11 Surfactant recovery at different airflow rates: (a) 500, (b) 1000, (c) 2000, and (d) 3000 mg dm^{-3} SDBS concentrations.

5.2.6. Water recovery

Water recovery is an important factor in foam fractionation. In this way, the reuse of water can be possible. During the experiment, only a small amount of water was lost. The feed contained 500 cm^3 of water. After the experiment was over, about 490 cm^3 of water was recovered (including the samples collected during the experiment). The presence of alcohol had no discernible effect on water recovery. It was observed that the recovery of water was nearly the same both in the presence of methanol and ethanol. The formation of foam was more effective at the high airflow rates (e.g., 1.6 dm^3 min^{-1}), resulting in a marginally higher loss of water.

5.3. Conclusions

Removal and recovery of an anionic surfactant (i.e., SDBS) in the presence of short-chain aliphatic alcohols (i.e., methanol and ethanol) by foam fractionation was investigated in this work. The mixed aqueous system comprised of water, surfactant, and alcohol is of interest in the chemical and biochemical industries. The effect of ethanol and methanol on foam

fractionation was studied at four concentrations of SDBS. The following conclusions can be drawn about the impact of various operational parameters:

- The foam volume increased with increasing surfactant concentration and airflow rate.
- The foam volume was higher in the presence of alcohol. Ethanol produced more foam than methanol.
- The recovery of SDBS decreased in the presence of alcohol. The recovery of SDBS in the absence of alcohol was 75%.
- The zeta potential increased with the increasing surfactant concentration. It also increased with the addition of alcohol.
- The surface tension of the aqueous solution decreased by the addition of alcohol.
- Water recovery was found to be excellent in all systems.

Nomenclature

Symbols

E	Gibbs film elasticity, N m^{-1}
A	surface area of foam lamella, m^2
R	gas constant, J mol^{-1} K^{-1}
T	temperature, K
K_L	equilibrium constant in the Langmuir adsorption equation, m^3 mol^{-1}
c_s	concentration of surfactant in the bulk solution, mol m^{-3}
h	thickness of foam film, m
ρ	recovery

Greek letters

γ	surface tension, N m^{-1}
Γ_∞	adsorption capacity, mol m^{-2}

References

[1] P. Wungrattanasopon, J.F. Scamehorn, S. Chavedej, C. Saiwan, J.H. Harwell, Use of foam flotation to remove tert-butylphenol from water, Sep. Sci. Technol. 31 (1996) 1523–1540.

[2] Y. Luo, W. Guo, H.H. Ngo, L.D. Nghiem, F.I. Hai, J. Zhang, S. Liang, X.C. Wang, A review on the occurrence of micropollutants in the aquatic environment and their fate and removal during wastewater treatment, Sci. Total Environ. 473 (2014) 619–641.

[3] N.H. Tran, M. Reinhard, K.Y.H. Gin, Occurrence and fate of emerging contaminants in municipal wastewater treatment plants from different geographical regions–a review, Water Res. 133 (2018) 182–207.

[4] I. Kruszelnicka, D. Ginter-Kramarczyk, B. Wyrwas, J. Idkowiak, Evaluation of surfactant removal efficiency in selected domestic wastewater treatment plants in Poland, J. Environ. Health. Sci. 17 (2019) 1257–1264.

[5] R. Leung, D.O. Shah, Dynamic properties of micellar solutions: I. effects of short-chain alcohols and polymers on micellar stability, J. Colloid Interface Sci. 113 (1986) 484–499.

[6] A. Pan, B. Naskar, G. Prameela, B.P. Kumar, A. Mandal, S. Bhattacharya, S. Moulik, Amphiphile behavior in mixed solvent media I: self-aggregation and ion association of sodium dodecylsulfate in 1, 4-dioxane–water and methanol–water media, Langmuir 28 (2012) 13830–13843.

[7] P. Chowdhary, A. Raj, R.N. Bharagava, Environmental pollution and health hazards from distillery wastewater and treatment approaches to combat the environmental threats: a review, Chemosphere 194 (2018) 229–246.

[8] P. Chowdhary, A. Yadav, G. Kaithwas, R.N. Bharagava, Distillery wastewater: a major source of environmental pollution and its biological treatment for environmental safety, Green technologies and environmental sustainability, Springer 2017, pp. 409–435.

[9] C. Varela, The impact of non-Saccharomyces yeasts in the production of alcoholic beverages, Appl. Microbiol. Biotechnol. 100 (2016) 9861–9874.

[10] H. Polat, D. Erdogan, Heavy metal removal from waste waters by ion flotation, J. Hazard. Mater. 148 (2007) 267–273.

[11] L. Blasco, M. Viñas, T.G. Villa, Proteins influencing foam formation in wine and beer: the role of yeast, Int. Microbiol. 14 (2011) 61–71.

[12] B. Medina, M. Torem, L. De Mesquita, On the kinetics of precipitate flotation of Cr III using sodium dodecylsulfate and ethanol, Miner. Eng. 18 (2005) 225–231.

[13] R. Krishna, M. Urseanu, A. Dreher, Gas hold-up in bubble columns: influence of alcohol addition versus operation at elevated pressures, Chem. Eng. Process. 39 (2000) 371–378.

[14] P. Lo Nostro, G. Gabrielli, Temperature and subphase effects on aliphatic alcohol films at the air–water interface, Langmuir 9 (1993) 3132–3137.

[15] H. Ghahremani, A. Moradi, J. Abedini-Torghabeh, S. Hassani, Measuring surface tension of binary mixtures of water + alcohols from the diffraction pattern of surface ripples, Der Chem. Sin. 2 (2011) 212–221.

[16] C. Panja, N. Saliba, B.E. Koel, Adsorption of methanol, ethanol and water on well-characterized Pt–Sn surface alloys, Surf. Sci. 395 (1998) 248–259.

[17] T.D. Hodgson, J.C. Lee, The effect of surfactants on the coalescence of a drop at an interface I, J. Colloid Interface Sci. 30 (1969) 94–108.

[18] L. Wang, R.-H. Yoon, Effects of surface forces and film elasticity on foam stability, Int. J. Miner. Process. 85 (2008) 101–110.

[19] W. Xu, A. Nikolov, D.T. Wasan, A. Gonsalves, R.P. Borwankar, Foam film rheology and thickness stability of foam-based food products, Colloids Surf. A 214 (2003) 13–21.

[20] Y. Chen, Y. Lapitsky, Interactions of anionic surfactants with cationic polyelectrolyte gels: competitive binding and application in separation processes, Colloids Surf. A 372 (2010) 196–203.

[21] S. Göktürk, U. Var, Effect of ethanol on partition and binding equilibrium of phenothiazine in anionic and nonionic micellar solutions, Curr. Res. Chem. 3 (2011) 49–61.

Chapter 6

Summary and Scope for Future Work

CHAPTER 6

Summary and Scope for Future Work

6.1 Summary of the work

An experimental study has been performed for the removal and recovery of a surfactant by foam fractionation. The airflow rate and the concentration of the surfactant were varied to analyze the recovery of the surfactant and foaming. The effects of inorganic salts on the removal and recovery of CTAB were investigated. The effects of benzene, toluene, and hexane on the recovery of SDS were studied. The effects of methanol and ethanol on the recovery of SDBS were studied. The major conclusions from this work are as follows:

- Surfactants used in this work showed a good foamability in the absence of the additives such as salt, oil, and alcohol. The foam volume reduced in the presence of these additives.
- The foam volume increased with increasing airflow rate.
- The concentrations of the surfactants in their aqueous solutions decreased with time.
- The surface tension of the aqueous surfactant solution increased with increasing airflow rate.
- The zeta potential increased with the increasing surfactant concentration. It was lower in the presence of salt in the CTAB system. It was highest in the presence of benzene and lowest for hexane in the SDS system. It increased with the addition of alcohol in the SDBS system.
- A good amount of surfactant was recovered by this process. The recovery was less in the presence of salt, oil, and alcohol.
- The recovery of water was good in all the experiments carried out in this study.

6.2 Future scope of research

Based on the work reported in this thesis, research can be extended in a few different ways in the future. Some of the interesting possibilities are as follows:

- Removal and recovery of a mixture of surfactants in the presence of salts and oils by foam fractionation may be studied. Mixed surfactant systems are encountered in nearly all practical applications of surfactants such as oil recovery, cosmetics, dyeing, paints, corrosion inhibition, and so on. Theoretical interest and practical importance of the mixed surfactant systems have been growing rapidly.
- Removal and recovery of surfactant in the presence of medium- and long-chain water-soluble alcohols by foam fractionation may be studied. Such alcohols are used in a wide variety of industrial applications including household laundry powders and liquids, dishwashing liquids, other household cleaners, and personal care products (e.g., shampoos and soaps).
- Modeling of the foam fractionation process, both in the batch and continuous modes of operation, may be attempted more rigorously. A few models have been developed on foam fractionation. However, hardly any model has incorporated the stability of foam, which depends on the stability of the thin liquid film. This stability depends on the intermolecular and surface forces such as van der Waals, electrostatic double layer, and hydration forces. No model has incorporated the DLVO and non-DLVO theories of thin film stability, which may be incorporated in the model of foam stability, its lifetime, and hence link it with the recovery of surfactant. A rigorous model for foam fractionation should include the drainage and stability of the foam film.

Appendix A

Appendix A: Cost estimation of the foam fractionation process

The estimated capital and running cost of the foam fractionation setup is given below. The summary of the capital cost of the experimental setup is given in Table A.1.

Table A.1 Capital cost of the experimental setup for foam fractionation

Item	*Cost (₹)*
Foam fractionation column	4000
Airflow system (compressor, voltage stabilizer, rotameter, and sparger)	7000
Total cost	11000

The main operational cost of this experimental setup is that of electricity, which is summarized in Table A2.2.

Table A.2 Operational cost of the foam fractionation setup

Item	*Power consumption (W)*	*Hours*	*Electricity consumption (kWh)*
Compressor	149	5*	0.75
Hot air oven	1250	24	30.00
Total units (kWh)			30.75

*Includes 1 h for cleaning

The cost of electricity for one unit in Assam (India) is ₹6.75. Therefore, the estimated total operating cost of a single run of the foam fractionation experiment is ₹207.56.

Cost estimation for SDS recovery:

The variation of operational cost with the surfactant recovery is shown in Figure A.1.

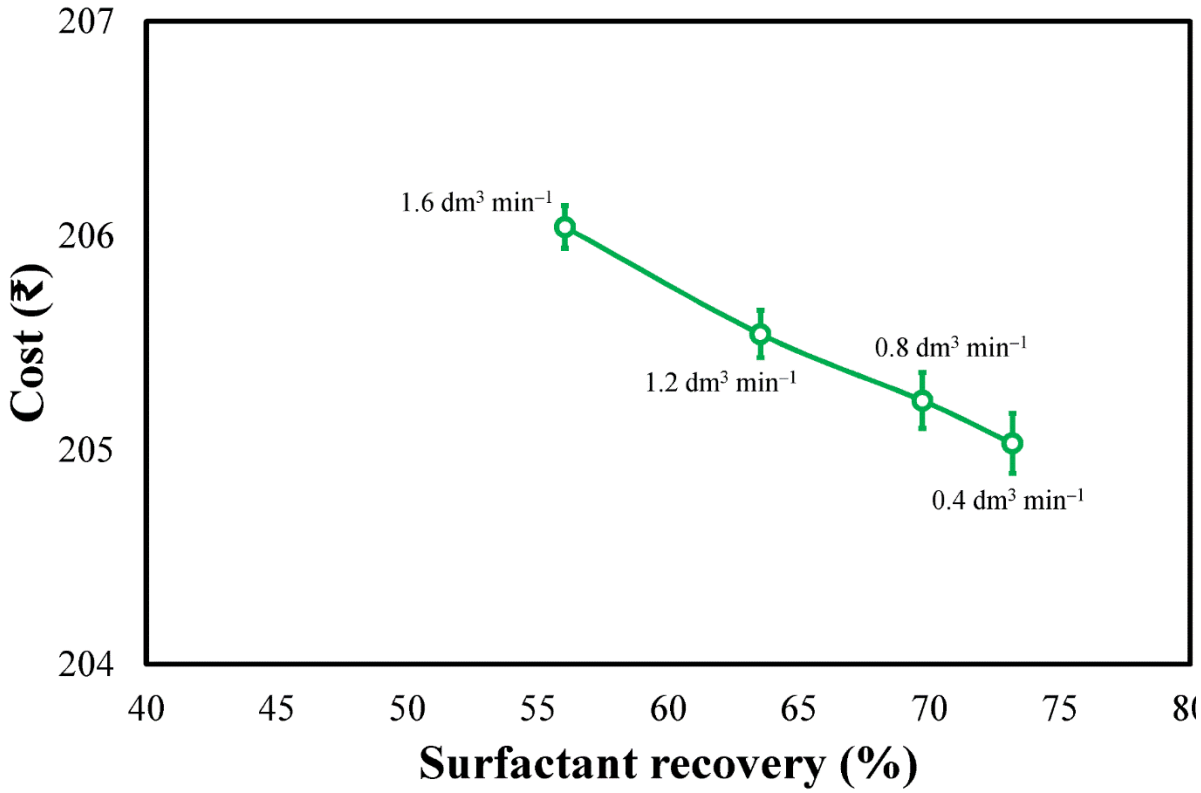

Figure A.1 The variation of operational cost with the recovery of SDS at different airflow rates.

Research Outcomes

Publications

1. **A.K. Kumar**, N. Rawat, P. Ghosh, Removal and recovery of a cationic surfactant from its aqueous solution by foam fractionation, J. Environ. Chem. Eng. 8 (2020) 103555.
2. **A.K. Kumar**, P. Ghosh, Recovery of an anionic surfactant in the presence of benzene, toluene, and hexane by foam fractionation, Int. J. Environ. Sci. Technol. (2021). Doi: 10.1007/s13762-021-03796-z
3. **A.K. Kumar**, P. Ghosh, Removal and recovery of an anionic surfactant in the presence of alcohol by foam fractionation, Ind. Eng. Chem. Res. (2022). Doi: 10.1021/acs.iecr.2c00372.

Conferences

1. Presented a poster in "Complex Fluids and Soft Matter 2021" organized by Indian Institute of Technology Gandhinagar, India, December 13–15, 2021.
2. Presented a poster in "Complex Fluids 2020" organized by IIT Bombay and the Indian Society of Rheology, December 10–12, 2020.
3. Presented a poster in the "International Conference on Advances in Chemical Engineering-2020 (AdChE-2020)" organized by the Department of Chemical Engineering, UPES, Dehradun (India), February 5–7, 2020.
4. Presented a poster in "The 8th Asian Conference on Colloid and Interface Science" organized by Asian Society of Colloid and Surface Science, Kathmandu (Nepal) September 24–27, 2019.

5. Presented a seminar on the "Advances in Chemical Engineering" organized by the Department of Chemical Engineering, Assam Engineering College, Guwahati, August 30, 2019.
6. Presented a poster in "Research Conclave 2019" organized by Students' Academic Board, Indian Institute of Technology Guwahati, March 14–17, 2019.
7. Presented a poster in "Research Conclave 2018" organized by Students' Academic Board, Indian Institute of Technology Guwahati, 8–11 March, 2018.